

Manuscript version: Author's Accepted Manuscript

The version presented in WRAP is the author's accepted manuscript and may differ from the published version or Version of Record.

Persistent WRAP URL:

<http://wrap.warwick.ac.uk/104860>

How to cite:

Please refer to published version for the most recent bibliographic citation information. If a published version is known of, the repository item page linked to above, will contain details on accessing it.

Copyright and reuse:

The Warwick Research Archive Portal (WRAP) makes this work by researchers of the University of Warwick available open access under the following conditions.

Copyright © and all moral rights to the version of the paper presented here belong to the individual author(s) and/or other copyright owners. To the extent reasonable and practicable the material made available in WRAP has been checked for eligibility before being made available.

Copies of full items can be used for personal research or study, educational, or not-for-profit purposes without prior permission or charge. Provided that the authors, title and full bibliographic details are credited, a hyperlink and/or URL is given for the original metadata page and the content is not changed in any way.

Publisher's statement:

Please refer to the repository item page, publisher's statement section, for further information.

For more information, please contact the WRAP Team at: wrap@warwick.ac.uk.

FORCE-BASED ATOMISTIC/CONTINUUM BLENDING FOR MULTILATTICES

DEREK OLSON, XINGJIE LI, CHRISTOPH ORTNER, BRIAN VAN KOTEN

ABSTRACT. We formulate the blended force-based quasicontinuum (BQCF) method for multilattices and develop rigorous error estimates in terms of the approximation parameters: atomistic region, blending region and continuum finite element mesh. Balancing the approximation parameters yields a convergent atomistic/continuum multiscale method for multilattices with point defects, including a rigorous convergence rate in terms of the computational cost. The analysis is illustrated with numerical results for a Stone–Wales defect in graphene.

1. INTRODUCTION

A full twenty years has passed since the original proposal of the quasicontinuum method [36] captivated the materials science community with the potential to model material phenomena spanning vastly different length scales. The quasicontinuum (QC) method was among the first of the so-called atomistic-to-continuum (AtC) coupling algorithms which sought to bridge the gap between length scales from the nano to macroscale. A remarkable number of these AtC methods have been proposed since (see e.g. [51, 31, 28] for a thorough discussion of many of these), and recently a mathematical framework has begun to emerge to analyze and compare several of these methods for defects in crystalline materials comprised of a Bravais lattice. Indeed, all three of the blended force-based quasicontinuum method (BQCF), blended energy-based quasicontinuum (BQCE), and blended ghost force correction (BGFC) methods have recently been analyzed in the context of a single defect in a two or three dimensional Bravais lattice [25, 41] as has the optimization-based AtC approach of [35]. Analyses in two and three dimensional Bravais lattices also exist for the AtC method of [26], but this has not yet been extended to allow for defects. Meanwhile, the methods [30, 46, 45] have been shown to be consistent (or free of ghost forces) for pair potential interactions only.

In the present work, we resolve the long-standing challenge to develop a rigorous numerical analysis for AtC methods in the context of *multilattices*, which allows for more than one atom to be present in the unit cell of the crystal. This description includes important materials such as hcp metals, diamond structures, and recently discovered 2D materials such as graphene and hexagonal boron nitride.

Concretely, we generalise the formulation and analysis of the blended force-based quasicontinuum (BQCF) method. Our main result is that, for a point defect in a homogeneous host crystal, the BQCF method for multilattices exhibits the same rate of convergence as in the Bravais lattice case. This is in sharp contrast with the blended energy-based quasicontinuum method for which a reduced convergence rate is expected in the multilattice setting [41].

The present work represents the first analysis that has been undertaken that remains valid for an AtC method which permits defects in a two or three dimensional multilattice. Even analyses of AtC

DO was supported by the NSF PIRE Grant OISE-0967140 and NSF RTG program DMS-1344962. XL was supported by the Simons Collaboration Grant with Award ID: 426935. CO was supported by ERC Starting Grant 335120.

methods for defect-free multilattices remain extremely sparse: the homogenized QC method [2, 1], for example, only allows for dead load external forces while the cascading Cauchy–Born method was rigorously analyzed only in one-dimensional multilattices for phase transforming materials [13].

As its name entails, the BQCF method is a force-based AtC method where a hybrid force operator is constructed instead of a hybrid energy functional [14, 47, 48, 26, 7, 5]. The primary advantage of force-based methods is that the forces can easily be defined in a way to avoid spurious interface effects (ghost forces); that is, the defect-free perfect crystal is a bona fide equilibrium configuration of the AtC force operator. The cost of defining the BQCF method and other force-based methods to be free of ghost forces is that these force fields are no longer conservative, which creates significant challenges in their numerical analysis [15, 27]. The blended force-based methods, originally studied in [23, 7, 5, 26], seek to overcome this problem by a smooth blending between atomistic and continuum forces over a region called the blending, overlap, or handshake region. Similar force-based blending methods have also been applied to coupling peridynamics with classical elasticity [43].

An alternative to the force-based paradigm is the energy-based paradigm where a global, hybrid energy is defined which is some combination of atomistic and continuum energies. This encompasses the original quasicontinuum method and many other offshoots and ancestors [36, 52, 3, 16, 49, 12, 18, 8]. The peril of these methods is the aforementioned ghost forces, and it remains open to construct a general, ghost-force free, energy-based AtC method for Bravais lattices in two or three dimensions. As such we do not concern ourselves with an energy-based AtC method for multilattices; however, see [41, 44] for promising directions.

1.1. Outline. We begin in Section 2 by formulating an atomistic model for a multilattice material describing a single point defect embedded in an infinite homogeneous crystal. This is a canonical extension of the framework adopted for Bravais lattices in [35, 25, 24, 17, 41].

In Section 3 we then formulate the BQCF method for this model and state our main results: (1) existence of a solution to the multilattice BQCF method and (2) a sharp error estimate. We also convert this error estimate to an estimate in terms of the computational complexity of the BQCF method in Section 3.4 which in particular allows us to balance approximation parameters to obtain a formulation optimised for the error / cost ratio. We present a numerical verification of these rates by testing the method on a Stone–Wales defect in graphene. The complexity estimates obtained for the BQCF method for point defects in multilattices match those estimates in [25] for Bravais lattices.

Finally, Section 4 covers the technical details needed to prove our main result, Theorem 6. These technical details can be seen as generalizations of the results of Bravais lattices, and the primary new component is having to account for shifts between atoms in the same unit cell.

1.2. Notation. We introduce new notation throughout the paper required to carry out the analysis. For the convenience of the reader, we have listed many of these in Appendix B. Here, we briefly establish several basic conventions we make throughout. We use d and n to denote the dimensions of the domain and range respectively, calligraphic fonts (e.g. \mathcal{L}, \mathcal{M}) to denote lattices, sans-serif fonts (e.g. \mathbf{F}, \mathbf{G}) for $n \times d$ matrices, the lower case Greek letters $\alpha, \beta, \gamma, \delta, \iota, \chi$ are used as subscripts denoting atomic species, and the lower case Greek letters ρ, τ, σ denote vectors (bond directions) between lattice sites.

The symbol $|\cdot|$ is used to denote the ℓ^2 norm of a single vector in \mathbb{R}^m , while $\|\cdot\|$ is used to denote either an ℓ^p or L^p norm over a specified set. We use \cdot for the dot product between two vectors, \otimes as the tensor product, and $:$ as the inner product on tensors.

Derivatives of functions $f : \mathbb{R}^d \rightarrow \mathbb{R}^n$ are denoted by $\nabla f : \mathbb{R}^d \rightarrow \mathbb{R}^{d \times n}$ and higher order derivatives by $\nabla^j f$. Given $F : X \rightarrow Y$ where X and Y are Banach spaces, we denote Fréchet or Gateaux derivatives by $\delta^j F$, j indicating the order. We will most commonly interpret these derivatives as (multi-)linear forms and use them when $Y = \mathbb{R}$, in which case we will then write the Gateaux derivatives as

$$\begin{aligned} \langle \delta F(x), y \rangle, \quad x, y \in X \\ \langle \delta^2 F(x)z, y \rangle, \quad x, y, z \in X \quad \text{and so on for higher order derivatives.} \end{aligned}$$

We reserve D for specific finite difference operators (defined in (2.3) and (2.4)), and use B_R to denote the ball of radius R about the origin.

We use the modified Vinogradov notation $x \lesssim y$ throughout the manuscript to mean there exists a positive constant C such that $x \leq Cy$. Where appropriate, we clarify what the constant C is allowed to depend on; in particular if there is any dependence on approximation parameters then it will always be made explicit.

2. ATOMISTIC MODEL

2.1. Defect-free Multilattice. We consider an infinite Bravais lattice, or simply a *lattice*, \mathcal{L} , defined by

$$\mathcal{L} := F\mathbb{Z}^d, \quad \text{for some } F \in \mathbb{R}^{d \times d}, \quad \det(F) = 1, \quad \text{and } d \in \{2, 3\},$$

where the requirement $\det(F) = 1$ is purely a notational convenience. From a physical standpoint by taking symmetry into account, it can be shown that there are only 14 unique physical lattices in 3D and five in 2D (see e.g. [51]); however, we consider the lattice to merely be a mathematical framework. A multilattice is then obtained by associating a basis of S atoms to each lattice site, and this is also referred to as a crystal when the Bravais lattice is interpreted as one of the unique physical lattices.

For each site $\xi \in \mathcal{L}$, these S atoms are located inside the unit cell of ξ at positions $\xi + p_\alpha^{\text{ref}}$ for $p_\alpha^{\text{ref}} \in \mathbb{R}^d$ and $\alpha = 0, \dots, S-1$. The multilattice is then defined by

$$\mathcal{M} := \bigcup_{\alpha=0}^{S-1} \mathcal{L} + p_\alpha^{\text{ref}}.$$

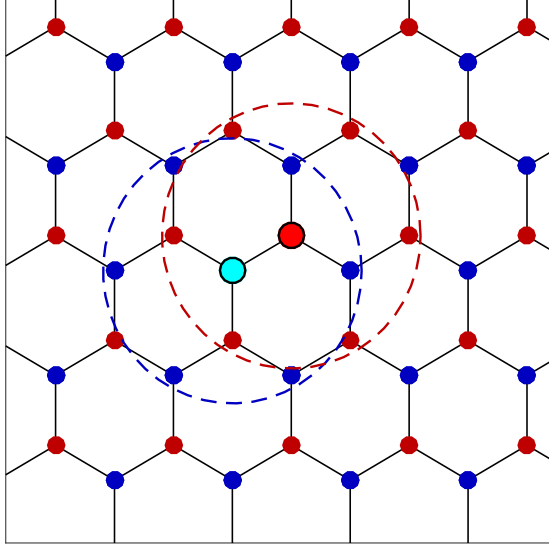
We call each $\mathcal{L} + p_\alpha^{\text{ref}}$ a sublattice; here the addition “+” means a translation of the lattice \mathcal{L} by the vector p_α^{ref} . Without loss of generality, we further assume $p_0^{\text{ref}} = 0$ (one atom is always located at a lattice site). Furthermore, we make the distinction between a lattice site, which we use to refer to a site in the Bravais lattice, \mathcal{L} , and an atom which is an element in the multilattice \mathcal{M} .

Two simple examples of multilattices are shown in Figure 1 including the 2D hexagonal lattice (e.g., graphene) for which

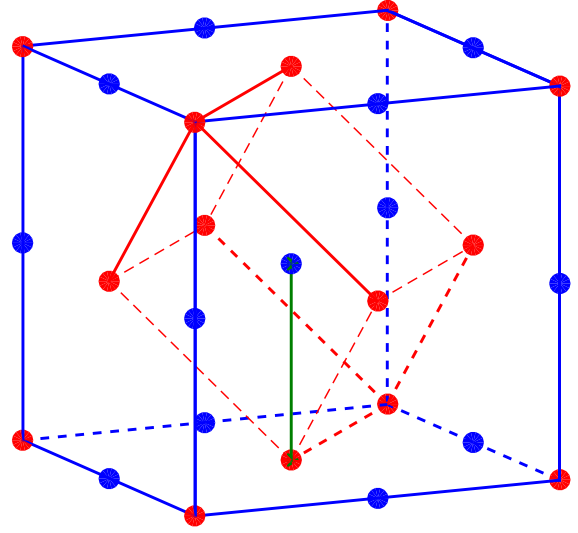
$$\mathcal{L} = a_0 \begin{pmatrix} \sqrt{3} & \sqrt{3}/2 \\ 0 & 3/2 \end{pmatrix} \mathbb{Z}^2, \quad S = 2, \quad p_0 = \begin{pmatrix} 0 \\ 0 \end{pmatrix}, \quad p_1 = a_0 \begin{pmatrix} \sqrt{3}/2 \\ 1/2 \end{pmatrix}, \quad a_0 = \frac{\sqrt{2}}{3^{3/4}}. \quad (2.1)$$

(The $a_0 = \frac{\sqrt{2}}{3^{3/4}}$ prefactor is due to the normalisation $\det(F) = 1$.)

For each species of atom, we define the deformation field $y_\alpha(\xi)$ as the deformation of the atom of species α at site ξ . We note that $y_\alpha : \mathcal{L} \rightarrow \mathbb{R}^n$ where the range dimension $n \in \{2, 3\}$ may be different than the domain dimension d to allow, e.g., for out of plane displacements in 2D. However, we remark that our later assumptions on stability of the multilattice (Assumption 3) will place a restriction on the out of plane behavior; for example bending, or rippling, cannot



(a) 2D graphene: the dashed circles indicate the interaction neighbourhoods of the highlighted atoms.



(b) 3D rock salt: the interior cube represents a possible choice of unit cell.

FIGURE 1. Examples of multilattice structures.

currently be incorporated into the analysis. We further discuss the issues involved in this in our concluding discussion, Section 5. In the case of these out of plane displacements, we will use $\xi \in \mathbb{R}^2$ as both a vector in \mathbb{R}^2 and as the vector $\begin{pmatrix} \xi \\ 0 \end{pmatrix} \in \mathbb{R}^3$. (We remark that though we will not consider dislocations, we could also consider $n = 1$ for an anti-plane screw dislocation model by fixing a second coordinate to be constant in this framework.)

The set of all sublattice deformations is denoted by $\mathbf{y} := (y_\alpha)_{\alpha=0}^{S-1}$ and displacements by $\mathbf{u} := (u_\alpha)_{\alpha=0}^{s-1}$. Equivalently we can describe the kinematics of a multilattice by a pair (Y, \mathbf{p}) where $Y : \mathcal{L} \rightarrow \mathbb{R}^n$ is a deformation field and $p_0, \dots, p_{S-1} : \mathcal{L} \rightarrow \mathbb{R}^n$ are shift fields. The two descriptions are related by

$$Y(\xi) = y_0(\xi), \quad p_\alpha(\xi) = y_\alpha(\xi) - y_0(\xi); \quad \text{and} \quad y_\alpha(\xi) = Y(\xi) + p_\alpha(\xi),$$

and analogous expressions hold for displacements as well.

We now turn to a description of the energy. We will make the fundamental modeling assumption that the total potential energy of the system can be written as a sum of *site potentials*—that is,

$$\hat{\mathcal{E}}_{\text{hom}}^{\text{a}}(\mathbf{y}) := \sum_{\xi \in \mathcal{L}} \hat{V}(D\mathbf{y}(\xi)), \quad (2.2)$$

where the various new symbols introduced are specified in the following. We also note that this assumption is not restrictive as almost any reasonable classical potential such as an n -body potential, pair functional, or bond-order potential may be written in this form. The main restriction is that long-range Coulomb interaction is excluded.

We use $D\mathbf{y}(\xi)$ to denote the collection of finite differences (relative atom positions) needed to compute the energy at site ξ . More precisely, we specify a *finite* set of triples

$$\mathcal{R} \subset \mathcal{L} \times \{0, 1, \dots, S-1\} \times \{0, 1, \dots, S-1\} \setminus \bigcup_{\alpha=0}^{S-1} \{(0\alpha\alpha)\},$$

and use

$$D_{(\rho\alpha\beta)}\mathbf{y}(\xi) := y_\beta(\xi + \rho) - y_\alpha(\xi) \quad (2.3)$$

to denote the relative positions of species β at site $\xi + \rho$ and species α at site ξ . The collection of finite differences, or finite difference stencils, $D\mathbf{y}$, is then defined by

$$D\mathbf{y}(\xi) := (D_{(\rho\alpha\beta)}\mathbf{y}(\xi))_{(\rho\alpha\beta) \in \mathcal{R}}. \quad (2.4)$$

In terms of (Y, \mathbf{p}) , this notation becomes

$$D_{(\rho\alpha\beta)}(Y, \mathbf{p}) := Y(\xi + \rho) - Y(\xi) + p_\beta(\xi + \rho) - p_\alpha(\xi) \quad \text{and} \quad D(Y, \mathbf{p}) := (D_{(\rho\alpha\beta)}(Y, \mathbf{p}))_{(\rho\alpha\beta) \in \mathcal{R}}.$$

For future reference we remark that we can write

$$D_{(\rho\alpha\beta)}\mathbf{y} = D_\rho y_\beta(\xi) + p_\beta(\xi) - p_\alpha(\xi),$$

where $D_\rho f(\xi) := f(\xi + \rho) - f(\xi)$. Moreover, we define the set of lattice vectors in \mathcal{R} as

$$\mathcal{R}_1 := \{\rho \in \mathcal{L} : \exists (\rho\alpha\beta) \in \mathcal{R}\}.$$

The site potential is then a function $\hat{V} : (\mathbb{R}^n)^{\mathcal{R}} \rightarrow \mathbb{R} \cup \{+\infty\}$, where $+\infty$ allows for singularities in the potential (though we will later assume certain smoothness of the potential for convenience of the analysis).

Since the homogeneous reference configuration, \mathbf{y}^{ref} , defined by

$$\mathbf{y}_\alpha^{\text{ref}}(\xi) := \xi + p_\alpha^{\text{ref}}, \quad (2.5)$$

for constant $p_\alpha^{\text{ref}} \in \mathbb{R}^n$ yields infinite energy, (due to an infinite sum over constant values of the site potential in the reference configuration), we thus will consider an energy difference functional defined on displacements from the reference state instead of (2.2). For a displacement $\mathbf{u} \equiv (U, \mathbf{p})$ from the reference state \mathbf{y}^{ref} let

$$V(D\mathbf{u}(\xi)) = \hat{V}(D(\mathbf{y}^{\text{ref}} + \mathbf{u})(\xi)),$$

and then the associated energy difference functional is defined by

$$\mathcal{E}_{\text{hom}}^a(\mathbf{u}) := \sum_{\xi \in \mathcal{L}} V(D\mathbf{u}(\xi)) - V(0). \quad (2.6)$$

where $V(0)$ is a constant which will not affect minimization or force computations, so for simplicity, we assume without loss of generality that $V(0) = 0$. In Theorem 2 below, we recall a result of [34] that characterizes for which displacements, \mathbf{u} , $\mathcal{E}_{\text{hom}}^a(\mathbf{u})$ is well-defined.

A convenient notation for derivatives of V is the following: if $(\rho\alpha\beta), (\tau\gamma\delta) \in \mathcal{R}$ and $\mathbf{g} = (\mathbf{g}_{(\rho\alpha\beta)})_{(\rho\alpha\beta) \in \mathcal{R}} \in (\mathbb{R}^n)^{\mathcal{R}}$, we set

$$\begin{aligned} [V_{,(\rho\alpha\beta)}(\mathbf{g})]_i &:= \frac{\partial V(\mathbf{g})}{\partial \mathbf{g}_{(\rho\alpha\beta)}^i}, \quad i = 1, \dots, n, \\ V_{,(\rho\alpha\beta)}(\mathbf{g}) &:= \frac{\partial V(\mathbf{g})}{\partial \mathbf{g}_{(\rho\alpha\beta)}}, \\ [V_{,(\rho\alpha\beta)(\tau\gamma\delta)}(\mathbf{g})]_{ij} &:= \frac{\partial^2 V(\mathbf{g})}{\partial \mathbf{g}_{(\tau\gamma\delta)}^j \partial \mathbf{g}_{(\rho\alpha\beta)}^i}, \quad i, j = 1, \dots, n, \\ V_{,(\rho\alpha\beta)(\tau\gamma\delta)}(\mathbf{g}) &:= \frac{\partial^2 V(\mathbf{g})}{\partial \mathbf{g}_{(\tau\gamma\delta)} \partial \mathbf{g}_{(\rho\alpha\beta)}}, \end{aligned}$$

and note that this can be extended to derivatives of arbitrary order. Furthermore, we adopt the convention that if $(\rho\alpha\beta) \notin \mathcal{R}$, then $V_{,(\rho\alpha\beta)} = 0$.

The following standing assumptions on the interaction range and site potentials are made.

Assumption 1.

(V.1) *The interaction range, \mathcal{R} , satisfies*

*For each $\alpha \in \{0, \dots, S-1\}$, the set of vectors ρ such that $(\rho\alpha\alpha) \in \mathcal{R}$ spans \mathbb{R}^d ,
and $(0\alpha\beta) \in \mathcal{R}$ for all $\alpha \neq \beta \in \{0, \dots, S-1\}$.*

(V.2) *V is four times continuously differentiable with uniformly bounded derivatives and satisfies $V(0) = 0$ (for simplicity of notation). Since $V : (\mathbb{R}^n)^{\mathcal{R}} \rightarrow \mathbb{R}$, the statement that V has uniformly bounded derivatives means there exists M such that for any multi-index γ with $|\gamma| \leq 4$, $|\partial_\gamma V| \leq M$.*

We remark that (V.1) may always be met by enlarging the interaction range, \mathcal{R} . On the other hand, (V.2) is made for simplicity of the analysis; it can be weakened to admit interatomic potentials with typical singularities under collisions of atoms, but this would introduce several additional technicalities in our analysis.

Next, we specify the function space over which $\mathcal{E}_{\text{hom}}^a(\mathbf{u})$ is defined, which can be achieved in several equivalent ways. A convenient route is by first defining a continuous, piecewise linear interpolant of an atomistic displacement. Let \mathcal{T}_a be a simplicial decomposition of \mathcal{L} obtained as in [25]: first let $\hat{T} := \text{conv}\{0, e_1, e_2\}$ (where conv represents the convex hull of a set) be the unit triangle in $2D$ and $\hat{T}_1, \dots, \hat{T}_6$ six congruent tetrahedra in $3D$ that subdivide the unit cube (see Figure 1 in [25] for an illustration in $3D$) and then define

$$\mathcal{T}_a = \begin{cases} \{\xi + F\hat{T}, \xi - F\hat{T} : \xi \in \mathcal{L}\}, & \text{if } d = 2, \\ \{\xi + F\hat{T}_i : \xi \in \mathcal{L}, i = 1, \dots, 6\}, & \text{if } d = 3. \end{cases}$$

We will often refer to this as the atomistic triangulation or *fully refined* triangulation. As noted before, we may always enlarge the interaction range, \mathcal{R} , so we may assume without loss of generality that

if $\text{conv}\{\xi, \xi + \rho\}$ is an edge of \mathcal{T}_a , then there exist α, β such that $(\rho\alpha\beta) \in \mathcal{R}$.

Given a discrete set of displacement values $u : \mathcal{L} \rightarrow \mathbb{R}^n$, we then denote the continuous, piecewise linear interpolant of u with respect to \mathcal{T}_a by $Iu \equiv \bar{u}$. We will use both notations, Iu and \bar{u} ,

depending on which is notationally more convenient. Subsequently, we define the function space

$$\mathcal{U} := \left\{ \mathbf{u} = (u_\alpha)_{\alpha=0}^{S-1} : u_\alpha : \mathcal{L} \rightarrow \mathbb{R}^n, \|\mathbf{u}\|_a < \infty \right\}, \text{ where}$$

$$\|\mathbf{u}\|_a^2 := \sum_{\alpha=0}^{S-1} \|\nabla I u_\alpha\|_{L^2(\mathbb{R}^d)}^2 + \sum_{\alpha \neq \beta} \|I u_\alpha - I u_\beta\|_{L^2(\mathbb{R}^d)}^2.$$

Clearly, $\|\cdot\|_a$ is not a norm on \mathcal{U} since $\|\mathbf{u}\|_a = 0$ only implies that each $u_\alpha(\xi)$ is a constant independent of α . However, $\|\cdot\|_a$ is a semi-norm on \mathcal{U} and hence a true norm on the quotient space

$$\mathcal{U} := \mathcal{U}/\mathbb{R}^n := \left\{ \{(u_\alpha + C)_{\alpha=0}^{S-1} : C \in \mathbb{R}^n\} : \mathbf{u} \in \mathcal{U} \right\}.$$

Since the atomistic energy is invariant with respect to addition by constants, it is exactly this quotient space which we utilize as our function space. We also note that \mathbf{u} and (U, \mathbf{p}) are two equivalent descriptions for the displacements, and an equivalent norm on this space which will be convenient in terms of the (U, \mathbf{p}) description is

$$\|(U, \mathbf{p})\|_a := \|\nabla I U\|_{L^2(\mathbb{R}^d)}^2 + \sum_{\alpha=1}^{S-1} \|I p_\alpha\|_{L^2(\mathbb{R}^d)}^2.$$

A dense subspace of \mathcal{U} that we will use as a test function space is \mathcal{U}_0 where

$$\mathcal{U}_0 := \left\{ \mathbf{u} \in \mathcal{U} : \text{supp}(\nabla I u_0), \text{ and } \text{supp}(I u_\alpha - I u_0) \text{ are compact} \right\},$$

$$\mathcal{U}_0 := \mathcal{U}_0/\mathbb{R}^n.$$

As proven in [34], this test space is dense in \mathcal{U} .

Lemma 1. [34, Lemma A.1] *The quotient space \mathcal{U}_0 is dense in \mathcal{U} .*

2.2. Point Defect. We now introduce a framework to embed a point defect in a homogeneous multilattice. This problem has been heavily used in analyzing and comparing different AtC methods for simple lattices in [35, 25, 28, 41] as it allows for a range of non-trivial benchmark problems and serves as a first step in analyzing more complicated scenarios such as interacting defects [21]. Point defects can be thought of as zero-dimensional defects representing a change to a single site in the lattice. Common examples include vacancies, interstitials, substitutions, and in graphene, the Stone–Wales defect which we use for our numerical verification.

Our first task is to define an analog of $\mathcal{E}_{\text{hom}}^a$ for point defects, which is well-defined on the function space \mathcal{U} . We accomplish this through a site-dependent site potential, V_ξ , which must take into account the defective structure of the lattice near the defect core, which we assume to be at or near the origin. We then write the atomistic potential energy as

$$\mathcal{E}^a(\mathbf{u}) := \sum_{\xi \in \mathcal{L}} V_\xi(D\mathbf{u}(\xi)). \quad (2.7)$$

As in Assumption 1, we require certain smoothness of the site-dependent site potential in addition to homogeneity outside of a defect core.

Assumption 2.

(V.3) *There exists $R_{\text{def}} > 0$ such that $V_\xi \equiv V$ for all $|\xi| \geq R_{\text{def}}$.*

(V.4) *Each V_ξ is four times continuously differentiable with uniformly bounded derivatives.*

We now recall from [34, Theorem 2.2] that \mathcal{E}^a and $\mathcal{E}_{\text{hom}}^a$ are well-defined on \mathcal{U} ; the main idea of the proof is that both are defined on displacements having compact support, and by density of \mathcal{U}_0 in \mathcal{U} , they may be uniquely extended by continuity to all of \mathcal{U} .

Theorem 2. [34, Lemma 3.3] *Assume the reference configuration \mathbf{y}^{ref} with $y_\alpha^{\text{ref}}(\xi) = \xi + p_\alpha^{\text{ref}}$ is an equilibrium configuration of the defect free energy meaning that*

$$\sum_{\xi \in \mathcal{L}} \sum_{(\rho\alpha\beta) \in \mathcal{R}} \hat{V}_{(\rho\alpha\beta)}(D\mathbf{y}^{\text{ref}}(\xi)) \cdot D\mathbf{v}(\xi) = 0, \quad \forall \mathbf{v} \in \mathcal{U}_0. \quad (2.8)$$

Then $\mathcal{E}_{\text{hom}}^a(\mathbf{u})$ and $\mathcal{E}^a(\mathbf{u})$ may be uniquely extended to continuous functions on \mathcal{U} which are C^3 (three times continuously differentiable) on \mathcal{U} .

Remark 1. The condition (2.8) that the reference configuration be an equilibrium is equivalent to requiring the shifts are equilibrated within each cell. See [34, Lemma 9] for details. Such reference configurations are thus straightforward to generate numerically. \square

Since we will eventually be working with a finite domain on which there is no difference between the original functionals and their extensions, we make no distinction between an energy and its continuous extension.

We are now able to pose the defect equilibration problem which we wish to approximate with the BQCF method, that is, to find $\mathbf{u}^\infty \in \mathcal{U}$ such that

$$\mathbf{u}^\infty \in \arg \min_{\mathbf{u} \in \mathcal{U}} \mathcal{E}^a(\mathbf{u}), \quad (2.9)$$

where $\arg \min$ represents the set of local minima of a functional.

While Assumptions 1 and 2 can be readily weakened in various ways, the next assumption concerning existence and stability of a defect configuration minimizing \mathcal{E}^a is essential for our analysis:

Assumption 3. (Strong Stability) *There exists a solution, \mathbf{u}^∞ , to (2.9) and a constant $\gamma_a > 0$ such that*

$$\langle \delta^2 \mathcal{E}^a(\mathbf{u}^\infty) \mathbf{v}, \mathbf{v} \rangle \geq \gamma_a \|\mathbf{v}\|_a^2 \quad \forall \mathbf{v} \in \mathcal{U}_0.$$

Proving Assumption 3 turns out to be notoriously difficult; indeed the only result of this kind we are aware of is for a special case of a screw dislocation in a simple lattice [21, Remark 3.2] under anti-plane deformation. Nevertheless, we expect it to hold for *virtually all* realistic defects and realistic interatomic potentials. We also mention that it can be numerically checked *a posteriori* once the defect configuration has been computed.

A useful consequence of Assumption 3 is the following regularity result, which is proven in [34] and extends the analogous simple lattice result [17]. These decay rates will be an essential component for converting the BQCF error estimates in terms of solution regularity that are presented in Section 3 into complexity estimates that are numerically verified in Section 3.4.

Theorem 3. [34, Theorem 2.5] *For $\boldsymbol{\rho} = \rho_1 \dots \rho_k$, the defect solution $(U^\infty, \mathbf{p}^\infty)$ satisfies*

$$\begin{aligned} |D_{\boldsymbol{\rho}} U^\infty(\xi)| &\lesssim (1 + |\xi|)^{1-d-k}, \quad \text{for } 1 \leq k \leq 3, \\ |D_{\boldsymbol{\rho}} p_\alpha^\infty(\xi)| &\lesssim (1 + |\xi|)^{-d-k}, \quad \text{for } 0 \leq k \leq 2, \text{ and all } \alpha = 0, \dots, S-1. \end{aligned} \quad (2.10)$$

The implied constant is allowed to depend on the interaction range through the maximum of $|\rho|$ for $\rho \in \mathcal{R}_1$, the site potential, and γ_a .

These decay rates will be an essential component for converting the BQCF error estimates in terms of solution regularity that are presented in Section 3 into complexity estimates that are numerically verified in Section 3.4.

Since we will compare discrete atomistic configurations with continuous finite element functions, it will be useful to reformulate Theorem 3 in terms of gradients of smooth interpolants, which we define in the next lemma (see [25] for further details and the proof).

Lemma 4. *Let $u : \mathcal{L} \rightarrow \mathbb{R}^n$, then there exists a unique function $\tilde{I}u : \mathbb{R}^d \rightarrow \mathbb{R}^n$ with $\tilde{I}u \in C^{2,1}(\mathbb{R}^d)$ such that*

- (1) $\tilde{I}u$ is multiquintic in $\xi + F(0, 1)^d$ for each $\xi \in \mathcal{L}$.
- (2) Given any multiindex γ with $|\gamma| \leq 2$, the interpolant satisfies $\partial_\gamma \tilde{I}u(\xi) = D_\gamma^{\text{nn}} u(\xi)$ where D_γ^{nn} are nearest-neighbor finite difference operators,

$$D_i^{\text{nn},0} u(\xi) := u(\xi),$$

$$D_i^{\text{nn},1} u(\xi) := \frac{1}{2}(u(\xi + Fe_i) - u(\xi - Fe_i)) \quad (e_i \text{ is the } i\text{th standard basis vector}),$$

$$D_i^{\text{nn},2} u(\xi) := u(\xi + Fe_i) - 2u(\xi) + u(\xi - Fe_i),$$

$$D_\gamma^{\text{nn}} u(\xi) := D_1^{\text{nn},|\gamma_1|} \dots D_d^{\text{nn},|\gamma_d|} u(\xi).$$

We will apply \tilde{I} to both displacements and shifts using the notation

$$\tilde{I}(U, \mathbf{p}) = (\tilde{I}U, \tilde{I}\mathbf{p}) = (\tilde{U}, \tilde{\mathbf{p}}).$$

Then, combining Theorem 3 and Lemma (4) yields the following result.

Theorem 5. *The defect solution $(U^\infty, \mathbf{p}^\infty)$ satisfies*

$$\begin{aligned} |\nabla^j \tilde{I}U^\infty(x)| &\lesssim (1 + |x|)^{1-d-j}, \quad \text{for } j = 1, 2, \\ |\nabla^j \tilde{I}\mathbf{p}^\infty(x)| &\lesssim (1 + |x|)^{-d-j}, \quad \text{for } j = 0, 1, 2, \text{ and all } \alpha = 0, \dots, S-1, \end{aligned} \tag{2.11}$$

where the implied constant is again allowed to depend on the interaction range, the site potential, and γ_a .

3. BQCF METHOD FORMULATION AND MAIN RESULTS

Any AtC approximation of the defect problem (2.9) must include the following ingredients: the atomistic and continuum domains, a coarsened finite element mesh in the continuum region, a specification of the continuum model, and finally and most importantly a mechanism for coupling the atomistic and continuum components.

We define the atomistic and continuum domains for the multilattice BQCF method by making similar choices as in the BQCF method for Bravais lattices [25]. We first give an intuitive description of the domains involved, but will (re-)define them again below after introducing the *blending function*. Choose a computational domain $\Omega \subset \mathbb{R}^d$ to be a (large) polygonal domain containing the origin (the defect). Fix a “defect core” region Ω_{core} such that, if $V_\xi \not\equiv V$, then $\xi \in \Omega_{\text{core}}$. Then take Ω_a , the atomistic domain, to be a polygonal domain with $\Omega_{\text{core}} \subset \Omega_a \subset \Omega$, and set Ω_c , the continuum domain to be $\Omega_c = \Omega \setminus \Omega_{\text{core}}$. In blending methods, the atomistic and continuum domains overlap in a blending region $\Omega_b = \Omega_c \cap \Omega_a$ over which the atomistic and continuum forces will be blended.

Next, we define a finite element mesh \mathcal{T}_h over Ω with nodes \mathcal{N}_h . For now we only require that the finite element mesh is fully refined over Ω_a , that is, if $T \cap \Omega_a \neq \emptyset$, then $T \in \mathcal{T}_h$ if and only if $T \in \mathcal{T}_a$, but we will state further assumptions in Section 3.1.

The continuum model we adopt is the Cauchy–Born model [11, 9, 36], a nonlinear hyperelastic model, which is amenable to AtC couplings due to the definition of the strain energy density function in terms of the atomistic potential V ,

$$W_{\text{CB}}(\mathbf{G}, \mathbf{p}) := V\left((\mathbf{G}\rho + p_\beta - p_\alpha)_{(\rho\alpha\beta) \in \mathcal{R}}\right) \quad \text{for } \mathbf{G} \in \mathbb{R}^{n \times d} \text{ and } \mathbf{p} \in (\mathbb{R}^n)^S,$$

without resorting to any constitutive laws. We note that G here is the deformation gradient of lattice sites in a unit cell while \mathbf{p} are the displacements of shift vectors; in contrast with typical continuum treatments of multilattices, we maintain the shift vectors as degrees of freedom in the Cauchy–Born model and do not minimize them out.

For $W^{1,\infty}$ displacement fields, U , and L^∞ shift fields, \mathbf{p} , this leads to a Cauchy–Born energy functional, formally (for now) defined by

$$\mathcal{E}^c(U, \mathbf{p}) := \int_{\mathbb{R}^d} W_{\text{CB}}(\nabla U(x), \mathbf{p}(x)) dx = \int_{\mathbb{R}^d} V(\nabla(U, \mathbf{p})) dx$$

where

$$\nabla(U, \mathbf{p}) := (\nabla_{(\rho\alpha\beta)}(U, \mathbf{p}))_{(\rho\alpha\beta) \in \mathcal{R}} := (\nabla_\rho U + p_\beta - p_\alpha)_{(\rho\alpha\beta) \in \mathcal{R}}$$

is a continuum variant of the atomistic finite difference stencil

$$D(U, \mathbf{p})(x) = (D_{(\rho\alpha\beta)}(U, \mathbf{p})(x))_{(\rho\alpha\beta) \in \mathcal{R}} := (D_\rho U(x) + p_\beta(x + \rho) - p_\alpha(x))_{(\rho\alpha\beta) \in \mathcal{R}}.$$

The admissible finite element space we consider will be \mathcal{P}_1 finite elements for both the displacements and the shifts subject to homogeneous boundary conditions. However, we will again consider equivalence classes of finite element functions by taking a quotient space. Thus, we define

$$\begin{aligned} \mathcal{U}_h &:= \{u \in C^0(\Omega) : u|_T \in \mathcal{P}_1(T), \quad \forall T \in \mathcal{T}_h\}, \\ \mathcal{U}_h &:= \mathcal{U}_h / \mathbb{R}^n, \\ \mathcal{U}_{h,0} &:= \{u \in C^0(\mathbb{R}^d) : u|_T \in \mathcal{P}_1(T), \quad \forall T \in \mathcal{T}_h, u = 0 \text{ on } \mathbb{R}^d \setminus \Omega\}, \\ \mathcal{U}_{h,0} &:= \mathcal{U}_{h,0} / \mathbb{R}^n, \\ \mathcal{P}_{h,0} &:= \left\{ \mathbf{p} = (p_0, \dots, p_{S-1}) : p_0 = 0, \text{ and } p_1, \dots, p_{S-1} \in (\mathcal{U}_{h,0})^{S-1} \right\}. \end{aligned}$$

These spaces are endowed with the norm

$$\|(U, \mathbf{p})\|_{\text{ml}}^2 := \|\nabla U\|_{L^2(\mathbb{R}^d)}^2 + \sum_{\alpha=0}^{S-1} \|p_\alpha\|_{L^2(\mathbb{R}^d)}^2 = \|\nabla U\|_{L^2(\mathbb{R}^d)}^2 + \|\mathbf{p}\|_{L^2(\mathbb{R}^d)}^2,$$

where $\|\mathbf{p}\|_{L^2(\mathbb{R}^d)}^2 = \sum_{\alpha=0}^{S-1} \|p_\alpha\|_{L^2(\mathbb{R}^d)}^2$ is used for brevity. Along with the finite element space, we also introduce the standard piecewise linear finite element interpolant, I_h , defined as usual through $I_h u(\nu) = u(\nu)$ for $\nu \in \mathcal{N}_h$.

The BQCF method is defined by blending forces on each degree of freedom, $(\nu, \alpha) \in \mathcal{N}_h \times \{0, \dots, S-1\}$, where the forces are defined by a weighted average of atomistic and continuum forces:

$$\mathcal{F}_{\nu,\alpha}^{\text{bqcf}}(U, \mathbf{p}) := (1 - \varphi(\nu)) \frac{\partial \mathcal{E}^a(U, \mathbf{p})}{\partial u_\alpha(\nu)} + \varphi(\nu) \frac{\partial \mathcal{E}^c(U, \mathbf{p})}{\partial u_\alpha(\nu)}, \quad (3.1)$$

where the *blending function*, φ , satisfies $\varphi \in C^{2,1}(\mathbb{R}^d)$ with $\varphi = 0$ in Ω_{core} and $\varphi = 1$ in $\mathbb{R}^d \setminus \Omega_a$. The BQCF method then seeks to solve $\mathcal{F}_{\nu,\alpha}^{\text{bqcf}}(U, \mathbf{p}) = 0$ for all $\nu \notin \partial\Omega$. Equivalently, we can write the force balance equations in weak form using the variational operator

$$\begin{aligned} & \langle \mathcal{F}^{\text{bqcf}}(U, \mathbf{p}), (W, \mathbf{r}) \rangle \\ &:= \sum_{\nu} \sum_{\alpha} \mathcal{F}_{\nu,\alpha}^{\text{bqcf}}(U, \mathbf{p}) \cdot (W + r_{\alpha})(\nu) \\ &= \sum_{\nu} \sum_{\alpha} (1 - \varphi(\nu)) \frac{\partial \mathcal{E}^a(U, \mathbf{p})}{\partial u_{\alpha}(\nu)} \cdot (W + r_{\alpha})(\nu) + \varphi(\nu) \frac{\partial \mathcal{E}^c(U, \mathbf{p})}{\partial u_{\alpha}(\nu)} \cdot (W + r_{\alpha})(\nu) \\ &= \langle \delta \mathcal{E}^a(U, \mathbf{p}), ((1 - \varphi)W, (1 - \varphi)\mathbf{r}) \rangle \\ &\quad + \langle \delta \mathcal{E}^c(U, \mathbf{p}), (I_h(\varphi W), I_h(\varphi \mathbf{r})) \rangle, \end{aligned} \tag{3.2}$$

where the last equal sign comes from direct calculation. The BQCF approximation to the defect optimization problem (2.9) is then to *find* $(U, \mathbf{p}) \in \mathcal{U}_{h,0} \times \mathcal{P}_{h,0}$ *such that*

$$\langle \mathcal{F}^{\text{bqcf}}(U, \mathbf{p}), (W, \mathbf{r}) \rangle = 0, \quad \forall (W, \mathbf{r}) \in \mathcal{U}_{h,0} \times \mathcal{P}_{h,0}. \tag{3.3}$$

The variational formulation is preferred for the analysis while the force-based formulation (from which the name BQCF is derived) is preferred for implementation. The pointwise formulation (3.1) was essentially how the original BQCF method was proposed for Bravais lattices [6], and this was analyzed in a finite-difference framework without defects for Bravais lattices in [26, 23]. The variational formulation (3.2) was introduced in [25] for Bravais lattices, and its subsequent analysis led to one of the first complete analyses of an AtC method capable of modeling defects.

3.1. Assumptions on the Approximation Parameters. We now summarise the precise technical requirements on the approximation parameters, $\varphi, \Omega, \Omega_a, \Omega_b, \Omega_c, \mathcal{T}_h$, which will be analogous to those in [25].

We begin by summarising basic assumptions on the blending function:

- (1) $\varphi \in C^{2,1}$ and $0 \leq \varphi \leq 1$
- (2) If $V_{\xi} \not\equiv V$, then $\varphi(\xi) = 0$. This means that φ vanishes near any defect, hence the pure atomistic force is employed in those regions.
- (3) There exists $K > 0$ such that $\varphi(x) = 1$ if $|x| \geq K$. That is, φ is identically one far away from the defect.

As the second step we specify the computational domain Ω and its corresponding partition \mathcal{T}_h . First, we shall require that $\text{supp}(1 - \varphi) \subset \Omega$ always holds. To state the required properties for \mathcal{T}_h , we first precisely specify the sub-domains in terms of φ and Ω . Let

$$r_{\text{cut}} := \max\{|\rho| : (\rho\alpha\beta) \in \mathcal{R}\}$$

be an interaction cut-off radius, let r_{cell} be the radius of the smallest ball circumscribing the unit cell of \mathcal{L} , and define $r_{\text{buff}} := \max\{r_{\text{cut}}, r_{\text{cell}}\}$. Then we set

$$\begin{aligned} \Omega_a &:= \text{supp}(1 - \varphi) + B_{4r_{\text{buff}}}, & \Omega_b &:= \text{supp}(\nabla\varphi) + B_{4r_{\text{buff}}}, \\ \Omega_c &:= \text{supp}(\varphi) \cap \Omega + B_{4r_{\text{buff}}}, & \Omega_{\text{core}} &:= \Omega \setminus \Omega_c. \end{aligned}$$

The size and shape regularity of the various subdomains are parameterized in terms of inner and outer radii: for $t \in \{a, c, b, \text{core}\}$, we set

$$r_t := \sup_r \{r > 0 : B_r \subset \Omega_t \cup \Omega_{\text{core}}\}, \quad R_t := \inf_R \{R > 0 : \Omega_t \subset B_R\},$$

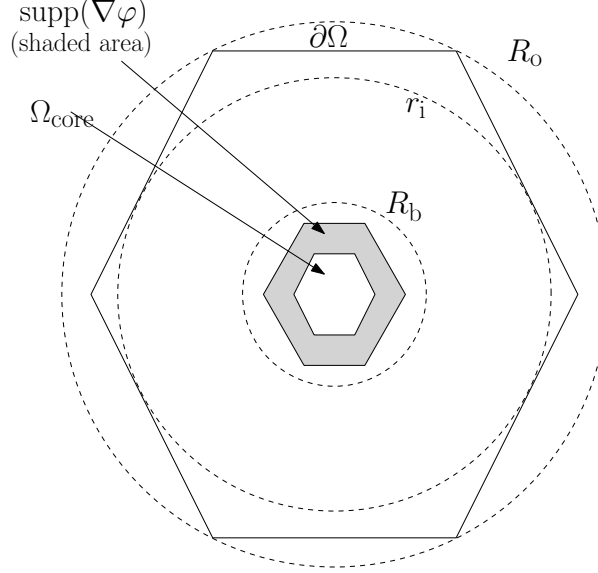


FIGURE 2. A diagram showing a selected number of domains and their inner and outer radii.

where we recall the notation B_R to denote the ball of radius R about the origin. The corresponding outer and inner radii for the complete domain Ω are, respectively, denoted by R_o and r_i :

$$r_i := \sup_r \{r > 0 : B_r \subset \Omega\}, \quad R_o := \inf_R \{R > 0 : \Omega \subset B_R\}.$$

Finally, we define an overlapping exterior domain,

$$\Omega_{\text{ext}} := \mathbb{R}^d \setminus B_{r_i/2},$$

which will be used to quantify the far-field error made by truncating to a finite computational domain.

For the sake of completeness, we now restate a crucial condition on the finite element mesh:

- (4) The finite element mesh is fully refined over Ω_a , that is, if $T \cap \Omega_a \neq \emptyset$, then $T \in \mathcal{T}_h$ if and only if $T \in \mathcal{T}_a$.

To conclude this discussion we note that only the blending function φ and the finite element mesh \mathcal{T}_h are free approximation parameters, while the subdomains and corresponding radii are derived (in particular, $\Omega = \bigcup \mathcal{T}_h$). In our analysis we will require bounds on the “shape regularity” of φ , \mathcal{T}_h , and the domains defined above:

Assumption 4. *In addition to (1)–(4) there exist constants $C_{\mathcal{T}_h}, C_\varphi > 0$, which shall be fixed throughout, such that*

$$\|\nabla^j \varphi\|_{L^\infty} \leq C_\varphi R_a^{-j} \quad \text{for } j = 1, 2, 3, \quad \text{and} \quad \max_{T \in \mathcal{T}_h} \frac{\sigma_T}{\rho_T} \leq C_{\mathcal{T}_h},$$

where σ_T denotes the radius of the smallest ball circumscribing T and ρ_T the radius of the largest ball contained in T . Defining the mesh size function

$$h(x) := \max_{\substack{T \in \mathcal{T}_h \\ x \in T}} \sigma_T,$$

there exists $s \geq 1$ such that the mesh satisfies the growth condition

$$|h(x)| \leq C_{\mathcal{T}_h} \left(\frac{|x|}{R_a} \right)^s, \quad |x| \geq R_a.$$

Moreover, there exists $C_o > 0$ and a positive integer λ such that

$$R_o \leq C_o R_{\text{core}}^\lambda \quad \text{and} \quad \frac{1}{4} R_a \leq R_{\text{core}} \leq \frac{3}{4} R_a. \quad (3.4)$$

While C_φ will feature heavily in our analysis, the parameter $C_{\mathcal{T}_h}$ will only enter implicitly in the form of constants in interpolation error estimates. The condition $\frac{1}{4} R_a \leq R_{\text{core}} \leq \frac{3}{4} R_a$ greatly simplifies the analysis. It is likely this could be weakened by an extremely refined analysis as can be done in one dimension [23], but the asymptotic estimates obtained would be unchanged with the exception of an improved prefactor so we do not pursue this. Moreover, though one can generate blending functions which satisfy these assumptions using splines, we point out that in practical implementations one can relax the regularity requirements on the blending functions, and this has provided no loss in performance in simulations carried out for lattices in [24].

3.2. Main Result. Our main result concerns the existence of a solution to (3.3) and an estimate on the error committed.

Theorem 6. *Suppose that Assumptions 1, 2, and 3 are valid. Then there exists R_{core}^* such that, for any approximation parameters satisfying Assumption 4 as well as $R_{\text{core}} \geq R_{\text{core}}^*$, there exists a solution $(U^{\text{bqcf}}, \mathbf{p}^{\text{bqcf}}) \in \mathcal{U}_{h,0} \times \mathcal{P}_{h,0}$ to the BQCF equations (3.3) that satisfies*

$$\begin{aligned} \|\nabla I U^\infty - \nabla U^{\text{bqcf}}\|_{L^2(\mathbb{R}^d)} + \|I \mathbf{p}^\infty - \mathbf{p}^{\text{bqcf}}\|_{L^2(\mathbb{R}^d)} &\lesssim \gamma_{\text{tr}} \left(\|h \nabla^2 \tilde{I} U^\infty\|_{L^2(\Omega_c)} \right. \\ &\quad \left. + \|h \nabla \tilde{I} \mathbf{p}^\infty\|_{L^2(\Omega_c)} + \|\nabla \tilde{I} U^\infty\|_{L^2(\Omega_{\text{ext}})} + \|\tilde{I} \mathbf{p}^\infty\|_{L^2(\Omega_{\text{ext}})} \right), \end{aligned} \quad (3.5)$$

where

$$\gamma_{\text{tr}} := \begin{cases} \sqrt{1 + \log(R_o/R_a)}, & \text{if } d = 2, \\ 1, & \text{if } d = 3. \end{cases}$$

The implied constant, as well as R_{core}^* , may depend on C_φ and $C_{\mathcal{T}_h}$, the interatomic potentials V, V_ξ , the maximum of $|\rho|$ for $\rho \in \mathcal{R}_1$, and the stability constant, γ_a .

Remark 2. The quantity γ_{tr} arises from a trace inequality that is needed when estimating interpolants on the atomistic mesh in terms of interpolants on the continuum mesh, c.f. [Lemma 4.6][25]. \square

Section 4 is devoted to proving Theorem 6, but before we embark on this, we first demonstrate how the error estimate can be combined with the regularity estimates of Theorem 5 to yield an optimised BQCF scheme with balanced approximation parameters. This is followed by a numerical test on a Stone–Wales defect in graphene, validating our theoretical convergence rates.

3.3. Optimal parameter choices. Once we restrict ourselves to a Cauchy–Born energy with \mathcal{P}_1 discretisation as the continuum model, the free parameters in the design of the BQCF method are the domain, Ω ; blending function, φ ; and finite element mesh, \mathcal{T}_h in the sense that once these are set according to Section 3.1, then the BQCF method (3.3) is fully formulated. Ideally, these parameters should be chosen in an optimal way so as to obtain the most efficient method.

The choice of blending function is, in the case of the BQCF method, arbitrary as long as Assumption 4 is satisfied. There are many choices to make for the blending function which meet these requirements, see e.g. [29].

The finite element mesh and hence the choice of Ω may, however, be optimized. The key to choosing the finite element mesh and size of Ω lies in applying the decay results of Theorem 5 to our error estimate (3.5), [28, 24, 29]. In obtaining our optimized parameters, we do not provide rigorous proofs but instead use heuristic assumptions to arrive at approximate choices which can then be rigorously analyzed numerically. To start, we assume that the mesh size function $h(x)$ is radial, i.e., $h(x) \equiv h(|x|)$. Then, ignoring logarithmic factors in γ_{tr} and employing the estimate $|1 + r|^{-1} \lesssim r^{-1}$ for $r \geq 1$, the error estimate (3.5) can be further estimated by

$$\begin{aligned} \|\nabla IU^\infty - \nabla U^{\text{bqcf}}\|_{L^2(\mathbb{R}^d)}^2 + \|I\mathbf{p}^\infty - \mathbf{p}^{\text{bqcf}}\|_{L^2(\mathbb{R}^d)}^2 \\ \lesssim \int_{r_{\text{core}}}^{R_c} |h(r)|^2 r^{-3-d} dr + \int_{1/2r_i}^{\infty} r^{-1-d} dr \end{aligned}$$

Next, we note that from the definitions of Ω_c, Ω , and r_i , we have $r_i = R_c + 4r_{\text{buff}}$ so that we may make the replacement $r_i \approx R_c$. Denoting the number of degrees of freedom by DoF (nodes in the continuum finite element mesh times the number of species in the multilattice), we can then carry out an optimization problem consisting of minimizing this error estimate subject to a fixed number of degrees of freedom, DoF. This problem is exactly the same as for the Bravais lattice and is

$$\min_{h \in L^2, R_c > 0} \int_{r_{\text{core}}}^{R_c} |h(r)|^2 r^{-3-d} dr + \int_{1/2R_c}^{\infty} r^{-1-d} dr.$$

This problem is solved in [32] where it is found that there are approximate minimisers of the form $h(r) = (r/R_a)^{\frac{1+d}{1+d/2}}$. A simplified approximate solution can be obtained by first minimizing $\int_{r_{\text{core}}}^{R_c} |h(r)|^2 r^{-3-d} dr$ with respect to h where the same expression for h will result, but instead of also minimizing with respect to R_c , one can simply note that the error then becomes

$$\int_{r_{\text{core}}}^{R_c} |h(r)|^2 r^{-3-d} dr + \int_{1/2R_c}^{\infty} r^{-1-d} dr \lesssim r_{\text{core}}^{-d-2} + R_c^{-d} \lesssim R_a^{-d-2} + R_c^{-d}. \quad (3.6)$$

In order to balance the sources of error, one should take $R_c = R_a^{2/d+1}$. Finally, by simply writing the number of degrees of freedom as the sum of those in the atomistic and continuum regions, it is possible to derive the result that $\#\text{DoF} \approx R_a^d$; further details can be found in [32, 33, 28, 25].

After making the estimation $\gamma_{\text{tr}} \leq (\log \text{DoF})^{1/2}$ [25] for $d = 2$, the main error estimate, (3.5), currently written in terms of solution regularity, may now be replaced by an estimate of (3.6) in terms of computational cost since $\#\text{DoF} \approx R_a^d$:

$$\begin{aligned} \|\nabla IU^\infty - \nabla U^{\text{bqcf}}\|_{L^2(\mathbb{R}^d)}^2 + \|I\mathbf{p}^\infty - \mathbf{p}^{\text{bqcf}}\|_{L^2(\mathbb{R}^d)}^2 \\ \lesssim \begin{cases} (\text{DoF})^{-1-2/d} \log \text{DoF}, & d = 2, \\ (\text{DoF})^{-1-2/d}, & d = 3, \end{cases} \end{aligned} \quad (3.7)$$

which exactly matches the rate for the Bravais lattice case [25]. This is due to the fact that the limiting factor in both error estimates is the \mathcal{P}_1 finite element approximation.

Remark 3. In the Bravais lattice analysis [25], the expression of R_c in terms of R_a is incorrect which has led to an error in the expression for the error estimate in terms of the degrees of freedom.

In that paper, a different mesh scaling is also used, but should the same mesh scaling be used, the error estimates in terms of the degrees of freedom would be identical up to a constant prefactor. \square

3.4. Numerical tests. In addition to providing a means to estimating the computational cost of the BQCF method, the estimate (3.7) is also convenient to verify numerically. We have carried this out for a Stone–Wales defect in graphene using both the BQCF method and a fully atomistic method.

For the latter we simply minimize the full atomistic energy over displacements that are non-zero only on the computational domain Ω (clamped boundary conditions). Using the methods discussed in Section 4, it is not difficult to show that the solution, $(U^{\text{Dir}}, \mathbf{p}^{\text{Dir}})$, to this atomistic Galerkin method exists and satisfies the error estimate

$$\|\nabla IU^\infty - \nabla U^{\text{Dir}}\|_{L^2(\mathbb{R}^d)} + \|I\mathbf{p}^\infty - \mathbf{p}^{\text{Dir}}\|_{L^2(\mathbb{R}^d)} \lesssim (\text{DoF})^{-1/2}. \quad (3.8)$$

We now set the model up for the Stone–Wales defect in graphene, recalling first the multilattice parameter values given in Section 2. We choose a Stillinger–Weber [50] type interatomic potential with a pair potential and bond angle potential component. The interaction range we consider is

$$\begin{aligned} \mathcal{R} = \{ & (\rho_1 00), (\rho_2 00), (-\rho_1 00), (-\rho_2 00), (\rho_1 - \rho_2 00), (\rho_2 - \rho_1 00), \\ & (001), (010), (-\rho_2 01), (\rho_2 10), (-\rho_1 01), (\rho_1 10), \\ & (\rho_1 11), (\rho_2 11), (-\rho_1 11), (-\rho_2 11), (\rho_1 - \rho_2 11), (\rho_2 - \rho_1 11) \}, \end{aligned}$$

which is depicted in Figure 1. In this notation, the site potential is given by

$$\begin{aligned} \hat{V}(D\mathbf{y}(\xi)) = & \sum_{(\rho\alpha\beta) \in \mathcal{R}} \frac{1}{2} \phi(D_{(\rho\alpha\beta)}\mathbf{y}(\xi)) + \vartheta(D_{(-\rho_1 01)}\mathbf{y}(\xi), D_{(-\rho_1 - \rho_2 01)}\mathbf{y}(\xi)) \\ & + \vartheta(D_{(-\rho_1 01)}\mathbf{y}(\xi), D_{(-\rho_2 01)}\mathbf{y}(\xi)) + \vartheta(D_{(-\rho_1 - \rho_2 01)}\mathbf{y}(\xi), D_{(-\rho_2 01)}\mathbf{y}(\xi)) \\ & + \vartheta(D_{(\rho_1 10)}\mathbf{y}(\xi), D_{(\rho_1 + \rho_2 10)}\mathbf{y}(\xi)) + \vartheta(D_{(\rho_1 10)}\mathbf{y}(\xi), D_{(\rho_2 10)}\mathbf{y}(\xi)) \\ & + \vartheta(D_{(\rho_1 + \rho_2 10)}\mathbf{y}(\xi), D_{(\rho_2 10)}\mathbf{y}(\xi)), \end{aligned}$$

where $\phi(r) = r^{-12} - 2r^{-6}$ is a pair potential term and

$$\vartheta(r_1, r_2) = \left(\frac{r_1 \cdot r_2}{|r_1| |r_2|} + 1/2 \right)^2$$

is a three-body term that penalizes angles that differ from $\frac{2\pi}{3}$.

The Stone–Wales defect shown in Figure 3 is obtained by rotating the bond between the two carbon atoms at the origin site by ninety degrees about the midpoint of this bond. One way of incorporating this defect into our framework is to define a reference configuration (Y_0, p_1) where $Y_0(\xi) = F\xi$ for all $\xi \neq 0$ with F and p_1 given by the graphene parameters in (2.1). At the origin, we set $Y_0(0) = \text{Rot}(0)$ and $p_1(0) = \text{Rot}(p_1)$, where Rot represents the ninety degree rotation about the midpoint of the segment $\text{conv}\{0, p_1\}$. Then we set $V_\xi(D(U, p)(\xi)) = \hat{V}(D(Y_0 + U, p_1 + p)(\xi))$.

We choose hexagonal domains for $\Omega_{\text{core}}, \Omega_a, \Omega$, etc., and use a blending function which approximately minimizes the L^2 norm of $\nabla^2 \varphi$ on Ω_b [29]. We select the inner width, r_{core} , of the hexagon Ω_{core} to be from the range $R_a = \{8, 12, 16, 20, 24\}$ with $\kappa = 1/2$, and then the remaining domains are chosen as scaled hexagons satisfying the requirements of Section 3 and Theorem 6 (see Figure 10 in [24] for a representative illustration of this domain decomposition for a Bravais lattice). Finally, our finite element mesh is graded radially with approximate mesh size $h(r) = \left(\frac{r}{R_a}\right)^{3/2}$ as described earlier in this section with $d = 2$. The BQCF equations were solved by a preconditioned nonlinear

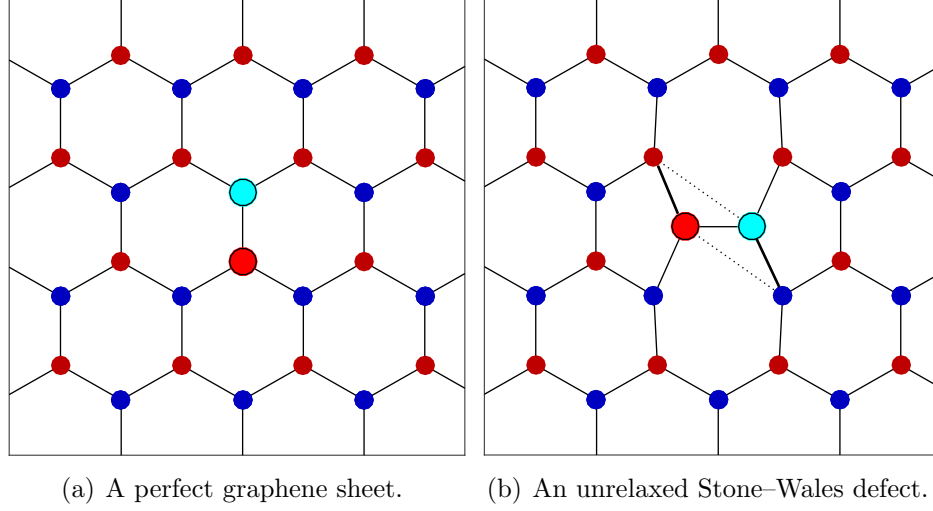
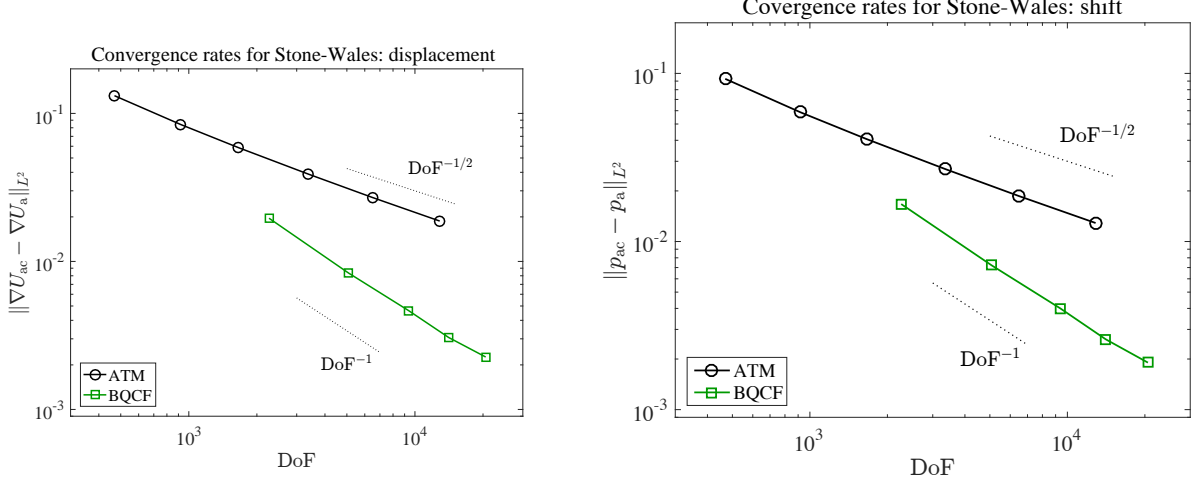


FIGURE 3. Examples of a perfect graphene sheet and a Stone–Wales defect. The dotted lines in the right display indicate bonds that are broken during the rotation of the highlighted atoms.

conjugate gradient algorithm with line-search based on force-orthogonality only (in BQCF there is no energy functional for which descent can be imposed).

In Figure 4 we show the error in the displacement gradients and the single graphene shift vector for the computed BQCF solution versus the number of degrees of freedom. Both match our theoretical predictions from (3.7) and indeed demonstrate that the error estimates are sharp (up to logarithms). We also show the error committed by the atomistic Galerkin method (which is estimated in (3.8)), to demonstrate the practical gain achieved by the BQCF method.



(a) Error in displacement field for Stone–Wales defect. (b) Error in shift field for Stone–Wales defect.

FIGURE 4. BQCF error plotted against degrees of freedom. We have also plotted the “purely atomistic” error, denoted by ATM, which is the solution obtained by truncating the infinite dimensional atomistic problem to a finite domain using homogeneous Dirichlet boundary conditions.

4. PROOFS

The remainder of this paper is devoted to proving our main result, Theorem 6. As in [25], the abstract framework for the proof is provided by the inverse function theorem [28, 37, 20], which we recall for reference and which is used to establish well-posedness of the nonlinear BQCF variational equation in Theorem 6.

Theorem 7 (Inverse Function Theorem [37, 20]). *Let X and Y be Banach spaces with $f : X \rightarrow Y$, $f \in C^1(U)$ with $U \subset X$ an open set containing x_0 . Suppose that $\eta > 0, \sigma > 0$, and $L > 0$ exist such that $\|f(x_0)\|_Y < \eta$, $\delta f(x_0)$ is invertible with $\|\delta f(x_0)^{-1}\|_{\mathcal{L}(Y,X)} < \sigma$, $B_{2\eta\sigma}(x_0) \subset U$, δf is Lipschitz continuous on $B_{2\eta\sigma}(x_0)$ with Lipschitz constant L , and $2L\eta\sigma^2 < 1$. Then there exists a C^1 inverse function $g : B_\eta(y_0) \rightarrow B_{2\eta\sigma}(x_0)$ and thus an element $\bar{x} \in X$ such that $f(\bar{x}) = 0$ and*

$$\|x_0 - \bar{x}\|_X < 2\eta\sigma.$$

The nonlinear operator we consider is the variational BQCF operator $\mathcal{F}^{\text{BQCF}}(U, \mathbf{p})$, and the point about which we linearize is $x_0 = (U_h, \mathbf{p}_h) := \Pi_h(U^\infty, \mathbf{p}^\infty)$ where Π_h is a projection operator defined in the following section. In Section 4.2 we prove a consistency estimate on the residual $\mathcal{F}^{\text{BQCF}}(U_h, \mathbf{p}_h)$:

$$\begin{aligned} \sup_{\|(W, \mathbf{r})\|_{\text{ml}}=1} |\langle \mathcal{F}^{\text{BQCF}}(U_h, \mathbf{p}_h), (W, \mathbf{r}) \rangle| &\lesssim \|h\nabla^2 \tilde{U}^\infty\|_{L^2(\Omega_c)} + \|h\nabla \tilde{\mathbf{p}}^\infty\|_{L^2(\Omega_c)} \\ &\quad + \|\nabla \tilde{U}^\infty\|_{L^2(\Omega_{\text{ext}})} + \|\tilde{\mathbf{p}}^\infty\|_{L^2(\Omega_{\text{ext}})}. \end{aligned} \tag{4.1}$$

The invertibility condition on the derivative of $\mathcal{F}^{\text{bqcf}}$ is proven as a coercivity condition in Section 4.3 where we show that

$$\langle \delta \mathcal{F}^{\text{BQCF}}(U_h, \mathbf{p}_h)(W, \mathbf{r}), (W, \mathbf{r}) \rangle \gtrsim \|(W, \mathbf{r})\|_{\text{ml}}^2, \quad \forall (W, \mathbf{r}) \in \mathcal{U}_{h,0} \times \mathcal{P}_{h,0}, \quad (4.2)$$

provided that the atomistic region is sufficiently large.

After we prove these two estimates, in Section 4.4 we combine them with a Lipschitz estimate on $\delta \mathcal{F}^{\text{bqcf}}$ and apply the inverse function theorem to prove Theorem 6.

Throughout this analysis, we continue to use the modified Vinogradov notation $x \lesssim y$, where the implied constants are allowed to depend on the shape regularity constants $C_{\mathcal{T}_h}, C_o$ (which are defined in Assumption 4 and (3.4)), the interatomic potentials (and their interaction range), and the stability constant γ_a .

4.1. Cauchy–Born Modeling Error. In preparation for the consistency analysis in Section 4.2 we first establish several auxiliary results about the Cauchy–Born model.

A central technical tool in the analysis of AtC coupling methods is the ability to compare discrete atomistic displacements which are the natural atomistic kinematic variables (recall that the atomistic displacements are equivalent to atomistic site displacements plus atomistic shift vectors), and continuous displacement and shift fields which capture the continuum kinematics. We have already introduced several interpolants which serve this task: a micro-interpolant, I ; a finite element interpolant, I_h ; and a smooth interpolant, \tilde{I} . We will also introduce a quasi-interpolant in this section which will allow us to define an analytically convenient atomistic version of stress [40].

We use $\bar{\zeta}(x)$ to denote the nodal basis function associated with the origin for the atomistic finite element mesh \mathcal{T}_a and $\bar{\zeta}_\xi(x) := \bar{\zeta}(x - \xi)$ to denote the nodal basis function at site ξ . We may then write the micro-interpolant $Iu = \bar{u}$ as

$$\bar{u}(x) = \sum_{\xi \in \mathcal{L}} u(\xi) \bar{\zeta}(x - \xi).$$

The quasi-interpolant of u is then defined by a convolution with $\bar{\zeta}$

$$u^*(x) := (\bar{\zeta} * \bar{u})(x). \quad (4.3)$$

It will later be important that this convolution operation is invertible and stable. This is a consequence of [38, Lemma 5], which we state here for reference.

Lemma 8. [38, Lemma 5] *For a given atomistic displacement, u , there exists a unique atomistic displacement \hat{u} with the property that $\bar{\zeta} * \hat{u}(\xi) = u(\xi)$ for all $\xi \in \mathcal{L}$.*

One of the primary uses of the u^* interpolant will be the development of an *atomistic stress function* which can be compared to the continuum stress in the Cauchy–Born model [40]. The first variation of the continuum model may be written in terms of a stress tensor,

$$\begin{aligned} \langle \delta \mathcal{E}^c(U, \mathbf{q}), (W, \mathbf{r}) \rangle &= \int_{\mathbb{R}^d} \sum_{(\rho\alpha\beta)} V_{(\rho\alpha\beta)}((\nabla_\tau U + q_\delta - q_\gamma)_{(\tau\gamma\delta) \in \mathbb{R}}) \cdot (\nabla_\rho W + r_\beta - r_\alpha) \\ &= \int_{\mathbb{R}^d} \sum_{(\rho\alpha\beta)} V_{(\rho\alpha\beta)}(\nabla(U, \mathbf{q})) \otimes \rho : \nabla W + \int_{\mathbb{R}^d} \sum_{(\rho\alpha\beta)} V_{(\rho\alpha\beta)}(\nabla(U, \mathbf{q}))_{(\tau\gamma\delta) \in \mathbb{R}} \cdot (r_\beta - r_\alpha) \\ &= \int_{\mathbb{R}^d} \sum_{\beta} [\mathcal{S}_d^c(U, \mathbf{q})(x)]_\beta : \nabla W + \int_{\mathbb{R}^d} \sum_{\alpha, \beta} [\mathcal{S}_s^c(U, \mathbf{q})(x)]_{\alpha\beta} (r_\beta - r_\alpha), \end{aligned} \quad (4.4)$$

where we defined

$$\begin{aligned} [S_d^c(U, \mathbf{q})(x)]_\beta &:= \sum_{\substack{\alpha, \rho: \\ (\rho\alpha\beta) \in \mathcal{R}}} V_{(\rho\alpha\beta)}(\nabla(U, \mathbf{q})(x)) \otimes \rho, \\ [S_s^c(U, \mathbf{q})(x)]_{\alpha\beta} &:= \sum_{\rho \in \mathcal{R}_1} V_{(\rho\alpha\beta)}(\nabla(U, \mathbf{q})(x)). \end{aligned} \quad (4.5)$$

To compare the atomistic and continuum models, we now construct an analogous atomistic stress tensor. Its definition will make it clear why we introduced the seemingly unnecessary sum over β in the first group in (4.4). The basic idea is to extend the construction of [40]: the argument $\nabla(U, \mathbf{q})(x)$ in (4.5) will be replaced by a local averaging of first order finite difference approximations $D(U, \mathbf{q})(\xi)$ for ξ near x .

Lemma 9. *For $(U, \mathbf{q}) \in \mathcal{U}$, define the atomistic stress tensors*

$$[S_d^a(U, \mathbf{q})(x)]_\beta := \sum_{\substack{\alpha, \rho: \\ (\rho\alpha\beta) \in \mathcal{R}}} \sum_{\xi \in \mathcal{L}} (V_{(\rho\alpha\beta)}(D(U, \mathbf{q})(\xi)) \otimes \rho) \omega_\rho(\xi - x), \quad (4.6)$$

$$[S_s^a(U, \mathbf{q})(x)]_{\alpha\beta} := \sum_{\rho \in \mathcal{R}_1} \sum_{\xi \in \mathcal{L}} V_{(\rho\alpha\beta)}(D(U, \mathbf{q})(\xi)) \omega_0(\xi - x).$$

$$\text{where} \quad \omega_\rho(x) := \int_0^1 \bar{\zeta}(x + t\rho) dt. \quad (4.7)$$

Then

$$\begin{aligned} \langle \delta \mathcal{E}_{\text{hom}}^a(U, \mathbf{q}), (W^*, \mathbf{r}^*) \rangle &= \int_{\mathbb{R}^d} \left\{ \sum_{\beta} [S_d^a(U, \mathbf{q})]_\beta : (\nabla \bar{W} + \nabla \bar{r}_\beta) \right. \\ &\quad \left. + \sum_{\alpha, \beta} [S_s^a(U, \mathbf{q})]_{\alpha\beta} \cdot (\bar{r}_\beta - \bar{r}_\alpha) \right\} dx. \end{aligned} \quad (4.8)$$

where W^* and \mathbf{r}^* are defined through (4.3).

Proof. We start by computing the first variation of $\mathcal{E}_{\text{hom}}^a(U, \mathbf{q})$ with the test pair (W^*, \mathbf{r}^*) :

$$\begin{aligned} &\langle \delta \mathcal{E}_{\text{hom}}^a(U, \mathbf{q}), (W^*, \mathbf{r}^*) \rangle \\ &= \sum_{\xi \in \mathcal{L}} \sum_{(\rho\alpha\beta) \in \mathcal{R}} V_{(\rho\alpha\beta)}(D(U, \mathbf{q})(\xi)) \cdot \left(D_\rho W^*(\xi) + D_\rho r_\beta^*(\xi) + r_\beta^*(\xi) - r_\alpha^*(\xi) \right). \end{aligned} \quad (4.9)$$

Arguing as in [40, Eq. (2.4)] we obtain

$$D_\rho W^*(\xi) + D_\rho r_\beta^*(\xi) = \int_{\mathbb{R}^d} \omega_\rho(\xi - x) (\nabla_\rho \bar{W} + \nabla_\rho \bar{r}_\beta) dx \quad \text{and} \quad (4.10)$$

$$r_\beta^*(\xi) - r_\alpha^*(\xi) = \int_{\mathbb{R}^d} \omega_0(\xi - x) (\bar{r}_\beta - \bar{r}_\alpha) dx. \quad (4.11)$$

Substituting (4.10) and (4.11) into (4.9) and recalling the definitions of the atomistic stress tensors from (4.6) yields the stated claim. \square

We refer to the error between the continuum and atomistic stress functions as the *Cauchy–Born modeling error* and quantify it in the next lemma; see [40] for an analogous result for Bravais lattices.

Lemma 10. *Assume that $U \in C^{2,1}(\mathbb{R}^d; \mathbb{R}^n)$ and $p_\alpha \in C^{1,1}(\mathbb{R}^d; \mathbb{R}^n)$ for each α . Fix $x \in \mathbb{R}^d$ and set*

$$r_{\text{cut}} = \max_{\rho \in \mathcal{R}_1} |\rho|, \quad \nu_x := B_{2r_{\text{cut}}}(0).$$

1. *If ∇U and \mathbf{p} are constant in ν_x , then*

$$[S_d^a(U, \mathbf{p})(x)]_\beta = [S_d^c(U, \mathbf{q})(x)]_\beta \quad \text{and} \quad [S_s^a(U, \mathbf{p})(x)]_{\alpha\beta} = [S_s^c(U, \mathbf{q})(x)]_{\alpha\beta}. \quad (4.12)$$

2. *In general,*

$$\begin{aligned} |[S_d^a(U, \mathbf{p})(x)]_\beta - [S_d^c(U, \mathbf{p})(x)]_\beta| &\lesssim \|\nabla^2 U\|_{L^\infty(\nu_x)} + \|\nabla \mathbf{q}\|_{L^\infty(\nu_x)}, \\ |[S_s^a(U, \mathbf{p})(x)]_{\alpha\beta} - [S_s^c(U, \mathbf{p})(x)]_{\alpha\beta}| &\lesssim \|\nabla^2 U\|_{L^\infty(\nu_x)} + \|\nabla \mathbf{q}\|_{L^\infty(\nu_x)}. \end{aligned}$$

with the implied constant depending only on the interatomic potential V .

Proof. 1. The identity (4.12) is an immediate consequence of the definitions (4.5), (4.6) and of

$$\sum_{\xi} \omega_\rho(\xi - x) = 1.$$

2. We define an auxiliary homogeneous displacement (U^h, \mathbf{q}^h) with $\nabla U^h \equiv \nabla U(x)$ and $\mathbf{q}^h \equiv \mathbf{q}(x)$. Then we have

$$[S_d^a(U, \mathbf{q})(x)]_\beta - [S_d^c(U, \mathbf{q})(x)]_\beta = [S_d^a(U, \mathbf{q})(x)]_\beta - [S_d^a(U^h, \mathbf{q}^h)(x)]_\beta.$$

Since we assumed that V is twice continuously differentiable, with globally bounded second derivatives, we obtain

$$\begin{aligned} &|[S_d^a(U, \mathbf{q})(x)]_\beta - [S_d^c(U, \mathbf{q})(x)]_\beta| = |[S_d^a(U, \mathbf{q})(x)]_\beta - [S_d^a(U^h, \mathbf{q}^h)(x)]_\beta| \\ &= \left| \sum_{\substack{\alpha, \rho: \\ (\rho\alpha\beta) \in \mathcal{R}}} \sum_{\xi \in \mathcal{L}} ([V_{(\rho\alpha\beta)}(D(U, \mathbf{q})(\xi)) - V_{(\rho\alpha\beta)}(D(U^h, \mathbf{q}^h)(\xi))] \otimes \rho) \omega_\rho(\xi - x) \right| \\ &\lesssim \sum_{\substack{\alpha, \rho: \\ (\rho\alpha\beta) \in \mathcal{R}}} \sum_{\xi \in \mathcal{L}} |D(U, \mathbf{q})(\xi) - D(U^h, \mathbf{q}^h)(\xi)| \omega_\rho(\xi - x) \\ &\lesssim \|\nabla U - \nabla U^h\|_{L^\infty(\nu_x)} + \|\mathbf{q} - \mathbf{q}^h\|_{L^\infty(\nu_x)} + \|\nabla^2 U\|_{L^\infty(\nu_x)} + \|\nabla \mathbf{q}\|_{L^\infty(\nu_x)} \\ &\lesssim \|\nabla^2 U\|_{L^\infty(\nu_x)} + \|\nabla \mathbf{q}\|_{L^\infty(\nu_x)}, \end{aligned}$$

where in obtaining the last two inequalities we have used a Taylor expansion of the finite differences and the fact that $\omega_\rho(\xi - x)$ as defined in (4.7) vanishes off of ν_x . The proof for the comparison of the “shift” stress tensors is nearly identical so is omitted. \square

With this pointwise estimate, and using the fact that \tilde{U} is piecewise polynomial, it is straightforward to deduce the following Cauchy–Born modeling error estimate over Ω_c .

Corollary 11. *For the atomistic and continuum stress tensors defined above,*

$$\begin{aligned} \|[S_d^a(\tilde{U}^\infty, \tilde{\mathbf{q}}^\infty)]_\beta - [S_d^c(\tilde{U}^\infty, \tilde{\mathbf{q}}^\infty)]_\beta\|_{L^2(\Omega_c)} &\lesssim \|\nabla^2 \tilde{U}^\infty\|_{L^2(\Omega_c)} + \|\nabla \tilde{\mathbf{q}}^\infty\|_{L^2(\Omega_c)}, \\ \|[S_s^a(\tilde{U}^\infty, \tilde{\mathbf{q}}^\infty)]_{\alpha\beta} - [S_s^c(\tilde{U}^\infty, \tilde{\mathbf{q}}^\infty)]_{\alpha\beta}\|_{L^2(\Omega_c)} &\lesssim \|\nabla^2 \tilde{U}^\infty\|_{L^2(\Omega_c)} + \|\nabla \tilde{\mathbf{q}}^\infty\|_{L^2(\Omega_c)}. \end{aligned}$$

Remark 4. The stress estimates for a multilattice are one order lower in terms of derivatives than the corresponding Bravais lattice estimates. A refined analysis shows that this estimate cannot be improved without an underlying point symmetry for the multilattice. When this symmetry is present in multilattices, it is possible to define a symmetrized Cauchy–Born energy with an improved estimate [22]. \square

4.2. Consistency. Our first task in completing the residual estimate (4.1) is to define the projection from atomistic functions to finite element functions satisfying the Dirichlet boundary conditions so we first truncate the solution to a finite domain. For that, let η be a smooth “bump function” with support in $B_1(0)$ and equal to one on $B_{3/4}(0)$. Let A_R be an “annular region” containing the support of $\nabla(I\eta(x/R))$, i.e., $A_R := B_{R+2r_{\text{buff}}}(0) \setminus B_{3/4R-2r_{\text{buff}}}(0) \supset \text{supp}(\nabla(I\eta(x/R)))$ and define the truncation operator by

$$T_R u_\alpha(x) = \eta(x/R) \left(I u_\alpha - \frac{1}{|A_R|} \int_{A_R} I u_0 dx \right).$$

Further, let S_h be the Scott–Zhang quasi-interpolation operator [42] onto the finite element mesh \mathcal{T}_h . We then define the projection operator by

$$\begin{aligned} \Pi_h u_\alpha &:= S_h(T_{r_i} u_\alpha), \quad \Pi_h \mathbf{u} := \{\Pi_h u_\alpha\}_{\alpha=0}^{S-1}, \\ \Pi_h p_\alpha &:= \Pi_h(u_\alpha - u_0), \quad \Pi_h \mathbf{p} := \{\Pi_h p_\alpha\}_{\alpha=0}^{S-1}, \quad \Pi_h(U, \mathbf{p}) := (\Pi_h U, \Pi_h \mathbf{p}). \end{aligned} \quad (4.13)$$

(Recall that r_i is the radius of the largest ball inscribed in Ω .) Note that $\nabla \Pi_h u_\alpha$ as well as

$$\Pi_h u_\alpha - \Pi_h u_\beta = S_h[\eta(x/r_i)(I u_\alpha - I u_\beta)]$$

have support contained in Ω . We also have the following approximation results.

Lemma 12. *Take $(U, \mathbf{p}) = \mathbf{u} \in \mathcal{U}$. Then*

$$\begin{aligned} \|\nabla \tilde{U} - \nabla \Pi_{h,R} U\|_{L^2(\mathbb{R}^d)} + \|\tilde{\mathbf{p}}_\alpha - \Pi_{h,R} \mathbf{p}_\alpha\|_{L^2(\mathbb{R}^d)} &\lesssim \|h \nabla^2 \tilde{U}^\infty\|_{L^2(\Omega_c)} + \|h \nabla \tilde{\mathbf{p}}^\infty\|_{L^2(\Omega_c)} \\ &\quad + \|\nabla \tilde{U}\|_{L^2(\Omega_{\text{ext}})} + \|\tilde{\mathbf{p}}\|_{L^2(\Omega_{\text{ext}})}, \\ \|\nabla \tilde{U} - \nabla \Pi_{h,R} U\|_{L^2(\Omega_c)} + \|\tilde{\mathbf{p}}_\alpha - \Pi_{h,R} \mathbf{p}_\alpha\|_{L^2(\Omega_c)} &\lesssim \|h \nabla^2 \tilde{U}^\infty\|_{L^2(\Omega_c)} + \|h \nabla \tilde{\mathbf{p}}^\infty\|_{L^2(\Omega_c)} \\ &\quad + \|\nabla \tilde{U}\|_{L^2(\Omega_{\text{ext}} \cap \Omega_c)} + \|\tilde{\mathbf{p}}\|_{L^2(\Omega_{\text{ext}} \cap \Omega_c)}. \end{aligned}$$

The proof is very similar to the proof of Lemma 1 (with only additional estimates required for the finite element interpolants) and therefore omitted. See also [35, Lemma 1.8] for similar estimates, the main difference being the usage of the Scott–Zhang interpolant which allows for L^2 interpolation bounds on H^1 functions, see [10, 42].

We can now prove the bound (4.1).

Theorem 13 (BQCF Consistency). *Define $(U_h, \mathbf{p}_h) := \Pi_h(U^\infty, \mathbf{p}^\infty)$ where $(U^\infty, \mathbf{p}^\infty)$ satisfies Assumption 3. If Assumptions 1 and 2 are valid also and if the blending function, φ , and finite element mesh, \mathcal{T}_h , satisfy the requirements of Section 3, then the BQCF consistency error is bounded by*

$$\begin{aligned} |\langle \mathcal{F}^{\text{bqcf}}(U_h, \mathbf{p}_h), (W, \mathbf{r}) \rangle| &\lesssim \gamma_{\text{tr}} \left(\|h \nabla^2 \tilde{U}\|_{L^2(\Omega_c)} + \|h \nabla \tilde{\mathbf{p}}_\alpha\|_{L^2(\Omega_c)} + \|\nabla \tilde{U}\|_{L^2(\Omega_{\text{ext}})} \right. \\ &\quad \left. + \|\tilde{\mathbf{p}}\|_{L^2(\Omega_{\text{ext}})} \right) \cdot \|(W, \mathbf{r})\|_{\text{ml}}, \quad \forall (W, \mathbf{r}) \in \mathcal{U}_{h,0} \times \mathcal{P}_{h,0}, \end{aligned}$$

and γ_{tr} is a trace inequality constant (see Lemma 4.6 in [25]) given by

$$\gamma_{\text{tr}} = \begin{cases} \sqrt{1 + \log(R_o/R_a)}, & \text{if } d = 2, \\ 1, & \text{if } d = 3. \end{cases}$$

Before beginning the proof, we make some preliminary remarks. First, we observe that, since the Scott–Zhang interpolation operator is a projection it follows that

$$D_{(\rho\alpha\beta)}U_h(\xi) = D_{(\rho\alpha\beta)}U^\infty(\xi) \quad \text{for } \xi \in \mathcal{L}^a,$$

where $\mathcal{L}^a := \mathcal{L} \cap (\text{supp}(1 - \varphi) + \mathcal{R}_1)$. Furthermore, since $\delta\mathcal{E}^a(U^\infty, \mathbf{p}^\infty) = 0$, the residual error in the BQCF variational operator is equivalent to

$$\begin{aligned} & \langle \mathcal{F}^{\text{bqcf}}(U_h, \mathbf{p}_h), (W, \mathbf{r}) \rangle - \langle \delta\mathcal{E}^a(U^\infty, \mathbf{p}^\infty), (U, \mathbf{q}) \rangle \\ &= \langle \delta\mathcal{E}^a(U^\infty, \mathbf{p}^\infty), (1 - \varphi)(W, \mathbf{r}) \rangle + \langle \delta\mathcal{E}^c(U_h, \mathbf{p}_h), (I_h(\varphi W), I_h(\varphi \mathbf{r})) \rangle \\ & \quad - \langle \delta\mathcal{E}^a(U^\infty, \mathbf{p}^\infty), (U, \mathbf{q}) \rangle, \end{aligned} \quad (4.14)$$

where $(W, \mathbf{r}) \in \mathcal{U}_{h,0} \times \mathcal{P}_{h,0}$ is an arbitrary given pair of test functions in the finite element test function space, while $(U, \mathbf{q}) \in \mathcal{U} \times \mathcal{P}$ is a test pair that we are free to choose. The obvious candidate choice is $(U, \mathbf{q}) = (W, \mathbf{r})$ in which case we would have

$$\begin{aligned} & \langle \mathcal{F}^{\text{bqcf}}(U_h, \mathbf{p}_h), (W, \mathbf{r}) \rangle - \langle \delta\mathcal{E}^a(U^\infty, \mathbf{p}^\infty), (U, \mathbf{q}) \rangle \\ &= -\langle \delta\mathcal{E}^a(U^\infty, \mathbf{p}^\infty), (\varphi)(W, \mathbf{r}) \rangle + \langle \delta\mathcal{E}^c(U_h, \mathbf{p}_h), (I_h(\varphi W), I_h(\varphi \mathbf{r})) \rangle. \end{aligned}$$

The resulting residual error is concentrated only over Ω_c due to $\nabla\varphi$ having support in Ω_c . The issue in estimating this quantity is that when we convert the atomistic residual into the atomistic-stress format, the test function appears as a piecewise linear function with respect to the atomistic mesh \mathcal{T}_a , whereas the test function is piecewise linear with respect to the graded mesh \mathcal{T}_h in the continuum portion. For this reason, we shall add correction terms to our previous candidate choice $(U, \mathbf{q}) = (W, \mathbf{r})$ via

$$U = W + (Z^* - \varphi W), \quad q_\alpha = r_\alpha + (z_\alpha^* - \varphi r_\alpha), \quad \alpha = 1, \dots, S-1, \quad (4.15)$$

where $(Z, \mathbf{z}) \in \mathcal{U} \times \mathcal{P}$ will be chosen to satisfy certain approximation estimates as stated in Lemma 14 below. The reason we use Z^* and z_α^* instead of merely Z and z_α is that we shall eventually make use of the atomistic stress representation from (4.8). The BQCF residual error from (4.14) then becomes

$$\begin{aligned} & \langle \mathcal{F}^{\text{bqcf}}(U_h, \mathbf{p}_h), (W, \mathbf{r}) \rangle - \langle \delta\mathcal{E}^a(U^\infty, \mathbf{p}^\infty), (W + (Z^* - \varphi W), \mathbf{r} + (\mathbf{z}^* - \varphi \mathbf{r})) \rangle \\ &= \langle \delta\mathcal{E}^c(U_h, \mathbf{p}_h), (I_h(\varphi W), I_h(\varphi \mathbf{r})) \rangle - \langle \delta\mathcal{E}^a(U^\infty, \mathbf{p}^\infty), (Z^*, \mathbf{z}^*) \rangle \end{aligned} \quad (4.16)$$

Moreover, since we are blending by site and using \mathcal{P}_1 elements for the shifts, we may use the same form for Z and \mathbf{z} as obtained in the simple lattice case [25] for both displacements *and* shifts.

Lemma 14. *Suppose $W \in \mathcal{U}_{h,0}$ and $\mathbf{r} \in \mathcal{P}_{h,0}$. Then for $f \in W_{\text{loc}}^{1,2}(\mathbb{R}^d)$ and for $Z_h, Z, z_{h\alpha}, z_\alpha$ as defined above,*

$$\int_{\Omega_c} f(\bar{Z} - Z_h) dx \lesssim \|\nabla f\|_{L^2(\Omega_c)} \cdot \|\nabla Z_h\|_{L^2(\Omega_c)}, \quad (4.17)$$

$$\int_{\Omega_c} f \cdot (z_{h\alpha} - \bar{z}_\alpha) dx \lesssim \|\nabla f\|_{L^2(\Omega_c)} \cdot \|z_{h\alpha}\|_{L^2(\Omega_c)} \quad (4.18)$$

$$\|Z_h - \bar{Z}\|_{L^2(\Omega_c)} \lesssim \|\nabla Z_h\|_{L^2(\Omega_c)}, \quad (4.19)$$

$$\|z_{h\alpha} - \bar{z}_\alpha\|_{L^2(\Omega_c)} \lesssim \|z_{h\alpha}\|_{L^2(\Omega_c)}, \quad (4.20)$$

$$\|\nabla Z_h\|_{L^2(\Omega_c)} \lesssim \gamma_{\text{tr}} \|\nabla W\|_{L^2(\Omega_c)}, \quad (4.21)$$

$$\|z_{h\alpha}\|_{L^2(\Omega_c)} \lesssim \|r_\alpha\|_{L^2(\Omega_c)}. \quad (4.22)$$

Proof. We begin by letting $\omega_\xi := \text{supp}(\bar{\zeta}(x - \xi))$ and $\mathcal{C} := \{\xi \in \mathcal{L} : \omega_\xi \subset \Omega_c\}$. Then we observe that Z_h and \bar{Z} are constant on any patch ω_ξ with $\xi \notin \mathcal{C}$, and furthermore $Z_h = \bar{Z}$. Intuitively, this should hold because if $\xi \notin \mathcal{C}$, then either ξ is near the defect core where $\varphi = 0$ and hence $Z_h = 0$ and $\bar{Z} = 0$; or ξ is near the exterior to the boundary of Ω where Z_h is constant. For this to rigorously hold, we need to recall the buffer, $B_{4\text{buff}}$, in the definition of Ω_c which then makes proving the statement possible. Moreover, $Z_h = \bar{Z}$ on any patch ω_ξ with $\xi \notin \mathcal{C}$ due to the normalization factor in the definition of Z . For $f \in W_{\text{loc}}^{1,2}(\mathbb{R}^d)$ we then have

$$\begin{aligned} \int_{\Omega_c} f(\bar{Z} - Z_h) dx &= \sum_{\xi \in \mathcal{L}} \int_{\omega_\xi \cap \Omega_c} f(x)(Z(\xi) - Z_h(x)) \bar{\zeta}(x - \xi) dx \\ &= \sum_{\substack{\xi \in \mathcal{L}: \\ \omega_\xi \subset \Omega_c}} \int_{\omega_\xi} f(x)(Z(\xi) - Z_h(x)) \bar{\zeta}(x - \xi) dx \quad \text{since } Z_h = Z \text{ is constant for } \xi \notin \mathcal{C} \\ &= \sum_{\xi \in \mathcal{C}} \int_{\omega_\xi} \left(f(x) - \int_{\omega_\xi} f \right) (Z(\xi) - Z_h(x)) \bar{\zeta}(x - \xi) dx \\ &\leq \sum_{\xi \in \mathcal{C}} \left\| f - \int_{\omega_\xi} f \right\|_{L^2(\omega_\xi)} \|Z(\xi) - Z_h\|_{L^2(\omega_\xi)} \\ &\lesssim \sum_{\xi \in \mathcal{C}} \|\nabla f\|_{L^2(\omega_\xi)} \|\nabla Z_h\|_{L^2(\omega_\xi)} \\ &\lesssim \|\nabla f\|_{L^2(\Omega_c)} \|\nabla Z_h\|_{L^2(\Omega_c)}. \end{aligned} \quad (4.23)$$

This proves (4.17). Proving (4.18) is analogous:

$$\int_{\Omega_c} f \cdot (z_{h\alpha} - \bar{z}_\alpha) dx \lesssim \|\nabla f\|_{L^2(\Omega_c)} \cdot \|\nabla z_{h\alpha}\|_{L^2(\Omega_c)} \lesssim \|\nabla f\|_{L^2(\Omega_c)} \cdot \|z_{h\alpha}\|_{L^2(\Omega_c)},$$

where in obtaining the final inequality we have used that for $T \in \mathcal{T}_a$,

$$\|\nabla z_h\|_{L^2(T)} \lesssim h_T \|z_h\|_{L^2(T)} \lesssim \|z_h\|_{L^2(T)}.$$

For these choices, we also have the following norm estimates (4.19) and (4.20):

$$\begin{aligned} \|Z_h - \bar{Z}\|_{L^2(\Omega_c)} &\lesssim \|\nabla Z_h\|_{L^2(\Omega_c)}, \\ \|z_{h\alpha} - \bar{z}_\alpha\|_{L^2(\Omega_c)} &\lesssim \|z_{h\alpha}\|_{L^2(\Omega_c)}. \end{aligned}$$

To obtain the first of these, we simply take $f = \bar{Z} - Z_h$ in (4.17) yielding

$$\begin{aligned} \|Z_h - \bar{Z}\|_{L^2(\Omega_c)}^2 &\lesssim \|\nabla Z_h - \nabla \bar{Z}\|_{L^2(\Omega_c)} \cdot \|\nabla Z_h\|_{L^2(\Omega_c)} \lesssim \|\nabla Z_h\|_{L^2(\Omega_c)}^2 + \|\nabla \bar{Z}\|_{L^2(\Omega_c)}^2 \\ &\lesssim \|\nabla Z_h\|_{L^2(\Omega_c)}^2 + \|\nabla Z\|_{L^2(\Omega_c)}^2 \lesssim \|\nabla Z_h\|_{L^2(\Omega_c)}^2 + \|\nabla Z_h\|_{L^2(\Omega_c)}^2, \end{aligned}$$

where we have applied Young's inequality to deduce the estimate

$$\|\nabla Z\|_{L^2(\Omega_c)}^2 = \|\nabla Z\|_{L^2(\mathbb{R}^d)}^2 = \left\| \frac{(\bar{\zeta} * \nabla Z_h)}{\int \bar{\zeta} dx} \right\|_{L^2(\mathbb{R}^d)}^2 \leq \|\nabla Z_h\|_{L^2(\mathbb{R}^d)}^2 \|\bar{\zeta}\|_{L^1(\mathbb{R}^d)}^2 \lesssim \|\nabla Z_h\|_{L^2(\Omega_c)}^2.$$

For the second of these, we simply have

$$\begin{aligned} \|z_{h\alpha} - \bar{z}_\alpha\|_{L^2(\Omega_c)} &\leq \|z_{h\alpha}\|_{L^2(\Omega_c)} + \|\bar{z}_\alpha\|_{L^2(\Omega_c)} \lesssim \|z_{h\alpha}\|_{L^2(\Omega_c)} + \|z_\alpha\|_{L^2(\Omega_c)} \\ &\lesssim \|z_{h\alpha}\|_{L^2(\Omega_c)} + \|z_{h\alpha}\|_{L^2(\Omega_c)}, \end{aligned}$$

where we have again used Young's inequality for convolutions. Next, upon recalling the definition

$$\gamma_{\text{tr}} = \begin{cases} \sqrt{1 + \log(R_o/R_a)}, & \text{if } d = 2, \\ 1, & \text{if } d = 3, \end{cases}$$

we have (4.21) and (4.22):

$$\begin{aligned} \|\nabla Z_h\|_{L^2(\Omega_c)} &\lesssim \gamma_{\text{tr}} \|\nabla W\|_{L^2(\Omega_c)}, \\ \|z_{h\alpha}\|_{L^2(\Omega_c)} &\lesssim \|r_\alpha\|_{L^2(\Omega_c)}. \end{aligned}$$

The first of these is a consequence of [25, Lemma 7]. The second is a result of $0 \leq \varphi \leq 1$:

$$\|z_{h\alpha}\|_{L^2(\Omega_c)} = \|I_h(\varphi r_\alpha)\|_{L^2(\Omega_c)} \leq \|I_h(r_\alpha)\|_{L^2(\Omega_c)} = \|r_\alpha\|_{L^2(\Omega_c)}.$$

□

We are now ready to prove Theorem 13.

Proof of Theorem 13. Since $\tilde{I}u$ interpolates u at $\xi \in \mathcal{L}$, we may replace discrete U^∞ with continuous $\tilde{I}U = \tilde{U}^\infty$ in (4.16) which leaves us with estimating

$$\begin{aligned} \langle \mathcal{F}^{\text{bqcf}}(U_h, \mathbf{p}_h), (W, \mathbf{r}) \rangle &= \langle \mathcal{F}^{\text{bqcf}}(U_h, \mathbf{p}_h), (W, \mathbf{r}) \rangle - \langle \delta \mathcal{E}^a(U^\infty, \mathbf{p}^\infty), (U, \mathbf{q}) \rangle \\ &= \langle \delta \mathcal{E}^c(U_h, \mathbf{p}_h), (I_h(\varphi W), I_h(\varphi \mathbf{r})) \rangle - \langle \delta \mathcal{E}^a(\tilde{U}^\infty, \tilde{\mathbf{p}}^\infty), (Z^*, \mathbf{z}^*) \rangle. \end{aligned} \quad (4.24)$$

Recalling that $Z_h := I_h(\varphi W)$, $\mathbf{z}_h := I_h(\varphi \mathbf{r})$, and the atomistic and continuum stress representations of (4.6) and (4.5), we split this into three terms using simple algebraic manipulations as

$$\begin{aligned} &\langle \delta \mathcal{E}^c(U_h, \mathbf{p}_h), (I_h(\varphi W), I_h(\varphi \mathbf{r})) \rangle - \langle \delta \mathcal{E}^a(\tilde{U}^\infty, \tilde{\mathbf{p}}^\infty), (Z^*, \mathbf{z}^*) \rangle \\ &\leq \left| \int_{\mathbb{R}^d} \sum_{\beta} [\mathcal{S}_d^c(U_h, \mathbf{p}_h)]_{\beta} : \nabla Z_h - [\mathcal{S}_d^a(\tilde{U}^\infty, \tilde{\mathbf{p}}^\infty)]_{\beta} : \nabla \bar{Z} \right| + \left| \int_{\mathbb{R}^d} \sum_{\alpha, \beta} [\mathcal{S}_s^c(U_h, \mathbf{p}_h)]_{\alpha\beta} \cdot (z_{h\alpha} - z_{h\beta}) \right. \\ &\quad \left. - \sum_{\alpha, \beta} [\mathcal{S}_s^a(\tilde{U}^\infty, \tilde{\mathbf{p}}^\infty)]_{\alpha\beta} \cdot (\bar{z}_\alpha - \bar{z}_\beta) \right| + \left| \int_{\mathbb{R}^d} \sum_{\beta} [\mathcal{S}_d^a(\tilde{U}^\infty, \tilde{\mathbf{p}}^\infty)]_{\beta} : \nabla \bar{z}_\beta \right| \\ &=: T_d^1 + T_s + T_d^2. \end{aligned}$$

Next, we analyze these terms separately.

Term T_d^1 : The T_d^1 term is identical to the simple lattice case after accounting for the additional approximation of the shifts. Following the ideas from the simple lattice case [25], we break down T_d^1 into three additional terms as in Section 6.4.1 of [25] (the difference being we do not consider a quadrature error), and apply the estimates of stress differences from Corollary 11 and the approximating estimates from Lemma 12 and (4.21). This produces

$$\begin{aligned} T_d^1 &\lesssim \left| \int_{\mathbb{R}^d} \sum_{\beta} \{ [S_d^c(U_h, \mathbf{p}_h)]_{\beta} - [S_d^c(\tilde{U}^{\infty}, \tilde{\mathbf{p}}^{\infty})]_{\beta} \} : \nabla Z_h \, dx \right| \\ &\quad + \left| \int_{\mathbb{R}^d} [S_d^c(\tilde{U}^{\infty}, \tilde{\mathbf{p}}^{\infty})]_{\beta} \} : (\nabla Z_h - \nabla \bar{Z}) \, dx \right| \\ &\quad + \left| \int_{\mathbb{R}^d} \sum_{\beta} \{ [S_d^c(\tilde{U}^{\infty}, \tilde{\mathbf{p}}^{\infty})]_{\beta} - [S_d^a(\tilde{U}^{\infty}, \tilde{\mathbf{p}}^{\infty})]_{\beta} \} : \nabla \bar{Z} \, dx \right| \\ &\lesssim \gamma_{\text{tr}} \left(\|h \nabla^2 \tilde{U}^{\infty}\|_{L^2(\Omega_c)} + \|h \nabla \tilde{\mathbf{p}}^{\infty}\|_{L^2(\Omega_c)} \right. \\ &\quad \left. + \|\nabla \tilde{U}^{\infty}\|_{L^2(\Omega_{\text{ext}})} + \|\tilde{\mathbf{p}}\|_{L^2(\Omega_{\text{ext}})} \right) \cdot \|\nabla W\|_{L^2(\mathbb{R}^d)}. \end{aligned}$$

Term T_s : For the shift term T_s , we have

$$\begin{aligned} T_s &\lesssim \left| \int_{\mathbb{R}^d} \sum_{\alpha, \beta} [S_s^c(U_h, \mathbf{p}_h)]_{\alpha\beta} \cdot (z_{h\alpha} - z_{h\beta}) - \sum_{\alpha, \beta} [S_s^c(\tilde{U}^{\infty}, \tilde{\mathbf{p}}^{\infty})]_{\alpha\beta} \cdot (z_{h\alpha} - z_{h\beta}) \right| \\ &\quad + \left| \int_{\mathbb{R}^d} \sum_{\alpha, \beta} [S_s^c(\tilde{U}^{\infty}, \tilde{\mathbf{p}}^{\infty})]_{\alpha\beta} \cdot (z_{h\alpha} - z_{h\beta} - (\bar{z}_{\alpha} - \bar{z}_{\beta})) \right| \\ &\quad + \left| \int_{\mathbb{R}^d} \sum_{\alpha, \beta} [S_s^c(\tilde{U}^{\infty}, \tilde{\mathbf{p}}^{\infty})]_{\alpha\beta} \cdot (\bar{z}_{\alpha} - \bar{z}_{\beta}) - \sum_{\alpha, \beta} [S_s^a(\tilde{U}^{\infty}, \tilde{\mathbf{p}}^{\infty})]_{\alpha\beta} \cdot (\bar{z}_{\alpha} - \bar{z}_{\beta}) \right| \\ &=: T_{s,1} + T_{s,2} + T_{s,3}. \end{aligned}$$

Using Lipschitz continuity of δV (in the definition of S_s^c) and the fact that \mathbf{z}_h is supported in Ω_c followed by an application of the test function estimate (4.22), we obtain

$$\begin{aligned} |T_{s,1}| &\lesssim \left(\|\nabla \Pi_h U - \nabla \tilde{U}\|_{L^2(\Omega_c)} + \|\Pi_h \mathbf{p} - \tilde{\mathbf{p}}\|_{L^2(\Omega_c)} \right) \|\mathbf{z}_h\|_{L^2(\mathbb{R}^d)} \\ &\lesssim \left(\|\nabla \Pi_h U - \nabla \tilde{U}\|_{L^2(\Omega_c)} + \|\Pi_h \mathbf{p} - \tilde{\mathbf{p}}\|_{L^2(\Omega_c)} \right) \|\mathbf{r}\|_{L^2(\mathbb{R}^d)} \end{aligned}$$

Using the stress estimate, Corollary 11, followed by the application of the test function norm estimates (4.20) and (4.22), we get

$$\begin{aligned} |T_{s,3}| &\lesssim \left(\|\nabla^2 \tilde{U}\|_{L^2(\Omega_c)} + \|\nabla \tilde{\mathbf{p}}\|_{L^2(\Omega_c)} \right) \|\bar{\mathbf{z}}\|_{L^2(\mathbb{R}^d)} \\ &\lesssim \left(\|\nabla^2 \tilde{U}\|_{L^2(\Omega_c)} + \|\nabla \tilde{\mathbf{p}}\|_{L^2(\Omega_c)} \right) \|\mathbf{r}\|_{L^2(\mathbb{R}^d)}. \end{aligned}$$

Finally, to treat $\mathbf{z}_h - \bar{\mathbf{z}}$ inside $T_{s,2}$, we use (4.18) of Lemma 14 with $f = [S_s^c(\tilde{U}^{\infty}, \tilde{\mathbf{p}}^{\infty})]_{\alpha\beta}$ followed by an application of (4.22), the chain rule, and (4.5):

$$\begin{aligned} |T_{s,2}| &\lesssim \left\| \nabla \left(S_s^c(\tilde{U}^{\infty}, \tilde{\mathbf{p}}^{\infty}) \right) \right\|_{L^2(\Omega_c)} \|\mathbf{z}_h\|_{L^2(\mathbb{R}^d)} \\ &\lesssim \|\nabla S_s^c(\tilde{U}^{\infty}, \tilde{\mathbf{p}}^{\infty}) \cdot \nabla (\nabla \tilde{U}^{\infty} + \tilde{\mathbf{p}}^{\infty})\|_{L^2(\Omega_c)} \|\mathbf{r}\|_{L^2(\mathbb{R}^d)}. \end{aligned}$$

Combining our estimates for $T_{s,1}$, $T_{s,2}$, and $T_{s,3}$ and appealing to Lemma 12 to estimate $T_{s,1}$ along with the crude estimate $h \gtrsim 1$ gives

$$|T_s| \lesssim \left(\|h \nabla^2 \tilde{U}^\infty\|_{L^2(\Omega_c)} + \|h \nabla \tilde{\mathbf{p}}^\infty\|_{L^2(\Omega_c)} + \|\nabla \tilde{U}^\infty\|_{L^2(\Omega_{\text{ext}})} + \|\tilde{\mathbf{p}}\|_{L^2(\Omega_{\text{ext}})} \right) \|\mathbf{r}\|_{L^2(\mathbb{R}^d)}.$$

Term T_d^2 : Finally, to estimate T_d^2 we split it into

$$\begin{aligned} |T_d^2| &= \left| \int_{\mathbb{R}^d} \sum_{\beta} [S_d^a(\tilde{U}^\infty, \tilde{\mathbf{p}}^\infty)]_{\beta} : \nabla \bar{z}_{\beta} \right| \\ &\lesssim \left| \int_{\mathbb{R}^d} \sum_{\beta} (S_d^c(\tilde{U}^\infty, \tilde{\mathbf{p}}^\infty)]_{\beta} - [S_d^a(\tilde{U}^\infty, \tilde{\mathbf{p}}^\infty)]_{\beta} : \nabla \bar{z}_{\beta} \right| \\ &\quad + \left| \int_{\mathbb{R}^d} \sum_{\beta} [S_d^c(\tilde{U}^\infty, \tilde{\mathbf{p}}^\infty)]_{\beta} : \nabla \bar{z}_{\beta} \right| \\ &=: T_{d,1}^2 + T_{d,2}^2. \end{aligned}$$

To estimate $T_{d,1}^2$, we note that it is similar to T_d^1 in that $\nabla_{\rho} \bar{z}_{\beta}$ is zero off Ω_c (which is due to the support of the blending function and the definition of Ω_c ; see the proof of Lemma 14 for further explanation) so we utilize the stress estimate in Corollary 11 along with the bound

$$\|\nabla \bar{z}_{\beta}\| \lesssim \|\bar{z}_{\beta}\| \lesssim \|r_{\beta}\|$$

which follows from

$$\begin{aligned} \|\bar{z}_{\beta}\| &\lesssim \|z_{h\beta}\|_{L^2(\Omega_c)} && \text{by (4.20)} \\ &\lesssim \|r_{\beta}\|_{L^2(\Omega_c)} && \text{by (4.22)}. \end{aligned}$$

This produces

$$\begin{aligned} T_{d,1}^2 &\lesssim \left(\|\nabla^2 \tilde{U}^\infty\|_{L^2(\Omega_c)} + \|\nabla \tilde{\mathbf{p}}^\infty\|_{L^2(\Omega_c)} \right) \|\nabla \bar{\mathbf{z}}\|_{L^2(\mathbb{R}^d)} \\ &\lesssim \left(\|\nabla^2 \tilde{U}^\infty\|_{L^2(\Omega_c)} + \|\nabla \tilde{\mathbf{p}}^\infty\|_{L^2(\Omega_c)} \right) \|\mathbf{r}\|_{L^2(\mathbb{R}^d)}. \end{aligned}$$

Meanwhile, we may integrate $T_{d,2}^2$ by parts and use the aforementioned fact that $\|\bar{z}_{\beta}\| \lesssim \|r_{\beta}\|$ to obtain

$$T_{d,2}^2 \lesssim \sum_{\beta} \left\| \operatorname{div} \left([S_d^c(\tilde{U}^\infty, \tilde{\mathbf{p}}^\infty)]_{\beta} \right) \right\|_{L^2(\Omega_c)} \|\mathbf{r}\|_{L^2(\mathbb{R}^d)}.$$

Applying the chain rule to $\operatorname{div} \left([S_d^c(\tilde{U}^\infty, \tilde{\mathbf{p}}^\infty)]_{\beta} \right)$ (just like for $T_{s,2}$), we get

$$\begin{aligned} |T_d^2| &\lesssim T_{d,1}^2 + T_{d,2}^2 \lesssim \left(\|\nabla^2 \tilde{U}^\infty\|_{L^2(\Omega_c)} + \|\nabla \tilde{\mathbf{p}}^\infty\|_{L^2(\Omega_c)} \right) \|\mathbf{r}\|_{L^2(\mathbb{R}^d)} \\ &\lesssim \left(\|h \nabla^2 \tilde{U}^\infty\|_{L^2(\Omega_c)} + \|h \nabla \tilde{\mathbf{p}}^\infty\|_{L^2(\Omega_c)} \right) \|\mathbf{r}\|_{L^2(\mathbb{R}^d)}. \end{aligned}$$

Combining our estimates for T_d^1 , T_s , and T_d^2 yields the stated result. \square

4.3. Stability. The second key ingredient in our proof of Theorem 6 is the stability estimate (4.2); this in turn implies a bound on the inverse of the linearised BQCF operator, which we will use in a quantitative version of the inverse function theorem to establish existence of the solution to our BQCF equations. Conceptually, the proof of stability is similar to that of the simple lattice case presented in [25].

Theorem 15 (Stability of BQCF). *Suppose that Assumptions 1, 2, and 3 hold. There exists a critical size, R_{core}^* , of the atomistic region such that, for all shape regular meshes and blending functions meeting the requirements of Section 3 and $R_{\text{core}} \geq R_{\text{core}}^*$,*

$$\frac{\gamma_a}{2} \|(W, \mathbf{r})\|_{\text{ml}}^2 \leq \langle \delta \mathcal{F}^{\text{bqcf}}(\Pi_h(U^\infty, \mathbf{p}^\infty))(W, \mathbf{r}), (W, \mathbf{r}) \rangle, \quad \forall (W, \mathbf{r}) \in \mathcal{U}_{h,0} \times \mathcal{P}_{h,0}.$$

As an intermediate step we also prove stability of the reference state.

Theorem 16 (Stability of BQCF at Reference State). *Suppose that Assumptions 1, 2, and 3 hold. There exists a critical size R_{core}^* of the atomistic region such that, for all meshes having shape regularity constant bounded below by $C_{\mathcal{T}_h}$ and blending functions meeting the requirements of Section 3 and $R_{\text{core}} \geq R_{\text{core}}^*$,*

$$\frac{3}{4} \gamma_a \|(W, \mathbf{r})\|_{\text{ml}}^2 \leq \langle \delta \mathcal{F}_{\text{hom}}^{\text{bqcf}}(0)(W, \mathbf{r}), (W, \mathbf{r}) \rangle, \quad \forall (W, \mathbf{r}) \in \mathcal{U}_{h,0} \times \mathcal{P}_{h,0}.$$

Before we present the proofs of these results in Sections 4.5 and 4.6 we apply them to complete the proof of our main result, Theorem 6.

4.4. Proof of the main result.

Proof of Theorem 6. We apply the inverse function theorem, Theorem 7, to the BQCF variational operator $\mathcal{F}^{\text{bqcf}}$ at the linearization point $\Pi_h(U^\infty, \mathbf{p}^\infty)$. The parameters η and σ defined in Theorem 7 are

$$\begin{aligned} \eta := & \gamma_{\text{tr}} \left(\|h \nabla^2 \tilde{U}\|_{L^2(\Omega_c)} + \|h \nabla \tilde{\mathbf{p}}\|_{L^2(\Omega_c)} + \|\nabla \tilde{U}\|_{L^2(\Omega_{\text{ext}})} \right. \\ & \left. + \|\tilde{\mathbf{p}}\|_{L^2(\Omega_{\text{ext}})} \right) \cdot \|(W, \mathbf{r})\|_{\text{ml}}, \quad \forall (W, \mathbf{r}) \in \mathcal{U}_{h,0} \times \mathcal{P}_{h,0}, \end{aligned}$$

which is the consistency error from Theorem (13), and

$$\sigma^{-1} := \frac{\gamma_a}{2},$$

which is the coercivity constant from Theorem (15) that exists so long as $R_{\text{core}} \geq R_{\text{core}}^*$, where R_{core}^* is furnished by Theorem (15). (The requirement $R_{\text{core}} \geq R_{\text{core}}^*$ means the domain decomposition procedure meets the requirements stated in Theorem 6.) The Lipschitz estimate on $\delta \mathcal{F}^{\text{bqcf}}$ is a direct result of the assumptions made on the site potential in Assumption 1. Applying the inverse function theorem with these parameters gives existence of $(U^{\text{bqcf}}, \mathbf{p}^{\text{bqcf}})$ and the stated error estimate, (3.5), follows from the inverse function theorem and the approximation lemma, Lemma 12. \square

The remainder of the paper is devoted to proving Theorems 15 and 16.

4.5. Stability of BQCF at defect-free reference state. We first prove Theorem 16, that is, coercivity of the homogeneous BQCF operator,

$$\begin{aligned} \langle \delta \mathcal{F}_{\text{hom}}^{\text{bqcf}}(0)(W, \mathbf{r}), (W, \mathbf{r}) \rangle &= \langle \delta^2 \mathcal{E}_{\text{hom}}^{\text{a}}(0)((1 - \varphi)W, (1 - \varphi)\mathbf{r}), (W, \mathbf{r}) \rangle \\ &\quad + \langle \delta^2 \mathcal{E}^{\text{c}}(0)(I_h(\varphi W), I_h(\varphi \mathbf{r})), (W, \mathbf{r}) \rangle. \end{aligned}$$

That is, we want to show that there exists γ_{bqcf} independent of the approximation parameters such that, for sufficiently large R_{core} ,

$$0 < \gamma_{\text{bqcf}} \|(W, \mathbf{r})\|_{\text{ml}}^2 \leq \langle \delta \mathcal{F}_{\text{hom}}^{\text{bqcf}}(0)(W, \mathbf{r}), (W, \mathbf{r}) \rangle. \quad (4.25)$$

The proof via contradiction is involved; hence we first outline and motivate the procedure and then give a number of technical results required to prove the theorem at the end of this section. The main idea is that the linearized BQCF operator consists of an atomistic second variation and a continuum second variation. Each of these can be individually shown to be coercive so intuitively, we would expect this linearized operator to be coercive for any test pair (W, \mathbf{r}) with support concentrated near the origin (in which case the blending function is zero) and for (W, \mathbf{r}) with support concentrated far from the origin (in which case the blending function would be one). Thus, we expect the only possible instabilities to occur with test pairs having some support over the blending region. Since there is no defect in the homogeneous case, any such instability should also occur for any geometric setup, i.e., we can consider the BQCF method for a sequence of growing atomistic domain sizes and should still have an unstable mode. Thus we shall consider such a sequence and then rescale this sequence so that the atomistic region in each case is contained in a ball of fixed radius about the origin and such that these unstable modes converge (in a sense to be made precise momentarily) to some continuum limit. We then consider evaluating the suitably rescaled linearized BQCF operator on this sequence and show using the aforementioned stability of the atomistic and continuum components *and* convergence of the test pairs (W, \mathbf{r}) that this leads to a contradiction. One of the main technical difficulties encountered here is that due to blending by forces, the individual atomistic/continuum components and hence the linearized BQCF operator is not a symmetric bilinear form. Thus we must take some care in converting the force-based formulation to a form suitable to using the existing coercivity estimates on the atomistic and continuum Hessians.

The negation of (4.25) is: “for all atomistic region sizes R_{a} , there exists a blending function φ and a mesh \mathcal{T}_h compatible with the assumptions of Section 3.1 (and in particular Assumption 4), as well as a test pair, (W, \mathbf{r}) with norm scaled to one, such that

$$\frac{3}{4}\gamma_{\text{a}} > \langle \delta \mathcal{F}_{\text{hom}}^{\text{bqcf}}(0)(W, \mathbf{r}), (W, \mathbf{r}) \rangle.” \quad (4.26)$$

Thus, for contradiction, suppose that there exists a sequence $R_{\text{a},n} \rightarrow \infty$ with associated meshes $\mathcal{T}_{h,n}$, blending functions φ_n , finite element spaces $\mathcal{U}_{h,0}^n \times \mathcal{P}_{h,0}^n$, and test pairs $(W_n, \mathbf{r}_n) \in \mathcal{U}_{h,0}^n \times \mathcal{P}_{h,0}^n$ with norm one such that

$$\begin{aligned} \frac{3}{4}\gamma_{\text{a}} &> \sum_{\xi \in \mathcal{L}} \sum_{(\rho\alpha\beta)} \sum_{(\tau\gamma\delta)} V_{,(\rho\alpha\beta)(\tau\gamma\delta)} : D_{(\rho\alpha\beta)}((1 - \varphi_n)W_n, (1 - \varphi_n)\mathbf{r}_n) : D_{(\rho\alpha\beta)}(W_n, \mathbf{r}_n) \\ &\quad + \int_{\mathbb{R}^d} \sum_{(\rho\alpha\beta)} \sum_{(\tau\gamma\delta)} V_{,(\rho\alpha\beta)(\tau\gamma\delta)} : \nabla_{(\rho\alpha\beta)}(I_h(\varphi_n(W_n, \mathbf{r}_n))) : \nabla_{(\rho\alpha\beta)}(W_n, \mathbf{r}_n) dx, \end{aligned} \quad (4.27)$$

where we have omitted the argument, 0, in $V_{,(\rho\alpha\beta)(\tau\gamma\delta)}(0)$ and where I_h is now the piecewise linear interpolant on $\mathcal{T}_{h,n}$.

We now rescale space in (4.26) and derive a continuum scaling limit, from which we will be able to obtain a contradiction. To that end, let $\epsilon_n = 1/R_{a,n}$, and define the set of scaled parameters

$$\begin{aligned}\hat{\xi}_n &= \epsilon_n \xi \\ \hat{x}_n &= \epsilon_n x \\ \hat{r}_n(\hat{x}_n) &= \epsilon_n^{-d/2} r_n(\hat{x}_n/\epsilon_n) \\ \hat{W}_n(\hat{x}_n) &= \epsilon_n^{1-d/2} W_n(\hat{x}_n/\epsilon_n) \\ \hat{\varphi}_n(\hat{x}_n) &= \varphi_n(\hat{x}_n/\epsilon_n).\end{aligned}\tag{4.28}$$

In terms of these rescaled quantities, we define $\hat{\nabla} := \epsilon_n^{-1} \nabla_x = \nabla_{\hat{x}_n}$ (when the subscript n is clear we use $\hat{\nabla}$) and then have

$$\begin{aligned}\|\nabla_{\hat{x}_n} \hat{W}_n\|_{L^2(\mathbb{R}^d)}^2 &= \|\nabla_x W_n\|_{L^2(\mathbb{R}^d)}^2, \quad \|\epsilon_n \nabla_{\hat{x}_n} \hat{r}_n\|_{L^2(\mathbb{R}^d)}^2 = \|\nabla_x r_n\|_{L^2(\mathbb{R}^d)}^2, \\ \|\hat{r}_n^\alpha\|_{L^2(\mathbb{R}^d)}^2 &= \|r_n^\alpha\|_{L^2(\mathbb{R}^d)}^2,\end{aligned}$$

and the rescaled BQCF operator is

$$\begin{aligned}\langle \delta \mathcal{F}_{\text{hom},n}^{\text{bqcf}}(0)(\hat{W}_n, \hat{\mathbf{r}}_n), (\hat{W}_n, \hat{\mathbf{r}}_n) \rangle &:= \\ \epsilon_n^d \sum_{\hat{\xi} \in \epsilon_n \mathcal{L}} \mathbb{C} : D_n((1 - \hat{\varphi}_n)(\hat{W}_n, \hat{\mathbf{r}}_n)) : D_n(\hat{W}_n, \hat{\mathbf{r}}_n)(\hat{\xi}) & \\ + \int_{\mathbb{R}^d} \mathbb{C} : \hat{\nabla}(I_{h,n}(\hat{\varphi}_n(\hat{W}_n, \hat{\mathbf{r}}_n))) : \hat{\nabla}(\hat{W}_n, \hat{\mathbf{r}}_n) d\hat{x}_n, &\end{aligned}\tag{4.29}$$

where $I_{h,n}$ is the piecewise linear interpolant on $\epsilon_n \mathcal{T}_{h,n}$ and

$$\begin{aligned}D_n(\hat{W}, \hat{\mathbf{r}}) &:= (D_{(\rho\alpha\beta),n}(\hat{W}, \hat{\mathbf{r}}))_{(\rho\alpha\beta) \in \mathcal{R}}, \\ D_{(\rho\alpha\beta),n}(\hat{W}, \hat{\mathbf{r}})(\hat{\xi}) &:= \frac{\hat{W}(\hat{\xi} + \epsilon_n \rho) + \epsilon_n \hat{r}_n^\beta(\hat{\xi} + \epsilon_n \rho) - \hat{W}(\hat{\xi}) - \epsilon_n \hat{r}_n^\alpha(\hat{\xi})}{\epsilon_n}.\end{aligned}$$

The rescaling of the shifts \hat{r}_n^α is one order lower than the rescaling of displacements, which is due to the fact that shifts are already discrete gradients.

We also define an interpolant onto the scaled lattice $\epsilon_n \mathcal{L}$ by I_n , a projection operator from the scaled lattice to finite element spaces $\mathcal{U}_{h,0}^n \times \mathcal{P}_{h,0}^n$ on $\mathcal{T}_{h,n}$ by $\Pi_{h,n} := S_{h,n} T_{r_{i,n}}$, and the scaled finite element basis function

$$\bar{\zeta}_n(x) := \epsilon_n^{-d} \bar{\zeta}(x/\epsilon_n).$$

Since $\hat{\nabla} \hat{W}_n$ is bounded in L^2 and since each \hat{r}_n^α is also bounded (both having norm less than one), we may extract weakly convergent subsequences. Furthermore, $\epsilon_n \hat{\nabla} \hat{r}_n^\alpha$ is also bounded in L^2 so we may take it to be weakly convergent as well. By replacing the original sequences with these weakly convergent subsequences (for notational convenience), we have $\hat{\nabla} \hat{W}_n \rightharpoonup \hat{\nabla} \hat{W}_0$, $\hat{r}_n^\alpha \rightharpoonup \hat{r}_0^\alpha$, and $\epsilon_n \hat{\nabla} \hat{r}_n^\alpha \rightharpoonup \hat{R}_0^\alpha$ in $L^2(\mathbb{R}^d)$ for some functions \hat{W}_0 , \hat{r}_0^α , and \hat{R}_0^α for each α . However, since \hat{r}_n^α is bounded in L^2 and $\epsilon_n \hat{r}_n^\alpha \rightarrow 0$ in L^2 , $\hat{R}_0^\alpha = 0$.

Next, we choose explicit equivalence representatives for \hat{W}_n ; namely, we choose \hat{W}_n such that $\int_{B_1(0)} \hat{W}_n = 0$. For this choice, we have $\|\hat{W}_n\|_{L^2(B_1(0))} \lesssim \|\hat{\nabla} \hat{W}_n\|_{L^2(B_1(0))}$, and as H^1 is compactly embedded in L^2 , there exists a strongly convergent subsequence, which we again denote by \hat{W}_n , such that $\hat{W}_n \rightarrow \hat{W}_0$ strongly in $L^2(B_1(0))$.

We also note here that $\hat{W}_n \rightharpoonup \hat{W}_0$ in the space

$$\dot{\mathbf{H}}^1(\mathbb{R}^d, \mathbb{R}^n) := \{f \in H_{\text{loc}}^1(\mathbb{R}^d, \mathbb{R}^n)/\mathbb{R}^n : \|\nabla f\|_{L^2(\mathbb{R}^d)} < \infty\},$$

and so $\hat{W}_0 \in \dot{\mathbf{H}}^1(\mathbb{R}^d, \mathbb{R}^n)$ as well [39].

The purpose of these subsequences is to use the pairs $(\hat{W}_n, \hat{\mathbf{r}}_n)$ to test with $\delta \mathcal{F}_{\text{hom},n}^{\text{bqcf}}(0)$. However, as these test pairs only consist of weakly convergent sequences and since the inner product of two weakly convergent sequences is not necessarily convergent, we further split \hat{W}_n and $\hat{\mathbf{r}}_n$ into the sum of a strongly convergent sequence and a sequence weakly convergent to zero.

This splitting is accomplished by setting

$$\hat{X}_n := \Pi_{h,n}(\eta_{j_n} * \hat{W}_0), \quad \hat{s}_n^\alpha := \Pi_{h,n}(\eta_{j_n} * \hat{r}_0^\alpha), \quad (4.30)$$

where η is a standard mollifier, $\eta_j(x) = j^{-d}\eta(x/j)$, and $j_n \rightarrow 0$ sufficiently slowly to ensure that the sequences \hat{X}_n and \hat{s}_n^α are strongly convergent to, respectively, \hat{W}_0 and \hat{r}_0^α . We will impose several further properties on the sequence j_n in Lemma 17 below, but for the remainder of the present section, we make the following conventions for notational convenience.

Remark 5. To simplify and lessen the notations hereafter, we drop the hat notation on the sequences $X_n, Z_n, \mathbf{s}_n, \mathbf{t}_n$ as well as on their derivatives, and so forth. \square

Further, we define

$$\psi_n := 1 - \varphi_n, \quad \text{and} \quad V_{,(\rho\alpha\beta)(\tau\gamma\delta)} := V_{,(\rho\alpha\beta)(\tau\gamma\delta)}(0),$$

and use the notation

$$\begin{aligned} V_{,(\rho\alpha\beta)(\tau\gamma\delta)}(\cdot) : v : w &:= w^\top [V_{,(\rho\alpha\beta)(\tau\gamma\delta)}(\cdot)] v \quad \forall v, w \in \mathbb{R}^n, \\ \mathbb{C} : D(W, \mathbf{q}) : D(Z, \mathbf{r}) &:= \sum_{(\rho\alpha\beta) \in \mathcal{R}} \sum_{(\tau\gamma\delta) \in \mathcal{R}} V_{,(\rho\alpha\beta)(\tau\gamma\delta)} : D_{(\rho\alpha\beta)}(W, \mathbf{q}) : D_{(\tau\gamma\delta)}(Z, \mathbf{r}), \\ \mathbb{C} : \nabla(W, \mathbf{q}) : \nabla(Z, \mathbf{r}) &:= \sum_{(\rho\alpha\beta) \in \mathcal{R}} \sum_{(\tau\gamma\delta) \in \mathcal{R}} V_{,(\rho\alpha\beta)(\tau\gamma\delta)} : (\nabla(W, \mathbf{q})) : (\nabla(Z, \mathbf{r})), \end{aligned}$$

where the argument of $V_{,(\rho\alpha\beta)(\tau\gamma\delta)}(\cdot)$ is omitted if evaluated at the reference state.

Lemma 17. *There exists $\psi_0 \in C^1$ is such that $\psi_n \rightarrow \psi_0$ in $C^1(B_1(0))$. Furthermore, there exists a sequence $j_n \rightarrow 0$ such that the sequences defined by X_n, \mathbf{s}_n in (4.30) and $Z_n := W_n - X_n$ and $t_n^\alpha := r_n^\alpha - s_n^\alpha$ satisfy the following convergence properties, where \rightarrow and \rightharpoonup denote respectively strong and weak $L^2(\mathbb{R}^d)$ convergence.*

$$\begin{aligned} \nabla W_n &\rightharpoonup \nabla W_0, \quad r_n^\alpha \rightharpoonup r_0^\alpha, \quad \epsilon_n \nabla r_n^\alpha \rightharpoonup 0, \quad \nabla X_n \rightarrow \nabla W_0, \quad s_n^\alpha \rightarrow r_0^\alpha, \\ \epsilon_n \nabla s_n^\alpha &\rightarrow 0, \quad \nabla Z_n \rightharpoonup 0, \quad t_n^\alpha \rightharpoonup 0, \quad \epsilon_n \nabla t_n^\alpha \rightharpoonup 0, \\ W_n &\rightarrow W_0 \text{ in } L^2(B_1(0)), \quad X_n \rightarrow W_0 \text{ in } L^2(B_1(0)), \quad Z_n \rightarrow 0 \text{ in } L^2(B_1(0)) \end{aligned} \quad (4.31)$$

Moreover, let I denote the identity and upon defining the quantities

$$\begin{aligned}
R_n^{\text{def}}(x) &:= R_n^{\text{def}}(\psi_n)(x) = \\
&\epsilon_n^d \sum_{\xi \in \epsilon_n \mathcal{L}} \sum_{\substack{(\rho\alpha\beta) \\ (\tau\gamma\delta)}} V_{(\rho\alpha\beta)(\tau\gamma\delta)}(0) D_{(\tau\gamma\delta),n}(\psi_n(X_n, s_n)) \otimes \frac{\rho}{\epsilon_n} \int_0^{\epsilon_n} \zeta_n(\xi + t\rho - x) dt, \\
R_n^{\text{shift}}(x) &:= R_n^{\text{shift}}(\psi_n)(x) = \\
&\epsilon_n^d \sum_{\xi \in \epsilon_n \mathcal{L}} \sum_{\substack{(\rho\alpha\beta) \\ (\tau\gamma\delta)}} V_{(\rho\alpha\beta)(\tau\gamma\delta)}(0) D_{(\tau\gamma\delta),n}(\psi_n X_n, \psi_n s_n) \bar{\zeta}_n(\xi - x), \\
S_n^{\text{def}}(x) &:= R_n^{\text{def}}(I)(x), \quad S_n^{\text{shift}}(x) := R_n^{\text{shift}}(I)(x) \\
S_n^{\text{inner}}(x) &:= \\
&\epsilon_n^d \sum_{\xi \in \epsilon_n \mathcal{L}} \sum_{\substack{(\rho\alpha\beta) \\ (\tau\gamma\delta)}} V_{(\rho\alpha\beta)(\tau\gamma\delta)} : D_{(\rho\alpha\beta),n}(\psi_n X_n, \psi_n s_n) : D_{(\tau\gamma\delta),n}(X_n, s_n),
\end{aligned}$$

the sequence j_n may further be chosen so that

$$\begin{aligned}
S_n^{\text{def}}(x) &\rightarrow \sum_{\substack{(\rho\alpha\beta) \\ (\tau\gamma\delta)}} V_{(\rho\alpha\beta)(\tau\gamma\delta)}(0) \nabla_{(\tau\gamma\delta)}(W_0, \mathbf{s}_0), \\
S_n^{\text{shift}}(x) &\rightarrow \sum_{\substack{(\rho\alpha\beta) \\ (\tau\gamma\delta)}} V_{(\rho\alpha\beta)(\tau\gamma\delta)}(0) \nabla_{(\tau\gamma\delta)}(W_0, \mathbf{s}_0), \\
R_n^{\text{def}}(x) &\rightarrow \sum_{\substack{(\rho\alpha\beta) \\ (\tau\gamma\delta)}} V_{(\rho\alpha\beta)(\tau\gamma\delta)}(0) \nabla_{(\tau\gamma\delta)}(\psi_0 W_0, \psi_0 \mathbf{s}_0), \\
R_n^{\text{shift}}(x) &\rightarrow \sum_{\substack{(\rho\alpha\beta) \\ (\tau\gamma\delta)}} V_{(\rho\alpha\beta)(\tau\gamma\delta)}(0) \nabla_{(\tau\gamma\delta)}(\psi_0 W_0, \psi_0 \mathbf{s}_0), \\
S_n^{\text{inner}}(x) &\rightarrow \int_{\mathbb{R}^d} \sum_{\substack{(\rho\alpha\beta) \\ (\tau\gamma\delta)}} V_{(\rho\alpha\beta)(\tau\gamma\delta)} : (\nabla_{(\rho\alpha\beta)}(\psi_0(W_0, \mathbf{s}_0))) : (\nabla_{(\tau\gamma\delta)}(W_0, \mathbf{s}_0)) dx,
\end{aligned} \tag{4.32}$$

with convergence being in $L^2(\mathbb{R}^d)$.

Proof. The key fact in proving this result is that j_n may be chosen to tend to zero sufficiently slowly such that any one of these properties holds individually, and by appropriately selecting subsequences using a diagonalization argument, they may be chosen so that all hold simultaneously. The full proof is given in the Appendix. \square

We now state a convergence result for “cross-terms” appearing in $\delta\mathcal{F}_{\text{hom},n}^{\text{bqcf}}(0)$ involving products of strongly and weakly convergent (to zero) sequences. The proof is given in the appendix.

Lemma 18. *With Z_n, X_n, \mathbf{t}_n , and \mathbf{s}_n as defined in Lemma 17,*

$$\epsilon_n^d \sum_{\xi \in \epsilon_n \mathcal{L}} \mathbb{C} : D_n(\psi_n Z_n, \psi_n \mathbf{t}_n) : D_n(X_n, \mathbf{s}_n) \rightarrow 0, \quad \text{and} \quad (4.33)$$

$$\epsilon_n^d \sum_{\xi \in \epsilon_n \mathcal{L}} \mathbb{C} : D_n(\psi_n X_n, \psi_n \mathbf{s}_n) : D_n(Z_n, \mathbf{t}_n) \rightarrow 0. \quad (4.34)$$

The next lemma manipulates the product of two weakly convergent sequences. The idea is that we may shift the blending function $\psi_n = 1 - \varphi_n$ in a way to use coercivity of the atomistic and continuum Hessians. The proof is again given in the appendix.

Lemma 19. *Let Z_n, X_n, \mathbf{t}_n , \mathbf{s}_n , $\theta_n = \sqrt{\psi_n}$, and $\theta_0 = \sqrt{\psi_0}$ be as defined above in Lemma 17. Then*

$$\begin{aligned} & \lim_{n \rightarrow \infty} \epsilon_n^d \sum_{\xi \in \epsilon_n \mathcal{L}} \mathbb{C} : D_n(\theta_n^2 Z_n, \theta_n^2 \mathbf{t}_n) : D_n(Z_n, \mathbf{t}_n) \\ &= \lim_{n \rightarrow \infty} \epsilon_n^d \sum_{\xi \in \epsilon_n \mathcal{L}} \mathbb{C} : D_n(\theta_n Z_n, \theta_n \mathbf{t}_n) : D_n(\theta_n Z_n, \theta_n \mathbf{t}_n). \end{aligned}$$

We are now positioned to prove Theorem 16.

Proof of Theorem 16, Stability of BQCF at Reference State. We use the scaling (4.29) and substitute (from Lemma 17) the quantities $W_n = Z_n + X_n$, $r_n^\alpha = t_n^\alpha + s_n^\alpha$, $\psi_n = 1 - \varphi_n$, and $\theta_n = \sqrt{1 - \varphi_n}$. We divide the proof into three steps: (1) we derive an expression for the atomistic portion of $\delta\mathcal{F}_{\text{hom},n}^{\text{bqcf}}(0)$ in the liminf as $n \rightarrow \infty$, (2) we derive an expression for the continuum component of $\delta\mathcal{F}_{\text{hom},n}^{\text{bqcf}}(0)$, and (3) we combine the results and use stability of the individual atomistic and continuum components to derive a contradiction.

Step 1: The first variation, $\delta\mathcal{F}_{\text{hom},n}^{\text{bqcf}}(0)$, computed in (4.29) is a sum of an atomistic and continuum component. The discrete, atomistic contribution is

$$\begin{aligned} & \langle \delta^2 \mathcal{E}_{\text{hom},n}^{\text{a}}(0)(1 - \varphi_n)(W_n, \mathbf{r}_n), (W_n, \mathbf{r}_n) \rangle \\ &= \epsilon_n^d \sum_{\xi \in \epsilon_n \mathcal{L}} \mathbb{C} : D_n(\theta_n^2 W_n, \theta_n^2 \mathbf{r}_n) : D_n(W_n, \mathbf{r}_n) \\ &= \epsilon_n^d \sum_{\xi \in \epsilon_n \mathcal{L}} \mathbb{C} : D_n(\theta_n^2 Z_n + \theta_n^2 X_n, \theta_n^2 \mathbf{t}_n + \theta_n^2 \mathbf{s}_n) : D_n(Z_n + X_n, \mathbf{t}_n + \mathbf{s}_n) \\ &= \epsilon_n^d \sum_{\xi \in \epsilon_n \mathcal{L}} \mathbb{C} : \left[D_n(\theta_n^2 Z_n, \theta_n^2 \mathbf{t}_n) : D_n(Z_n, \mathbf{t}_n) + D_n(\theta_n^2 Z_n, \theta_n^2 \mathbf{t}_n) : D_n(X_n, \mathbf{s}_n) \right. \\ & \quad \left. + D_n(\theta_n^2 X_n, \theta_n^2 \mathbf{s}_n) : D_n(Z_n, \mathbf{t}_n) + D_n(\theta_n^2 X_n, \theta_n^2 \mathbf{s}_n) : D_n(X_n, \mathbf{s}_n) \right]. \end{aligned} \quad (4.35)$$

This final expression consists of four different pairings of the form $D_n(\cdot, \cdot) : D_n(\cdot, \cdot)$; upon taking liminf as $n \rightarrow \infty$, we use Lemma 19 on the first pairing, Lemma 18 on the second and third

pairings, and the final convergence property of $S_n^{\text{inner}}(x)$ from Lemma 17 on the fourth pairing to arrive at the following expression for the atomistic contribution:

$$\begin{aligned} & \liminf_{n \rightarrow \infty} \langle \delta^2 \mathcal{E}_{\text{hom},n}^a(0)(1 - \varphi)(W_n, \mathbf{r}_n), (W_n, \mathbf{r}_n) \rangle \\ &= \liminf_{n \rightarrow \infty} \epsilon_n^d \sum_{\xi \in \epsilon_n \mathcal{L}} \mathbb{C} : D_n(\theta_n Z_n, \theta_n \mathbf{t}_n) : D_n(\theta_n Z_n, \theta_n \mathbf{t}_n) \\ & \quad + \int_{\mathbb{R}^d} \mathbb{C} : \nabla(\theta_0^2 W_0, \theta_0^2 \mathbf{r}_0) : \nabla(W_0, \mathbf{r}_0) dx. \end{aligned} \quad (4.36)$$

Step 2: Meanwhile, the continuum component of $\delta \mathcal{F}_{\text{hom},n}^{\text{bqcf}}(0)$ from (4.29) is

$$\langle \delta^2 \mathcal{E}^c(0) I_{h,n}(\varphi_n W_n, \varphi_n \mathbf{r}_n), (W_n, \mathbf{r}_n) \rangle = \int_{\mathbb{R}^d} \mathbb{C} : \nabla(I_{h,n}(\varphi_n W_n), I_{h,n}(\varphi_n \mathbf{r}_n)) : \nabla(W_n, \mathbf{r}_n) dx. \quad (4.37)$$

Using standard \mathcal{P}_1 -nodal interpolation error estimates and the fact that each $\nabla \varphi_n$ has support on B_1 , it is straightforward to prove that (c.f. Lemma 21)

$$\begin{aligned} & \lim_{n \rightarrow \infty} \|\nabla I_{h,n}(\varphi_n W_n) - \nabla(\varphi_n W_n)\|_{L^2(\mathbb{R}^d)} = 0, \\ & \lim_{n \rightarrow \infty} \|I_{h,n}(\varphi_n \mathbf{r}_n^\alpha) - (\varphi_n \mathbf{r}_n^\alpha)\|_{L^2(\mathbb{R}^d)} = 0. \end{aligned} \quad (4.38)$$

Thus, taking the \liminf of (4.37) and applying (4.38) we obtain

$$\liminf_{n \rightarrow \infty} \langle \delta^2 \mathcal{E}^c(0) I_{h,n}(\varphi W_n, \varphi \mathbf{r}_n), (W_n, \mathbf{r}_n) \rangle = \liminf_{n \rightarrow \infty} \int_{\mathbb{R}^d} \mathbb{C} : \nabla(\varphi_n W_n, \varphi_n \mathbf{r}_n) : \nabla(W_n, \mathbf{r}_n) dx. \quad (4.39)$$

Substituting the decomposition $(W_n, \mathbf{r}_n) := (Z_n + X_n, \mathbf{t}_n + \mathbf{s}_n)$ into (4.39) yields

$$\begin{aligned} & \liminf_{n \rightarrow \infty} \langle \delta^2 \mathcal{E}^c(0) I_{h,n}(\varphi W_n, \varphi \mathbf{r}_n), (W_n, \mathbf{r}_n) \rangle \\ &= \liminf_{n \rightarrow \infty} \int_{\mathbb{R}^d} \left[\mathbb{C} : \nabla(\varphi_n Z_n, \varphi_n \mathbf{t}_n) : \nabla(Z_n, \mathbf{t}_n) + \mathbb{C} : \nabla(\varphi_n Z_n, \varphi_n \mathbf{t}_n) : \nabla(X_n, \mathbf{s}_n) \right. \\ & \quad \left. + \mathbb{C} : \nabla(\varphi_n X_n, \varphi_n \mathbf{s}_n) : \nabla(Z_n, \mathbf{t}_n) + \mathbb{C} : \nabla(\varphi_n X_n, \varphi_n \mathbf{s}_n) : \nabla(X_n, \mathbf{s}_n) \right] dx. \end{aligned} \quad (4.40)$$

This final expression again gives four pairings just as in step one but now of the form $\nabla(\cdot, \cdot) : \nabla(\cdot, \cdot)$. The first pairing we momentarily leave alone, the second and third pairings both converge to zero by virtue of strong convergence of $\nabla X_n, \mathbf{s}_n$ and weak convergence of $\nabla Z_n, \mathbf{t}_n$ to 0 from Lemma 17, and the final pairing converges to $\nabla(\varphi_0 W_0, \varphi_0 \mathbf{r}_0) : \nabla(W_0, \mathbf{r}_0)$ again as a result of the strong convergence properties of $\nabla X_n, \mathbf{s}_n$ from Lemma 17. These facts simplify (4.40) to

$$\begin{aligned} & \liminf_{n \rightarrow \infty} \langle \delta^2 \mathcal{E}^c(0) I_{h,n}(\varphi W_n, \varphi \mathbf{r}_n), (W_n, \mathbf{r}_n) \rangle \\ &= \liminf_{n \rightarrow \infty} \int_{\mathbb{R}^d} \left[\mathbb{C} : \nabla(\varphi_n Z_n, \varphi_n \mathbf{t}_n) : \nabla(Z_n, \mathbf{t}_n) \right. \\ & \quad \left. + \mathbb{C} : \nabla(\varphi_0 W_0, \varphi_0 \mathbf{r}_0) : \nabla(W_0, \mathbf{r}_0) \right] dx. \end{aligned} \quad (4.41)$$

As in the atomistic case, our goal is again to think of φ_n as a square, $\varphi_n := \sqrt{\varphi_n}^2$ and to shift one factor of $\sqrt{\varphi_n}$ to each component of the duality pairing. Using an argument very similar to that

in the proof of Lemma 19 (which we therefore omit) we obtain

$$\begin{aligned} & \liminf_{n \rightarrow \infty} \int_{\mathbb{R}^d} \mathbb{C} : \nabla(\varphi_n Z_n, \varphi_n \mathbf{t}_n) : \nabla(Z_n, \mathbf{t}_n) \\ &= \liminf_{n \rightarrow \infty} \int_{\mathbb{R}^d} \mathbb{C} : \nabla(\sqrt{\varphi_n} Z_n, \sqrt{\varphi_n} \mathbf{t}_n) : \nabla(\sqrt{\varphi_n} Z_n, \sqrt{\varphi_n} \mathbf{t}_n). \end{aligned}$$

Inserting the last result into (4.41), we obtain

$$\begin{aligned} & \liminf_{n \rightarrow \infty} \langle \delta^2 \mathcal{E}^c(0) I_{h,n}(\varphi W_n, \varphi \mathbf{r}_n), (W_n, \mathbf{r}_n) \rangle \\ &= \liminf_{n \rightarrow \infty} \int_{\mathbb{R}^d} [\mathbb{C} : \nabla(\sqrt{\varphi_n} Z_n, \sqrt{\varphi_n} \mathbf{t}_n) : \nabla(\sqrt{\varphi_n} Z_n, \sqrt{\varphi_n} \mathbf{t}_n) + \mathbb{C} : \nabla(\varphi_0 W_0, \varphi_0 \mathbf{r}_0) : \nabla(W_0, \mathbf{r}_0)] dx. \end{aligned} \quad (4.42)$$

Step 3: Upon adding the atomistic components from (4.36) to the continuum contributions (4.42) and recalling that $\theta_0^2 = 1 - \varphi_0$, we have the following expression for $\delta \mathcal{F}_{\text{hom},n}^{\text{bqcf}}(0)$:

$$\begin{aligned} & \liminf_{n \rightarrow \infty} \langle \delta \mathcal{F}_{\text{hom},n}^{\text{bqcf}}(0)(W_n, \mathbf{r}_n), (W_n, \mathbf{r}_n) \rangle \\ &= \liminf_{n \rightarrow \infty} \int_{\mathbb{R}^d} [\mathbb{C} : \nabla(\sqrt{\varphi_n} Z_n, \sqrt{\varphi_n} \mathbf{t}_n) : \nabla(\sqrt{\varphi_n} Z_n, \sqrt{\varphi_n} \mathbf{t}_n) + \mathbb{C} : \nabla(W_0, \mathbf{r}_0) : \nabla(W_0, \mathbf{r}_0)] dx \\ & \quad + \liminf_{n \rightarrow \infty} \epsilon_n^d \sum_{\xi \in \epsilon_n \mathcal{L}} \mathbb{C} : D_n(\sqrt{1 - \varphi_n} Z_n, \sqrt{1 - \varphi_n} \mathbf{t}_n) : D_n(\sqrt{1 - \varphi_n} Z_n, \sqrt{1 - \varphi_n} \mathbf{t}_n) \end{aligned} \quad (4.43)$$

Next, using stability of the homogeneous atomistic model in this scaling,

$$\langle \delta^2 \mathcal{E}_{\text{hom},n}^a(0)(W_n, \mathbf{r}_n), (W_n, \mathbf{r}_n) \rangle \geq \gamma_a \|(W_n, \mathbf{r}_n)\|_a^2,$$

(which can easily be proven (c.f. [34, 17]) due to Assumption 3) and the fact that atomistic stability implies Cauchy–Born Stability [34, Theorem 3.6], that is,

$$\langle \delta^2 \mathcal{E}^c(0)(W_n, \mathbf{r}_n), (W_n, \mathbf{r}_n) \rangle \geq \gamma_a \|(W, \mathbf{r})\|_{\text{ml}}^2,$$

we hence have from (4.43) that

$$\begin{aligned} & \liminf_{n \rightarrow \infty} \langle \delta \mathcal{F}_{\text{hom},n}^{\text{bqcf}}(0)(W_n, \mathbf{r}_n), (W_n, \mathbf{r}_n) \rangle \\ &= \liminf_{n \rightarrow \infty} [\langle \delta^2 \mathcal{E}^c(\sqrt{\varphi_n} Z_n, \sqrt{\varphi_n} \mathbf{t}_n), (\sqrt{\varphi_n} Z_n, \sqrt{\varphi_n} \mathbf{t}_n) \rangle + \langle \delta^2 \mathcal{E}^c(W_0, \mathbf{r}_0), (W_0, \mathbf{r}_0) \rangle \\ & \quad + \langle \delta^2 \mathcal{E}_{\text{hom},n}^a(\sqrt{1 - \varphi_n} Z_n, \sqrt{1 - \varphi_n} \mathbf{t}_n), (\sqrt{1 - \varphi_n} Z_n, \sqrt{1 - \varphi_n} \mathbf{t}_n) \rangle] \\ &\geq \liminf_{n \rightarrow \infty} \gamma_a \left[\|\nabla(\sqrt{\varphi_n} Z_n)\|_{L^2(\mathbb{R}^d)}^2 + \|\sqrt{\varphi_n} \mathbf{t}_n\|_{L^2(\mathbb{R}^d)}^2 + \|\nabla W_0\|_{L^2(\mathbb{R}^d)}^2 + \|\mathbf{r}_0\|_{L^2(\mathbb{R}^d)}^2 \right. \\ & \quad \left. + \|\nabla I_n(\sqrt{1 - \varphi_n} Z_n)\|_{L^2(\mathbb{R}^d)}^2 + \|I_n(\sqrt{1 - \varphi_n} \mathbf{t}_n)\|_{L^2(\mathbb{R}^d)}^2 \right]. \end{aligned} \quad (4.44)$$

Similar to (4.38) (c.f. Lemma 21), standard nodal interpolation error estimates imply that

$$\begin{aligned} & \lim_{n \rightarrow \infty} \|\nabla I_n(\sqrt{1 - \varphi_n} Z_n) - \nabla(\sqrt{1 - \varphi_n} Z_n)\|_{L^2(\mathbb{R}^d)} = 0, \quad \text{and} \\ & \lim_{n \rightarrow \infty} \|I_n(\sqrt{1 - \varphi_n} \mathbf{t}_n) - (\sqrt{1 - \varphi_n} \mathbf{t}_n)\|_{L^2(\mathbb{R}^d)} = 0. \end{aligned}$$

Thus, (4.44) becomes

$$\begin{aligned}
& \liminf_{n \rightarrow \infty} \langle \delta \mathcal{F}_{\text{hom},n}^{\text{bqcf}}(0)(W_n, \mathbf{r}_n), (W_n, \mathbf{r}_n) \rangle \\
& \geq \liminf_{n \rightarrow \infty} \gamma_a \left[\|\nabla(\sqrt{\varphi_n} Z_n)\|_{L^2(\mathbb{R}^d)}^2 + \|\sqrt{\varphi_n} \mathbf{t}_n\|_{L^2(\mathbb{R}^d)}^2 + \|\nabla W_0\|_{L^2(\mathbb{R}^d)}^2 + \|\mathbf{r}_0\|_{L^2(\mathbb{R}^d)}^2 \right. \\
& \quad \left. + \|\nabla(\sqrt{1-\varphi_n} Z_n)\|_{L^2(\mathbb{R}^d)}^2 + \|\sqrt{1-\varphi_n} \mathbf{t}_n\|_{L^2(\mathbb{R}^d)}^2 \right] \\
& = \liminf_{n \rightarrow \infty} \gamma_a \left[\|\nabla(\sqrt{\varphi_n} Z_n)\|_{L^2(\mathbb{R}^d)}^2 + \|\nabla(\sqrt{1-\varphi_n} Z_n)\|_{L^2(\mathbb{R}^d)}^2 + \|\mathbf{t}_n\|_{L^2(\mathbb{R}^d)}^2 \right. \\
& \quad \left. + \|\nabla W_0\|_{L^2(\mathbb{R}^d)}^2 + \|\mathbf{r}_0\|_{L^2(\mathbb{R}^d)}^2 \right].
\end{aligned} \tag{4.45}$$

Next observe

$$\begin{aligned}
& \|\nabla(\sqrt{\varphi_n} Z_n)\|_{L^2(\mathbb{R}^d)}^2 + \|\nabla(\sqrt{1-\varphi_n} Z_n)\|_{L^2(\mathbb{R}^d)}^2 \\
& = \int \left[|\nabla(\sqrt{\varphi_n}) \otimes Z_n + \sqrt{\varphi_n} \nabla Z_n|^2 + |\nabla(\sqrt{1-\varphi_n}) \otimes Z_n + \sqrt{1-\varphi_n} \nabla Z_n|^2 \right] dx \\
& = \int \left[2\nabla(\sqrt{\varphi_n}) \otimes Z_n : \sqrt{\varphi_n} \nabla Z_n + |\nabla(\sqrt{\varphi_n}) \otimes Z_n|^2 + \varphi_n |\nabla Z_n|^2 \right] dx \\
& \quad + \int \left[2\nabla(\sqrt{1-\varphi_n}) \otimes Z_n : \sqrt{1-\varphi_n} \nabla Z_n + |\nabla(\sqrt{1-\varphi_n}) \otimes Z_n|^2 + (1-\varphi_n) |\nabla Z_n|^2 \right] dx.
\end{aligned} \tag{4.46}$$

Since Z_n converges strongly to zero in $L^2(\text{supp}(\nabla(\sqrt{1-\varphi_n})))$ by Lemma 17 ($\text{supp}(\nabla(\sqrt{1-\varphi_n})) \subset B_1(0)$), it follows from (4.46) that

$$\liminf_{n \rightarrow \infty} \|\nabla(\sqrt{\varphi_n} Z_n)\|_{L^2(\mathbb{R}^d)}^2 + \|\nabla(\sqrt{1-\varphi_n} Z_n)\|_{L^2(\mathbb{R}^d)}^2 = \liminf_{n \rightarrow \infty} \|\nabla Z_n\|_{L^2(\mathbb{R}^d)}^2. \tag{4.47}$$

Substituting (4.47) into (4.45) produces

$$\begin{aligned}
& \liminf_{n \rightarrow \infty} \langle \delta \mathcal{F}_{\text{hom},n}^{\text{bqcf}}(0)(W_n, \mathbf{r}_n), (W_n, \mathbf{r}_n) \rangle \\
& \geq \liminf_{n \rightarrow \infty} \gamma_a \left[\|\nabla Z_n\|_{L^2(\mathbb{R}^d)}^2 + \|\mathbf{t}_n\|_{L^2(\mathbb{R}^d)}^2 + \|\nabla W_0\|_{L^2(\mathbb{R}^d)}^2 + \|\mathbf{r}_0\|_{L^2(\mathbb{R}^d)}^2 \right] \\
& \geq \liminf_{n \rightarrow \infty} \gamma_a \left[\|\nabla Z_n\|_{L^2(\mathbb{R}^d)}^2 + \|\mathbf{t}_n\|_{L^2(\mathbb{R}^d)}^2 + \|\nabla X_n\|_{L^2(\mathbb{R}^d)}^2 + \|\mathbf{s}_n\|_{L^2(\mathbb{R}^d)}^2 \right] \\
& = \liminf_{n \rightarrow \infty} \gamma_a \left[\|\nabla W_n\|_{L^2(\mathbb{R}^d)}^2 + \|\mathbf{r}_n\|_{L^2(\mathbb{R}^d)}^2 \right] = \gamma_a,
\end{aligned} \tag{4.48}$$

which contradicts our assumption in (4.27). \square

4.6. Reference Stability Implies Defect Stability. Having established stability of the homogeneous BQCF operator we obtain stability of $\delta \mathcal{F}^{\text{bqcf}}(\Pi_{h,n}(U^\infty, \mathbf{p}^\infty))$, i.e. Theorem 15, as a relatively straightforward consequence. Before entering into the proof we remark that we now no longer employ the rescalings of Section 4.5. The basic idea of the proof is that the linearized homogeneous BQCF operator and linearized BQCF operator agree for any (W, \mathbf{r}) which is zero in a large enough neighborhood about the origin. Thus, to prove stability of the true linearized BQCF operator, we again consider the possibility of a sequence, (W_n, \mathbf{r}_n) , of unstable modes whose support is contained in larger and larger balls about the origin. We will then split each (W_n, \mathbf{r}_n) into components concentrated near the origin (where we can use atomistic stability) and correction terms supported far from the origin where we use stability of the linearized homogeneous operator. As before, the main difficulty is converting the atomistic component of the BQCF operator to a form where we may utilize atomistic coercivity.

Proof of Theorem 15. We prove this result by contradiction as well. Therefore suppose, as in the proof of Theorem 16, that there exists $R_{a,n} \rightarrow \infty$ with associated meshes $\mathcal{T}_{h,n}$, blending functions φ_n , and test pairs $(W_n, \mathbf{r}_n) \in \mathcal{U}_{h,0}^n \times \mathcal{P}_{h,0}^n$ with norm scaled to one, such that

$$\begin{aligned} \frac{\gamma_a}{2} &> \sum_{\xi \in \mathcal{L}} \sum_{(\rho\alpha\beta)} \sum_{(\tau\gamma\delta)} V_{(\rho\alpha\beta)(\tau\gamma\delta)}(D\mathbf{U}_n) : D_{(\rho\alpha\beta)}((1 - \hat{\varphi}_n)\hat{W}_n, (1 - \hat{\varphi}_n)\hat{\mathbf{r}}_n) : D_{(\rho\alpha\beta)}(\hat{W}_n, \hat{\mathbf{r}}_n) \\ &\quad + \int_{\mathbb{R}^d} \sum_{(\rho\alpha\beta)} \sum_{(\tau\gamma\delta)} V_{(\rho\alpha\beta)(\tau\gamma\delta)}(\nabla\mathbf{U}_n) : \nabla_{\rho\alpha\beta}(I_{h,n}(\hat{\varphi}_n(\hat{W}_n, \hat{\mathbf{r}}_n))) : \nabla_{\rho\alpha\beta}(\hat{W}_n, \hat{\mathbf{r}}_n) dx \quad (4.49) \\ &=: \langle \delta\mathcal{F}_n^{\text{bqcf}}(\mathbf{U}_n)(W_n, \mathbf{r}_n), (W_n, \mathbf{r}_n) \rangle, \end{aligned}$$

where, for notational simplicity we have defined $\mathbf{U}_n := \Pi_{h,n}(U^\infty, \mathbf{p}^\infty)$ and redefined $\delta\mathcal{F}_n^{\text{bqcf}}$ from the previous section without a scaling by ϵ .

Upon extracting a subsequence, we may assume without loss of generality that $\nabla W_n \rightharpoonup \nabla W_0$ for $W_0 \in \dot{H}^1$ and $\mathbf{r}_n \rightharpoonup \mathbf{r}_0 \in L^2$. For each $R_{a,n}$, W_n and \mathbf{r}_n are piecewise linear with respect to the mesh \mathcal{T}_a on $\Omega_{a,n}$. Hence the convergence is strong on any finite collection of elements on \mathcal{T}_a since weak convergence implies strong convergence on finite dimensional spaces. It also follows from the full refinement of the mesh assumption on $\Omega_{a,n}$ that W_0 and \mathbf{r}_0 are also piecewise linear with respect to \mathcal{T}_a .

Having established these basic facts, we will yet again split (W_n, \mathbf{r}_n) into the sum of a strongly convergent sequence and weakly convergent sequence as in [25, Theorem 4.9]. For each n , we take $\eta_n(x)$ to be a smooth bump function satisfying $\eta_n(x) = 1$ on $B_{1/2r_{\text{core},n}}(0)$ and $\eta_n(x)$ has support contained in $B_{r_{\text{core},n}}(0)$. Similar to the definition of Π_h , we then set

$$A_n := B_{r_{\text{core},n}} \setminus B_{(1/2)r_{\text{core},n}} + B_{2r_{\text{buff}}}$$

and

$$X_n := I_n(\eta_n W_0) - I_n(\eta_n) \int_{A_n} W_0 dx, \quad Z_n := W_n - X_n, \quad \mathbf{s}_n := I_n(\eta_n \mathbf{r}_0), \quad \mathbf{t}_n := \mathbf{r}_n - \mathbf{s}_n. \quad (4.50)$$

Similar to Lemma 12, we have, with these definitions,

$$\nabla X_n \rightarrow \nabla W_0, \quad \text{and} \quad \nabla Z_n \rightharpoonup 0 \quad \text{in } L^2(\mathbb{R}^d)$$

and

$$\mathbf{s}_n \rightarrow \mathbf{r}_0, \quad \text{and} \quad \mathbf{t}_n \rightharpoonup 0 \quad \text{in } L^2(\mathbb{R}^d).$$

Then we note that the norm defined by

$$\|(U, \mathbf{p})\|_{a1}^2 := \sum_{\xi \in \mathcal{L}} |D(U, \mathbf{p})(\xi)|^2, \quad \text{where} \quad |D(U, \mathbf{p})(\xi)|^2 := \sum_{(\rho\alpha\beta) \in \mathcal{R}} |D_{(\rho\alpha\beta)}(U, \mathbf{p})(\xi)|^2.$$

is equivalent to the $\|\cdot\|_a$ norm on \mathcal{U} by [34, Lemma 2.1]. Thus, since we are dealing with functions which are \mathcal{P}^1 with respect to \mathcal{T}_a on a growing atomistic region, then the continuous convergence results for $\nabla X_n, \nabla Z_n, \mathbf{s}_n$, and \mathbf{t}_n imply corresponding discrete convergence results:

$$D(X_n, \mathbf{s}_n) \rightarrow D(W_0, \mathbf{r}_0) \quad \text{and} \quad D(Z_n, \mathbf{t}_n) \rightharpoonup 0 \quad \text{in } \ell^2(\mathcal{L}). \quad (4.51)$$

With this decomposition, we now substitute the test pair $(W_n, \mathbf{r}_n) = (X_n + Z_n, \mathbf{s}_n + \mathbf{t}_n)$ from (4.50) into

$$\begin{aligned} & \langle \delta \mathcal{F}_n^{\text{bqcf}}(\mathbf{U}_n)(X_n + Z_n, \mathbf{s}_n + \mathbf{t}_n), (X_n + Z_n, \mathbf{s}_n + \mathbf{t}_n) \rangle \\ &= \langle \delta \mathcal{F}_n^{\text{bqcf}}(\mathbf{U}_n)(X_n, \mathbf{s}_n), (X_n, \mathbf{s}_n) \rangle + \langle \delta \mathcal{F}_n^{\text{bqcf}}(\mathbf{U}_n)(X_n, \mathbf{s}_n), (Z_n, \mathbf{t}_n) \rangle \\ & \quad + \langle \delta \mathcal{F}_n^{\text{bqcf}}(\mathbf{U}_n)(Z_n, \mathbf{t}_n), (X_n, \mathbf{s}_n) \rangle + \langle \delta \mathcal{F}_n^{\text{bqcf}}(\mathbf{U}_n)(Z_n, \mathbf{t}_n), (Z_n, \mathbf{t}_n) \rangle. \end{aligned} \quad (4.52)$$

Also recall the definition of $\delta \mathcal{F}_n^{\text{bqcf}}$, which is

$$\begin{aligned} & \langle \delta \mathcal{F}_n^{\text{bqcf}}(\mathbf{U}_n)(W_n, \mathbf{r}_n), (W_n, \mathbf{r}_n) \rangle \\ &= \langle \delta^2 \mathcal{E}^a(\mathbf{U}_n)((1 - \varphi_n)(W_n, \mathbf{r}_n)), (W_n, \mathbf{r}_n) \rangle \\ & \quad + \langle \delta^2 \mathcal{E}^c(\mathbf{U}_n)(\varphi_n(W_n, \mathbf{r}_n)), (W_n, \mathbf{r}_n) \rangle. \end{aligned}$$

Since $D(X_n, \mathbf{s}_n)$ each have support where $\varphi_n = 0$ and $\Pi_{h,n}(\mathbf{U}_n) = (\mathbf{U}_n)$ there, we can rewrite the first three terms of (4.52) without the blending function as

$$\begin{aligned} & \langle \delta \mathcal{F}_n^{\text{bqcf}}(\mathbf{U}_n)(X_n + Z_n, \mathbf{s}_n + \mathbf{t}_n), (X_n + Z_n, \mathbf{s}_n + \mathbf{t}_n) \rangle \\ &= \langle \delta^2 \mathcal{E}^a(\mathbf{U}_n)(X_n, \mathbf{s}_n), (X_n, \mathbf{s}_n) \rangle + \langle \delta^2 \mathcal{E}^a(\mathbf{U}_n)(X_n, \mathbf{s}_n), (Z_n, \mathbf{t}_n) \rangle \\ & \quad + \langle \delta^2 \mathcal{E}^a(\mathbf{U}_n)(Z_n, \mathbf{t}_n), (X_n, \mathbf{s}_n) \rangle + \langle \delta \mathcal{F}_n^{\text{bqcf}}(\mathbf{U}_n)(Z_n, \mathbf{t}_n), (Z_n, \mathbf{t}_n) \rangle. \end{aligned} \quad (4.53)$$

Moreover, $D(Z_n, \mathbf{t}_n)$ has support only where $V_\xi \equiv V$ and so from the convergence properties (4.51), it follows that $\langle \delta^2 \mathcal{E}^a(\mathbf{U}_n)(X_n, \mathbf{s}_n), (Z_n, \mathbf{t}_n) \rangle$ and $\langle \delta^2 \mathcal{E}^a(\mathbf{U}_n)(Z_n, \mathbf{t}_n), (X_n, \mathbf{s}_n) \rangle$ both go to zero as $n \rightarrow \infty$.

For the first term in (4.53), using the atomistic stability assumption, Assumption 3, we obtain

$$\langle \delta^2 \mathcal{E}^a(\mathbf{U}_n)(X_n, \mathbf{s}_n), (X_n, \mathbf{s}_n) \rangle \geq \gamma_a \|(X_n, \mathbf{s}_n)\|_{\text{ml}}^2. \quad (4.54)$$

Thus, taking the lim inf as $n \rightarrow \infty$ in (4.53) yields

$$\begin{aligned} & \liminf_{n \rightarrow \infty} \langle \delta \mathcal{F}_n^{\text{bqcf}}(\mathbf{U}_n)(X_n + Z_n, \mathbf{s}_n + \mathbf{t}_n), (X_n + Z_n, \mathbf{s}_n + \mathbf{t}_n) \rangle \\ & \geq \liminf_{n \rightarrow \infty} \gamma_a \|(X_n, \mathbf{s}_n)\|_{\text{ml}}^2 + \liminf_{n \rightarrow \infty} \langle \delta \mathcal{F}_n^{\text{bqcf}}(\mathbf{U}_n)(Z_n, \mathbf{t}_n), (Z_n, \mathbf{t}_n) \rangle \end{aligned} \quad (4.55)$$

Thus, we are only left to treat $\langle \delta \mathcal{F}_n^{\text{bqcf}}(\mathbf{U}_n)(Z_n, \mathbf{t}_n), (Z_n, \mathbf{t}_n) \rangle$, the far-field contribution, as defined in (4.50). The strategy here is that far from the defect core we may replace $\delta \mathcal{F}_n^{\text{bqcf}}(\mathbf{U}_n)$ with $\delta \mathcal{F}_{\text{hom},n}^{\text{bqcf}}(0)$ and then apply Theorem 16. Thus, we first estimate,

$$\begin{aligned} & \langle \delta \mathcal{F}_n^{\text{bqcf}}(\mathbf{U}_n)(Z_n, \mathbf{t}_n), (Z_n, \mathbf{t}_n) \rangle \\ &= \langle \delta \mathcal{F}_{\text{hom},n}^{\text{bqcf}}(\mathbf{U}_n)(Z_n, \mathbf{t}_n), (Z_n, \mathbf{t}_n) \rangle \\ &= \langle \delta \mathcal{F}_{\text{hom},n}^{\text{bqcf}}(0)(Z_n, \mathbf{t}_n), (Z_n, \mathbf{t}_n) \rangle + \langle [\delta \mathcal{F}_{\text{hom},n}^{\text{bqcf}}(\mathbf{U}_n) - \delta \mathcal{F}_{\text{hom},n}^{\text{bqcf}}(0)](Z_n, \mathbf{t}_n), (Z_n, \mathbf{t}_n) \rangle \\ & \geq \frac{3}{4} \gamma_a \|(Z_n, \mathbf{t}_n)\|_{\text{ml}}^2 + \langle [\delta \mathcal{F}_{\text{hom},n}^{\text{bqcf}}(\mathbf{U}_n) - \delta \mathcal{F}_{\text{hom},n}^{\text{bqcf}}(0)](Z_n, \mathbf{t}_n), (Z_n, \mathbf{t}_n) \rangle. \end{aligned} \quad (4.56)$$

where we applied Theorem 16 in the final step. (Note that there is a slight notational discrepancy in that our $\mathcal{F}_{\text{hom},n}^{\text{bqcf}}$ is indexed by n here while there is no index in Theorem 16. However, we may still use this theorem since $R_{\text{core},n} \rightarrow \infty$ so we may assume $R_{\text{core},n} \geq R_{\text{core}}^*$ in the statement of that theorem.)

Next, we estimate the remaining group in (4.56),

$$\begin{aligned}
& \langle [\delta \mathcal{F}_{\text{hom},n}^{\text{bqcf}}(\mathbf{U}_n) - \delta \mathcal{F}_{\text{hom},n}^{\text{bqcf}}(0)](Z_n, \mathbf{t}_n), (Z_n, \mathbf{t}_n) \rangle \\
& \leq \left| \langle [\delta^2 \mathcal{E}_{\text{hom}}^{\text{a}}(\mathbf{U}_n) - \delta^2 \mathcal{E}_{\text{hom}}^{\text{a}}(0)](1 - \varphi_n)(Z_n, \mathbf{t}_n), (Z_n, \mathbf{t}_n) \rangle \right| \\
& \quad + \left| \langle [\delta^2 \mathcal{E}^{\text{c}}(\mathbf{U}_n) - \delta^2 \mathcal{E}^{\text{c}}(0)]I_{h,n}(\varphi_n(Z_n, \mathbf{t}_n)), (Z_n, \mathbf{t}_n) \rangle \right| \\
& \leq \sum_{(\rho\alpha\beta)(\tau\gamma\delta)} \|V_{(\rho\alpha\beta)(\tau\gamma\delta)}(D\mathbf{U}_n) - V_{(\rho\alpha\beta)(\tau\gamma\delta)}(0)\|_{\ell^\infty(\text{supp}(D(Z_n, \mathbf{t}_n)))} \\
& \quad \cdot \|D_{(\rho\alpha\beta)}((1 - \varphi_n)(Z_n, \mathbf{t}_n))\|_{\ell^2(\mathbb{R}^d)} \|D_{(\tau\gamma\delta)}(Z_n, \mathbf{t}_n)\|_{\ell^2(\mathbb{R}^d)} \\
& + \sum_{(\rho\alpha\beta)(\tau\gamma\delta)} \|V_{(\rho\alpha\beta)(\tau\gamma\delta)}(\nabla \mathbf{U}_n) - V_{(\rho\alpha\beta)(\tau\gamma\delta)}(0)\|_{L^\infty(\text{supp}(\nabla(Z_n, \mathbf{t}_n)))} \\
& \quad \cdot \|\nabla_{(\rho\alpha\beta)}((1 - \varphi_n)(Z_n, \mathbf{t}_n))\|_{L^2(\mathbb{R}^d)} \|\nabla_{(\tau\gamma\delta)}(Z_n, \mathbf{t}_n)\|_{L^2(\mathbb{R}^d)}.
\end{aligned}$$

From Lemma 12 and the decay rates from Theorem 5 we have

$$\begin{aligned}
& \|V_{(\rho\alpha\beta)(\tau\gamma\delta)}(D\mathbf{U}_n) - V_{(\rho\alpha\beta)(\tau\gamma\delta)}(0)\|_{\ell^\infty(\text{supp}(D(Z_n, \mathbf{t}_n)))} \rightarrow 0, \quad \text{and} \\
& \|V_{(\rho\alpha\beta)(\tau\gamma\delta)}(\nabla \mathbf{U}_n) - V_{(\rho\alpha\beta)(\tau\gamma\delta)}(0)\|_{L^\infty(\text{supp}(\nabla(Z_n, \mathbf{t}_n)))} \rightarrow 0.
\end{aligned} \tag{4.57}$$

Consequently,

$$\langle [\delta \mathcal{F}_{\text{hom},n}^{\text{bqcf}}(\mathbf{U}_n) - \delta \mathcal{F}_{\text{hom},n}^{\text{bqcf}}(0)](Z_n, \mathbf{t}_n), (Z_n, \mathbf{t}_n) \rangle \rightarrow 0,$$

and from (4.56),

$$\liminf_{n \rightarrow \infty} \langle \delta \mathcal{F}_n^{\text{bqcf}}(\mathbf{U}_n)(Z_n, \mathbf{t}_n), (Z_n, \mathbf{t}_n) \rangle \geq \frac{3}{4} \gamma_{\text{a}} \|(Z_n, \mathbf{t}_n)\|_{\text{ml}}^2. \tag{4.58}$$

Combining (4.55) and (4.58), we can therefore conclude that

$$\begin{aligned}
& \liminf_{n \rightarrow \infty} \langle \delta \mathcal{F}_n^{\text{bqcf}}(\Pi_{h,n}(\mathbf{U}_n))(X_n + Z_n, \mathbf{s}_n + \mathbf{t}_n), (X_n + Z_n, \mathbf{s}_n + \mathbf{t}_n) \rangle \\
& \geq \liminf_{n \rightarrow \infty} \left[\gamma_{\text{a}} \|(X_n, \mathbf{s}_n)\|_{\text{ml}}^2 + \frac{3}{4} \gamma_{\text{a}} \|(Z_n, \mathbf{t}_n)\|_{\text{ml}}^2 \right] \\
& \geq \liminf_{n \rightarrow \infty} \frac{3}{4} \gamma_{\text{a}} \left[\|\nabla X_n\|_{L^2(\mathbb{R}^d)}^2 + \|\mathbf{s}_n\|_{L^2(\mathbb{R}^d)}^2 + \|\nabla Z_n\|_{L^2(\mathbb{R}^d)}^2 + \|\mathbf{t}_n\|_{L^2(\mathbb{R}^d)}^2 \right].
\end{aligned} \tag{4.59}$$

Notice that we have

$$\begin{aligned}
\|\nabla W_n\|_{L^2(\mathbb{R}^d)}^2 &= \langle \nabla W_n, \nabla W_n \rangle = \langle \nabla(X_n + Z_n), \nabla(X_n + Z_n) \rangle \\
&= \|\nabla X_n\|_{L^2(\mathbb{R}^d)}^2 + 2\langle \nabla X_n, \nabla Z_n \rangle + \|\nabla Z_n\|_{L^2(\mathbb{R}^d)}^2,
\end{aligned}$$

so we get

$$\|\nabla X_n\|_{L^2(\mathbb{R}^d)}^2 + \|\nabla Z_n\|_{L^2(\mathbb{R}^d)}^2 = \|\nabla W_n\|_{L^2(\mathbb{R}^d)}^2 - 2\langle \nabla X_n, \nabla Z_n \rangle.$$

Applying the same treatments to $\|\mathbf{r}_n\|^2$, we have from (4.59) that

$$\begin{aligned}
& \liminf_{n \rightarrow \infty} \langle \delta \mathcal{F}_n^{\text{bqcf}}(\Pi_{h,n}(\mathbf{U}_n))(X_n + Z_n, \mathbf{s}_n + \mathbf{t}_n), (X_n + Z_n, \mathbf{s}_n + \mathbf{t}_n) \rangle \\
& \geq \liminf_{n \rightarrow \infty} \frac{3}{4} \gamma_{\text{a}} \left[\|\nabla W_n\|_{L^2(\mathbb{R}^d)}^2 - 2\langle \nabla Z_n, \nabla X_n \rangle_{L^2(\mathbb{R}^d)} + \sum_{\alpha} \|r_n^\alpha\|_{L^2(\mathbb{R}^d)}^2 \right. \\
& \quad \left. - \sum_{\alpha} 2\langle s_n^\alpha, t_n^\alpha \rangle_{L^2(\mathbb{R}^d)} \right] \\
& \geq \liminf_{n \rightarrow \infty} \frac{3}{4} \gamma_{\text{a}} \left[\|\nabla W_n\|_{L^2(\mathbb{R}^d)}^2 + \sum_{\alpha} \|r_n^\alpha\|_{L^2(\mathbb{R}^d)}^2 \right] = \frac{3}{4} \gamma_{\text{a}},
\end{aligned}$$

which is a contradiction to (4.49). In attaining the last equality, we have used $(\cdot, \cdot)_{L^2}$ to denote the L^2 inner product, and we have again used the fact that the inner product of the strongly convergent sequence ∇X_n and weakly convergent sequence ∇Z_n (c.f. Lemma 17) converges to zero and similarly for the inner product of the strongly convergent \mathbf{s}_n and weakly convergent \mathbf{t}_n . \square

5. DISCUSSION

We presented the first complete error analysis of an atomistic-to-continuum coupling method for multilattices capable of incorporating defects in the analysis. Our results for the blended force-based quasicontinuum method extend the existing results for Bravais lattices [25], with the striking conclusion that the convergence rates in the simple and multi-lattice cases coincide for the optimal mesh coarsening. Our computational results for a Stone-Wales defect in graphene confirm our theoretical predictions.

We have concerned ourselves here with the case of point defects, though we see no conceptually challenging obstacles to include dislocations in the analysis so long as there is an analogous decay result to Theorem 3. However, as previously mentioned, we are still limited in our ability to model physical effects such as bending or rippling in two-dimensional materials such as graphene due to several factors. First, our assumption concerning stability of the multilattice, Assumption 3 uses a norm, $\|\nabla IU\|_{L^2} + \|I\mathbf{p}\|_{L^2}$, which does not take any bending energy into account and so we do not guarantee our lattice is stable in this situation. We could have of course formulated a different assumption using a discrete variant of $\|\nabla^2 U_3\|$ (where U_3 represents the out of plane displacement), but it is a very challenging question to extend the BQCF method and its analysis to such a situation. The next issue that must be answered is what continuum model to use since the Cauchy–Born model used herein is not adequate to model such effects. Possible alternatives would be to use higher-order Cauchy–Born rules [19, 53] which rely on higher-order strain gradients, or the so-called exponential Cauchy–Born rule [4]. In either of these cases, to use a similar analysis to what we have presented, one would have to establish new stress estimates akin to Corollary 11 as well ensuring that the continuum model chosen is stable provided the atomistic model is. We are also confronted with the problem of choosing a finite element space capable of approximating H^2 functions, which likewise challenges the analysis as well as the implementation.

Finally, we remark that extensions to charged defects in ionic crystals, which represent a wide class of important multilattice crystals, represent yet another difficult challenge, largely due to the long-range nature of the interatomic forces.

APPENDIX A. PROOFS OF CONVERGENCE LEMMAS

The following elementary lemma will be used to construct the “diagonal” sequence alluded to when we first introduced Lemma 17.

Lemma 20. *Let $\{\mathcal{L}_m^\alpha\}_{m=1}^\infty$ be a sequence of functions from $H^1(\mathbb{R}^d) \times (L^2(\mathbb{R}^d))^S \rightarrow V^\alpha$ for V^α a Banach space where α ranges in some finite index set S . Let $(v_0, \mathbf{s}_0) \in H^1(\mathbb{R}^d) \times (L^2(\mathbb{R}^d))^S$ with η the standard mollifier ($\eta_j(x) = j^{-d}\eta(x/j)$), $v_j := \eta_j * v_0$, $\mathbf{s}_j := \eta_j * \mathbf{s}_0$, $j > 0$, and $f^\alpha : (H^1, (L^2)^S) \rightarrow V^\alpha$ continuous. Further assume that for each fixed $j > 0$, $\mathcal{L}_m^\alpha(v_j, \mathbf{s}_j) \rightarrow f^\alpha(v_j, \mathbf{s}_j)$ in V^α as $m \rightarrow \infty$ for each α . Then there exists a sequence $j_n \rightarrow 0$ such that*

$$\mathcal{L}_n^\alpha(v_{j_n}, \mathbf{s}_{j_n}) \rightarrow f^\alpha(v_0, \mathbf{s}_0) \quad \text{for each } \alpha.$$

Moreover, the sequence j_n may be taken to satisfy $j_n \geq 1/\sqrt{R_{a,n}}$ where $R_{a,n}$ is taken from (4.28)

Proof. Fix α and $j > 0$ and note that $\mathcal{L}_m^\alpha(v_j, \mathbf{s}_j) \rightarrow f^\alpha(v_j, \mathbf{s}_j)$ as $m \rightarrow \infty$. Thus we may choose $n_0^\alpha(j)$ large enough such that for $n \geq n_0^\alpha(j)$

$$\|\mathcal{L}_n^\alpha(v_j, \mathbf{s}_j) - f^\alpha(v_j, \mathbf{s}_j)\|_{V^\alpha} \leq j. \quad (\text{A.1})$$

Since α belongs to a finite set S , we may define $n_0(j) = \max_\alpha n_0^\alpha(j)$. Now define j_n by

$$\begin{aligned} j_n &= \max\{1, 1/\sqrt{R_{a,1}}\} \quad \text{for } n = 1, \dots, n_0(1/2) - 1, \\ j_n &= \max\{1/2, 1/\sqrt{R_{a,2}}\} \quad \text{for } n = n_0(1/2), \dots, n_0(1/3) - 1, \\ j_n &= \max\{1/m, 1/\sqrt{R_{a,m}}\} \quad \text{for } n = n_0(1/m), \dots, n_0(1/(m+1)) - 1. \end{aligned}$$

For $n \geq n_0(1)$, we obtain from (A.1) that

$$\|\mathcal{L}_n^\alpha(v_{j_n}, \mathbf{s}_{j_n}) - f^\alpha(v_{j_n}, \mathbf{s}_{j_n})\|_{V^\alpha} \leq j_n \rightarrow 0. \quad (\text{A.2})$$

By continuity of f^α , $f^\alpha(v_{j_n}, \mathbf{s}_{j_n}) \rightarrow f^\alpha(v_0, \mathbf{s}_0)$, and so (A.2) implies the desired result. \square

Remark 6. In the above proof, we made the requirement $j_n \geq 1/\sqrt{R_{a,n}}$ so that $1/R_{a,n} = \epsilon_n \leq j_n^2$, where ϵ_n is used in the scaling (4.28). This ensures that

$$\begin{aligned} \|\epsilon_n \nabla(\eta_{j_n} * \hat{s}_0)\|_{L^2(\mathbb{R}^d)} &= \epsilon_n \|(\nabla \eta_{j_n}) * \hat{s}_0\|_{L^2(\mathbb{R}^d)} \\ &\leq \epsilon_n \|(\nabla \eta_{j_n})\|_{L^1(\mathbb{R}^d)} \|\hat{s}_0\|_{L^2(\mathbb{R}^d)} \quad \text{by Young's Inequality} \\ &= \epsilon_n \cdot 1/j_n \|\nabla \eta\|_{L^1(\mathbb{R}^d)} \|\hat{s}_0\|_{L^2(\mathbb{R}^d)} \\ &\leq j_n \|\nabla \eta\|_{L^1(\mathbb{R}^d)} \|\hat{s}_0\|_{L^2(\mathbb{R}^d)} \rightarrow 0. \end{aligned}$$

\square

The collection of operators and continuous functions that we apply this lemma to are the ones enumerated in Lemma 17, which may now prove.

Proof of Lemma 17. We begin by noting that the properties of (4.31) are clear from the definitions of $W_n, X_n, Z_n, \mathbf{r}_n, \mathbf{s}_n, \mathbf{t}_n$ provided that we can show $\nabla X_n \rightarrow \nabla W_0$ and $\mathbf{s}_n \rightarrow \mathbf{r}_0$. Moreover, we can immediately note that with $\psi_m = 1 - \varphi_m$, $\nabla \psi_m$ and $\nabla^2 \psi_m$ are uniformly bounded on the compact set $\text{supp}(\psi_m) \subset \epsilon_m B_{R_{a,m}}(0) = B_1(0)$ by the assumptions on the blending function in Assumption 4 and the definition of ϵ_n . Thus, by Arzela-Ascoli and by replacing the original sequence by a subsequence if necessary, we may assume $\psi_m \rightarrow \psi_0$ in C^1 for some $\psi_0 \in C^1(B_1(0))$.

We now set about proving $\nabla X_n \rightarrow \nabla W_0$ and $\mathbf{s}_n \rightarrow \mathbf{r}_0$ and the remaining properties in Lemma (17). To that end, define

$$\begin{aligned}
\mathcal{L}_m^1 &:= \Pi_{h,m}, \quad f^1(W, \mathbf{s}) = (W, \mathbf{s}), \\
\mathcal{L}_m^2(W, \mathbf{s}) &:= \epsilon_m^d \sum_{\xi \in \epsilon_m \mathcal{L}} \sum_{(\rho\alpha\beta)} \sum_{(\tau\gamma\delta)} V_{(\rho\alpha\beta)(\tau\gamma\delta)} : D_{(\tau\gamma\delta),m}(W, \mathbf{s}) \otimes \frac{\rho}{\epsilon_m} \int_0^{\epsilon_m} \bar{\zeta}_m(\xi + t\rho - x), \\
f^2(W, \mathbf{s}) &:= \sum_{(\rho\alpha\beta)} \sum_{(\tau\gamma\delta)} V_{(\rho\alpha\beta)(\tau\gamma\delta)} : \nabla_{(\tau\gamma\delta)}(W(x), \mathbf{s}(x)) \otimes \rho, \\
\mathcal{L}_m^3(W, \mathbf{s}) &:= \epsilon_m^d \sum_{\xi \in \epsilon_m \mathcal{L}} \sum_{(\rho\alpha\beta)} \sum_{(\tau\gamma\delta)} V_{(\rho\alpha\beta)(\tau\gamma\delta)} : (D_{(\tau\gamma\delta),m}(W, \mathbf{s})) \bar{\zeta}_m(\xi - x), \\
f^3(W, \mathbf{s}) &:= \sum_{(\rho\alpha\beta)} \sum_{(\tau\gamma\delta)} V_{(\rho\alpha\beta)(\tau\gamma\delta)} : \nabla_{(\tau\gamma\delta)}(W(x), \mathbf{s}(x)), \\
\mathcal{L}_m^4(W, \mathbf{s}) &:= \epsilon_m^d \sum_{\xi \in \epsilon_m \mathcal{L}} \sum_{(\rho\alpha\beta)} \sum_{(\tau\gamma\delta)} V_{(\rho\alpha\beta)(\tau\gamma\delta)} : D_{(\tau\gamma\delta),m}(\psi_m W, \psi_m \mathbf{s}) \otimes \frac{\rho}{\epsilon_m} \int_0^{\epsilon_m} \bar{\zeta}_m(\xi + t\rho - x), \\
f^4(W, \mathbf{s}) &:= \sum_{(\rho\alpha\beta)} \sum_{(\tau\gamma\delta)} V_{(\rho\alpha\beta)(\tau\gamma\delta)} : \nabla_{(\tau\gamma\delta)}(\psi_0 W(x), \psi_0 \mathbf{s}(x)) \otimes \rho, \\
\mathcal{L}_m^5(W, \mathbf{s}) &:= \epsilon_m^d \sum_{\xi \in \epsilon_m \mathcal{L}} \sum_{(\rho\alpha\beta)} \sum_{(\tau\gamma\delta)} V_{(\rho\alpha\beta)(\tau\gamma\delta)} : (D_{(\tau\gamma\delta),m}(\psi_m W, \psi_m \mathbf{s})) \bar{\zeta}_m(\xi - x), \\
f^5(W, \mathbf{s}) &:= \sum_{(\rho\alpha\beta)} \sum_{(\tau\gamma\delta)} V_{(\rho\alpha\beta)(\tau\gamma\delta)} : \nabla_{(\tau\gamma\delta)}(\psi_0 W(x), \psi_0 \mathbf{s}(x)), \\
\mathcal{L}_m^6(W, \mathbf{s}) &:= \epsilon_m^d \sum_{\xi \in \epsilon_m \mathcal{L}} \sum_{(\rho\alpha\beta)} \sum_{\tau\gamma\delta} V_{(\rho\alpha\beta)(\tau\gamma\delta)} : D_{(\rho\alpha\beta),m}(\psi_m W, \psi_m \mathbf{s}) : D_{\tau\gamma\delta,m}(W, \mathbf{s}), \\
f^6(W, \mathbf{s}) &:= \int_{\mathbb{R}^d} \sum_{(\rho\alpha\beta)} \sum_{(\tau\gamma\delta)} V_{(\rho\alpha\beta)(\tau\gamma\delta)} : (\nabla_\rho(\psi_0 W) + \psi_0(s^\beta - s^\alpha)) : (\nabla_\tau W + s^\delta - s^\gamma) dx.
\end{aligned}$$

If we can show that each of these satisfies the hypothesis of Lemma 20, then we may apply the conclusion of that lemma to deduce Lemmma 17. We focus primarily on \mathcal{L}^4 and f^4 and briefly touch on the other cases at the end.

We fix j and set $W := v_j$ and $\mathbf{s} := \mathbf{s}_j$ and set $\mu_m(x) := \frac{1}{\epsilon_m} \int_0^{\epsilon_m} \bar{\zeta}_m(x + t\rho) dt$. Then note that $\mu_m(\xi - x) = 0$ unless $|x - \xi| \lesssim \epsilon_m |\rho|$. Hence

$$\begin{aligned}
& \lim_{m \rightarrow \infty} \mathcal{L}_m^2(W, \mathbf{s})(x) \\
&= \lim_{m \rightarrow \infty} \epsilon_m^d \sum_{\xi \in \epsilon_m \mathcal{L}} \sum_{(\rho\alpha\beta)} \sum_{(\tau\gamma\delta)} V_{(\rho\alpha\beta)(\tau\gamma\delta)} : D_{(\tau\gamma\delta),m}(\psi_m W(\xi), \psi_m \mathbf{s}(\xi)) \otimes \rho \mu_m(\xi - x) \\
&= \lim_{m \rightarrow \infty} \epsilon_m^d \sum_{\xi \in \epsilon_m \mathcal{L}} \sum_{(\rho\alpha\beta)} \sum_{(\tau\gamma\delta)} V_{(\rho\alpha\beta)(\tau\gamma\delta)} : [D_{(\tau\gamma\delta),m}(\psi_m W(\xi), \psi_m \mathbf{s}(\xi)) - \nabla_{(\tau\gamma\delta)}(\psi_m W(x), \psi_m \mathbf{s}(x)) \\
&\quad + \nabla_{(\tau\gamma\delta)}(\psi_m W(x), \psi_m \mathbf{s}(x))] \otimes \rho \mu_m(\xi - x) \\
&= \lim_{m \rightarrow \infty} \epsilon_m^d \sum_{\xi \in \epsilon_m \mathcal{L}} \sum_{(\rho\alpha\beta)} \sum_{(\tau\gamma\delta)} V_{(\rho\alpha\beta)(\tau\gamma\delta)} : [D_{(\tau\gamma\delta),m}(\psi_m W(\xi), \psi_m \mathbf{s}(\xi)) \\
&\quad - \nabla_{(\tau\gamma\delta)}(\psi_m W(x), \psi_m \mathbf{s}(x))] \otimes \rho \mu_m(\xi - x) \\
&\quad + \lim_{m \rightarrow \infty} \sum_{(\rho\alpha\beta)} \sum_{(\tau\gamma\delta)} V_{(\rho\alpha\beta)(\tau\gamma\delta),m} : \nabla_{(\tau\gamma\delta)}(\psi_m W(x), \psi_m \mathbf{s}(x)) \otimes \rho \epsilon_m^d \sum_{\xi \in \epsilon_m \mathcal{L}} \mu_m(\xi - x) \\
&= \lim_{m \rightarrow \infty} \epsilon_m^d \sum_{\xi \in \epsilon_m \mathcal{L}} \sum_{(\rho\alpha\beta)} \sum_{(\tau\gamma\delta)} V_{(\rho\alpha\beta)(\tau\gamma\delta)} : [D_{(\tau\gamma\delta),m}(\psi_m W(\xi), \psi_m \mathbf{s}(\xi)) \\
&\quad - \nabla_{(\tau\gamma\delta)}(\psi_m W(x), \psi_m \mathbf{s}(x))] \otimes \rho \mu_m(\xi - x) \\
&\quad + \sum_{(\rho\alpha\beta)} \sum_{(\tau\gamma\delta)} V_{(\rho\alpha\beta)(\tau\gamma\delta),m} : \nabla_{(\tau\gamma\delta)}(\psi_0 W(x), \psi_0 \mathbf{s}(x)) \otimes \rho,
\end{aligned}$$

since $\epsilon_m^d \sum_{\xi \in \epsilon_m \mathcal{L}} \mu_m(\xi - x) = 1$ and since $\psi_m \rightarrow \psi_0$ in C^1 . For the first limit above, we note that $\mu_m(\xi - x) = 0$ unless $|x - \xi| \lesssim \epsilon_m |\rho|$ implies

$$[D_{(\tau\gamma\delta),m}(\psi_m W(\xi), \psi_m \mathbf{s}(\xi)) - \nabla_{(\tau\gamma\delta)}(\psi_m W(x), \psi_m \mathbf{s}(x))] = \mathcal{O}(\epsilon_m)$$

Thus

$$\begin{aligned}
& \lim_{m \rightarrow \infty} \epsilon_m^d \sum_{\xi \in \epsilon_m \mathcal{L}} \sum_{(\rho\alpha\beta)} \sum_{(\tau\gamma\delta)} V_{(\rho\alpha\beta)(\tau\gamma\delta)} : [D_{(\tau\gamma\delta),m}(\psi_m W(\xi), \psi_m \mathbf{s}(\xi)) \\
&\quad - \nabla_{(\tau\gamma\delta)}(\psi_m W(x), \psi_m \mathbf{s}(x))] \otimes \rho \mu_m(\xi - x) \\
&= \lim_{m \rightarrow \infty} \sum_{(\rho\alpha\beta)} \sum_{(\tau\gamma\delta)} V_{(\rho\alpha\beta)(\tau\gamma\delta)} : [\mathcal{O}(\epsilon_m)] \otimes \rho \epsilon_m^d \sum_{\xi \in \epsilon_m \mathcal{L}} \mu_m(\xi - x) \\
&= \lim_{m \rightarrow \infty} \sum_{(\rho\alpha\beta)} \sum_{(\tau\gamma\delta)} V_{(\rho\alpha\beta)(\tau\gamma\delta)} : [\mathcal{O}(\epsilon_m)] \otimes \rho = 0.
\end{aligned}$$

We have thus shown that

$$\lim_{m \rightarrow \infty} \mathcal{L}_m^4(W, \mathbf{s}) = \sum_{(\rho\alpha\beta)} \sum_{(\tau\gamma\delta)} V_{(\rho\alpha\beta)(\tau\gamma\delta)} : \nabla_{(\tau\gamma\delta)}(\psi_0 W(x), \psi_0 \mathbf{s}(x)) \otimes \rho = f^4(W, \mathbf{s}).$$

The proof for \mathcal{L}^5 proceeds in exactly the same manner, and the proofs for \mathcal{L}^2 and \mathcal{L}^3 are likewise very similar with the exception that ψ_m is no longer present.

For \mathcal{L}^6 , using a Taylor expansion and the fact that $\nabla^2 \psi_m$ is uniformly bounded in m by Assumption 4,

$$\begin{aligned} D_{\tau,m} \psi_m(\xi) &= D_{\tau,m} \psi_m(\xi) - \nabla_\tau \psi_m(\xi) + \nabla_\tau \psi_m(\xi) \\ &= \mathcal{O}(\epsilon_m) + \nabla_\tau \psi_m(\xi) \rightarrow \nabla_\tau \psi_0(\xi). \end{aligned}$$

Furthermore, since W and \mathbf{s} are smooth, $D_{\tau,m} W$ converges to $\nabla_\tau W$ in L^2 and ℓ^2 on compact subsets, and the same holds for $D_{\tau,m} \mathbf{s}_\beta$ converging to $\nabla_\tau \mathbf{s}_\beta$. Consequently,

$$D_{(\tau\gamma\delta),m}(\psi_m W, \psi_m \mathbf{s}) \rightarrow \nabla_{(\tau\gamma\delta)}(\psi_0 W, \psi_0 \mathbf{s}) \quad \text{in } L^2 \text{ and } \ell^2 \text{ on bounded sets.}$$

Convergence of $\mathcal{L}^6(W, \mathbf{s})$ to $f^6(W, \mathbf{s})$ now follows from this and convergence of the quadrature rule

$$\lim_{m \rightarrow \infty} \epsilon_m^d \sum_{\xi \in \epsilon_m \mathcal{L}} \sum_{(\rho\alpha\beta)} \sum_{\tau\gamma\delta} V_{(\rho\alpha\beta)(\tau\gamma\delta)} : \nabla_{(\rho\alpha\beta),m}(\psi_0 W, \psi_0 \mathbf{s}) : \nabla_{\tau\gamma\delta,m}(W, \mathbf{s}),$$

to

$$\int_{B_1(0)} \sum_{(\rho\alpha\beta)} \sum_{\tau\gamma\delta} V_{(\rho\alpha\beta)(\tau\gamma\delta)} : \nabla_{(\rho\alpha\beta),m}(\psi_0 W, \psi_0 \mathbf{s}) : \nabla_{\tau\gamma\delta,m}(W, \mathbf{s}) dx.$$

Lastly, we note that $\mathcal{L}^1(W, \mathbf{s}) \rightarrow f^1(W, \mathbf{s})$ as a result of first approximating (W, \mathbf{s}) by smooth functions having support contained in $B_{\epsilon_m^{-\gamma}}(0)$ for some $0 < \gamma < 1$ and then using standard interpolation estimates for smooth functions along with the mesh growth assumption of Assumption 4. Specifically, let $W_m, \mathbf{s}_m \in C_0^\infty$ such that $\nabla W_m \rightarrow \nabla W, \nabla^2 W_m \rightarrow \nabla^2 W, \mathbf{s}_m \rightarrow \mathbf{s}$, and $\nabla \mathbf{s}_m \rightarrow \nabla \mathbf{s}$ in L^2 where ∇W_m and \mathbf{s}_m have support in $B_{\epsilon_m^{-\gamma}}(0)$. Then

$$\begin{aligned} \|\Pi_{h,m}(W, \mathbf{s}) - (W, \mathbf{s})\|_{\text{ml}} &\leq \|\Pi_{h,m}(W, \mathbf{s}) - \Pi_{h,m}(W_m, \mathbf{s}_m)\|_{\text{ml}} + \|\Pi_{h,m}(W_m, \mathbf{s}_m) - (W_m, \mathbf{s}_m)\|_{\text{ml}} \\ &\quad + \|(W_m, \mathbf{s}_m) - (W, \mathbf{s})\|_{\text{ml}} \\ &\lesssim \|(W, \mathbf{s}) - (W_m, \mathbf{s}_m)\|_{\text{ml}} + \|\Pi_{h,m}(W_m, \mathbf{s}_m) - (W_m, \mathbf{s}_m)\|_{\text{ml}}, \end{aligned} \tag{A.3}$$

after using stability of $\Pi_{h,m}$ with respect to the ml norm. By our choice of (W_m, \mathbf{s}_m) , it follows that

$$\|(W, \mathbf{s}) - (W_m, \mathbf{s}_m)\|_{\text{ml}} \rightarrow 0. \tag{A.4}$$

Using the definition of the ml norm and standard interpolation estimates, we also possess

$$\|\Pi_{h,m}(W_m, \mathbf{s}_m) - (W_m, \mathbf{s}_m)\|_{\text{ml}} \lesssim \|h_m \nabla^2 W_m\|_{L^2(\mathbb{R}^d)} + \|h_m \nabla \mathbf{s}_m\|_{L^2(\mathbb{R}^d)}. \tag{A.5}$$

Since, ∇W_m and \mathbf{s}_m have support in $B_{\epsilon_m^{-\gamma}}(0)$ and since we have the mesh growth $|h_m(x)| \lesssim \epsilon_m(\epsilon_m|x/\epsilon_m|)^s$ from our choice of scaling and Assumption 4, it follows that $|h_m(x)| \lesssim \epsilon_m^{1-s\gamma}$ on $B_{\epsilon_m^{-\gamma}}(0)$. It then follows from (A.5) that

$$\|\Pi_{h,m}(W_m, \mathbf{s}_m) - (W_m, \mathbf{s}_m)\|_{\text{ml}} \lesssim \epsilon_m^{1-s\gamma} \|\nabla^2 W_m\|_{L^2(\mathbb{R}^d)} + \epsilon_m^{1-s\gamma} \|\nabla \mathbf{s}_m\|_{L^2(\mathbb{R}^d)} \rightarrow 0, \tag{A.6}$$

for appropriately chosen γ . Applying the results (A.4) and (A.6) to (A.3) then produces

$$\|\Pi_{h,m}(W, \mathbf{s}) - (W, \mathbf{s})\|_{\text{ml}} \rightarrow 0,$$

as desired.

Then as a consequence of Lemma 20 applied to each of these operators, we obtain a sequence $j_n \rightarrow 0$ which satisfies the desired convergence results of (17). \square

Proof of Lemma 18. To prove the first convergence result (4.33), we note by Lemma 8, there exists $Y_n = (\psi_n Z_n)$ such that $\psi_n Z_n(\xi) = (\bar{\zeta}_n * \bar{Y}_n)(\xi) =: (Y_n^*)(\xi)$ for all $\xi \in \epsilon_n \mathcal{L}$, and similarly there exists $\mathbf{b}_n = (\psi_n \mathbf{t}_n)$ such that $\psi_n \mathbf{t}_n(\xi) = (\bar{\zeta}_n * \bar{\mathbf{b}}_n)(\xi) := (\mathbf{b}_n^*)(\xi)$. We further note that from the proof of [25, Lemma 4.10, Step 3] and the fact that $\nabla(\psi_n Z_n) \rightharpoonup 0$, we also have $\nabla \bar{Y}_n \rightharpoonup 0$. To show that $\bar{b}_n^\alpha \rightharpoonup 0$, observe for a smooth function μ with compact support that

$$\begin{aligned} \lim_{n \rightarrow \infty} \int \bar{b}_n^\alpha \cdot \mu &= \lim_{n \rightarrow \infty} \int \bar{b}_n^\alpha \cdot (\bar{\zeta}_n * \mu) + \lim_{n \rightarrow \infty} \int \bar{b}_n^\alpha \cdot (\mu - \bar{\zeta}_n * \mu) \\ &= \lim_{n \rightarrow \infty} \int (\bar{b}_n^\alpha * \bar{\zeta}_n) \cdot \mu = \lim_{n \rightarrow \infty} \int t_n^\alpha (\psi_n \mu). \end{aligned}$$

From Lemma 17, we have $\psi_n \rightarrow \psi_0$ in L^2 (since these functions are compactly supported), and this latter expression is then an inner product of a weakly convergent sequence ($t_n^\alpha \rightharpoonup 0$) and strongly convergent sequence which therefore converges to zero.

Having established that $\nabla \bar{Y}_n, \bar{b}_n^\alpha \rightharpoonup 0$, we can use the functions $S_n^{\text{def}}(x)$ and $S_n^{\text{shift}}(x)$ from Lemma 17 to write

$$\begin{aligned} \epsilon^d \sum_{\xi \in \epsilon_n \mathcal{L}} \sum_{(\rho\alpha\beta)} \sum_{(\tau\gamma\delta)} V_{(\rho\alpha\beta)(\tau\gamma\delta)} : D_{(\rho\alpha\beta),n}(\psi_n Z_n, \psi_n \mathbf{t}_n) : D_{(\tau\gamma\delta),n}(X_n, \mathbf{s}_n) \\ = \int S_n^{\text{def}}(x) : (\nabla \bar{Y}_n + \epsilon_n \nabla \bar{b}_n^\beta) + \int S_n^{\text{shift}}(x) : (\bar{b}_n^\beta - \bar{b}_n^\alpha) \rightarrow 0, \end{aligned}$$

using the strong convergence of $S_n^{\text{def}}(x)$ and $S_n^{\text{shift}}(x)$ from Lemma 17 and the weak convergence: $\nabla \bar{Y}_n, \bar{b}_n^\alpha \rightharpoonup 0$.

The second convergence result (4.34) is proven in nearly an identical manner by choosing $Y_n = \dot{Z}_n$ and $\mathbf{b}_n = \dot{\mathbf{t}}_n$ such that $Z_n = \bar{\zeta}_n * \dot{Z}_n$ and $\mathbf{t}_n = \bar{\zeta}_n * \dot{\mathbf{t}}_n$ and using the convergence results for $R_n^{\text{def}}(x)$ and $R_n^{\text{shift}}(x)$ from Lemma 17. \square

Proof of Lemma 19. Observe

$$\begin{aligned} \lim_{n \rightarrow \infty} \epsilon_n^d \sum_{\xi \in \epsilon_n \mathcal{L}} \sum_{(\rho\alpha\beta)} \sum_{(\tau\gamma\delta)} V_{(\rho\alpha\beta)(\tau\gamma\delta)} : D_{(\rho\alpha\beta),n}(\theta_n^2 Z_n, \theta_n^2 \mathbf{t}_n) : D_{(\tau\gamma\delta),n}(Z_n, \mathbf{t}_n), \\ = \lim_{n \rightarrow \infty} \epsilon_n^d \sum_{\xi \in \epsilon_n \mathcal{L}} \sum_{(\rho\alpha\beta)} \sum_{(\tau\gamma\delta)} V_{(\rho\alpha\beta)(\tau\gamma\delta)} : (D_{\rho,n}(\theta_n^2 Z_n) + \epsilon_n D_{\rho,n}(\theta_n^2 t_n^\beta) - \theta_n^2(t_n^\alpha - t_n^\beta)) : (D_{\tau,n}(Z_n) + \\ \epsilon_n D_{\tau,n}(t_n^\delta) - (t_n^\gamma - t_n^\delta)) \\ = \lim_{n \rightarrow \infty} \epsilon_n^d \sum_{\xi \in \epsilon_n \mathcal{L}} \sum_{(\rho\alpha\beta)} \sum_{(\tau\gamma\delta)} V_{(\rho\alpha\beta)(\tau\gamma\delta)} : D_{\rho,n}(\theta_n^2 Z_n) : D_{\tau,n}(Z_n) \\ + \lim_{n \rightarrow \infty} \epsilon_n^d \sum_{\xi \in \epsilon_n \mathcal{L}} \sum_{(\rho\alpha\beta)} \sum_{(\tau\gamma\delta)} V_{(\rho\alpha\beta)(\tau\gamma\delta)} : D_{\rho,n}(\theta_n^2 Z_n) : (\epsilon_n D_{\tau,n}(t_n^\delta) - (t_n^\gamma - t_n^\delta)) \\ + \lim_{n \rightarrow \infty} \epsilon_n^d \sum_{\xi \in \epsilon_n \mathcal{L}} \sum_{(\rho\alpha\beta)} \sum_{(\tau\gamma\delta)} V_{(\rho\alpha\beta)(\tau\gamma\delta)} : (T_{\rho,n}(\theta_n^2 t_n^\beta) - \theta_n^2 t_n^\alpha) : D_{\tau,n}(Z_n) \\ + \lim_{n \rightarrow \infty} \epsilon_n^d \sum_{\xi \in \epsilon_n \mathcal{L}} \sum_{(\rho\alpha\beta)} \sum_{(\tau\gamma\delta)} V_{(\rho\alpha\beta)(\tau\gamma\delta)} : (T_{\rho,n}(\theta_n^2 t_n^\beta) - \theta_n^2 t_n^\alpha) : (\epsilon_n D_{\tau,n}(t_n^\delta) - (t_n^\gamma - t_n^\delta)). \end{aligned} \tag{A.7}$$

This gives four terms to manipulate, which we label in order as A_1^n, A_2^n, A_3^n , and A_4^n . The first of these is, after using the product rule for finite differences (and the associated notation $T_{\rho,n}f(\xi) =$

$$f(\xi + \epsilon_n \rho)),$$

$$\begin{aligned} & \lim_{n \rightarrow \infty} A_1^n \\ &= \lim_{n \rightarrow \infty} \epsilon_n^d \sum_{\xi \in \epsilon_n \mathcal{L}} \sum_{(\rho\alpha\beta)} \sum_{(\tau\gamma\delta)} V_{(\rho\alpha\beta)(\tau\gamma\delta)} : \{ \theta_n Z_n D_{\rho,n}(\theta_n) : D_{\tau,n}(Z_n) + T_{\rho,n}(\theta_n) D_{\rho,n}(\theta_n Z_n) : D_{\tau,n}(Z_n) \}. \end{aligned} \quad (\text{A.8})$$

Recall that $Z_n \rightarrow 0$ in L^2 on $B_1(0) \supset \text{supp}(\theta_n)$ and hence also in ℓ^2 due to being piecewise linear. Therefore, continuing the limit in (A.8),

$$\begin{aligned} & \lim_{n \rightarrow \infty} A_1^n \\ &= \lim_{n \rightarrow \infty} \epsilon_n^d \sum_{\xi \in \epsilon_n \mathcal{L}} \sum_{(\rho\alpha\beta)} \sum_{(\tau\gamma\delta)} V_{(\rho\alpha\beta)(\tau\gamma\delta)} : \{ T_{\rho,n}(\theta_n) D_{\rho,n}(\theta_n Z_n) : D_{\tau,n}(Z_n) \\ & \quad + D_{\rho,n}(\theta_n Z_n) : D_{\tau,n}(\theta_n) Z_n \} \\ &= \lim_{n \rightarrow \infty} \epsilon_n^d \sum_{\xi \in \epsilon_n \mathcal{L}} \sum_{(\rho\alpha\beta)} \sum_{(\tau\gamma\delta)} V_{(\rho\alpha\beta)(\tau\gamma\delta)} : \{ D_{\rho,n}(\theta_n Z_n) : (T_{\rho,n}(\theta_n) - T_{\tau,n}(\theta_n)) D_{\tau,n}(Z_n) \\ & \quad + D_{\rho,n}(\theta_n Z_n) : T_{\tau,n}(\theta_n) D_{\tau,n}(Z_n) + D_{\rho,n}(\theta_n Z_n) : D_{\tau,n}(\theta_n) Z_n \} \\ &= \lim_{n \rightarrow \infty} \epsilon_n^d \sum_{\xi \in \epsilon_n \mathcal{L}} \sum_{(\rho\alpha\beta)} \sum_{(\tau\gamma\delta)} V_{(\rho\alpha\beta)(\tau\gamma\delta)} : \{ D_{\rho,n}(\theta_n Z_n) : D_{\tau,n}(\theta_n Z_n) \}, \end{aligned} \quad (\text{A.9})$$

where in arriving at the last line we used the fact that $(T_{\rho,n}(\theta_n) - T_{\tau,n}(\theta_n)) \rightarrow 0$ in L^∞ and H^1 boundedness of Z_n .

By replacing Z_n with $\epsilon_n t_n^\delta$, we have may write the second of the terms in (A.7) as

$$\begin{aligned} & \lim_{n \rightarrow \infty} A_2^n \\ &= \lim_{n \rightarrow \infty} \epsilon_n^d \sum_{\xi \in \epsilon_n \mathcal{L}} \sum_{(\rho\alpha\beta)} \sum_{(\tau\gamma\delta)} V_{(\rho\alpha\beta)(\tau\gamma\delta)} : \{ D_{\rho,n}(\theta_n Z_n) : D_{\tau,n}(\epsilon_n \theta_n t_n^\delta) + D_{\rho,n}(\theta_n^2 Z_n) : (t_n^\delta - t_n^\gamma) \} \\ &= \lim_{n \rightarrow \infty} \epsilon_n^d \sum_{\xi \in \epsilon_n \mathcal{L}} \sum_{(\rho\alpha\beta)} \sum_{(\tau\gamma\delta)} V_{(\rho\alpha\beta)(\tau\gamma\delta)} : \{ D_{\rho,n}(\theta_n Z_n) : D_{\tau,n}(\epsilon_n \theta_n t_n^\delta) \\ & \quad + (D_{\rho,n}(\theta_n)(\theta_n Z_n) + T_{\rho,n}(\theta_n) D_{\rho,n}(\theta_n Z_n)) : (t_n^\delta - t_n^\gamma) \} \\ &= \lim_{n \rightarrow \infty} \epsilon_n^d \sum_{\xi \in \epsilon_n \mathcal{L}} \sum_{(\rho\alpha\beta)} \sum_{(\tau\gamma\delta)} V_{(\rho\alpha\beta)(\tau\gamma\delta)} : \{ D_{\rho,n}(\theta_n Z_n) : D_{\tau,n}(\epsilon_n \theta_n t_n^\delta) \\ & \quad + D_{\rho,n}(\theta_n Z_n) : (T_{\rho,n}(\theta_n) - \theta_n + \theta_n)(t_n^\delta - t_n^\gamma) \} \\ &= \lim_{n \rightarrow \infty} \epsilon_n^d \sum_{\xi \in \epsilon_n \mathcal{L}} \sum_{(\rho\alpha\beta)} \sum_{(\tau\gamma\delta)} V_{(\rho\alpha\beta)(\tau\gamma\delta)} : \{ D_{\rho,n}(\theta_n Z_n) : (D_{\tau,n}(\epsilon_n \theta_n t_n^\delta) + \theta_n(t_n^\delta - t_n^\gamma)) \}. \end{aligned} \quad (\text{A.10})$$

The third term from (A.7) is, after using the previously established convergence properties of Z_n, t_n and θ_n ,

$$\begin{aligned}
& \lim_{n \rightarrow \infty} A_3^n \\
&= \lim_{n \rightarrow \infty} \epsilon_n^d \sum_{\xi \in \epsilon_n \mathcal{L}} \sum_{(\rho\alpha\beta)} \sum_{(\tau\gamma\delta)} V_{(\rho\alpha\beta)(\tau\gamma\delta)} : (T_{\rho,n}(\theta_n^2 t_n^\beta) - \theta_n^2 t_n^\alpha) : D_{\tau,n}(Z_n) \\
&= \lim_{n \rightarrow \infty} \epsilon_n^d \sum_{\xi \in \epsilon_n \mathcal{L}} \sum_{(\rho\alpha\beta)} \sum_{(\tau\gamma\delta)} V_{(\rho\alpha\beta)(\tau\gamma\delta)} : ((T_{\rho,n}(\theta_n) - \theta_n)T_{\rho,n}(\theta_n t_n^\beta) + \theta_n T_{\rho,n}(\theta_n t_n^\beta) - \theta_n^2 t_n^\alpha) : D_{\tau,n}(Z_n) \\
&= \lim_{n \rightarrow \infty} \epsilon_n^d \sum_{\xi \in \epsilon_n \mathcal{L}} \sum_{(\rho\alpha\beta)} \sum_{(\tau\gamma\delta)} V_{(\rho\alpha\beta)(\tau\gamma\delta)} : \{(T_{\rho,n}(\theta_n t_n^\beta) - \theta_n t_n^\alpha) : \theta_n D_{\tau,n}(Z_n)\} \\
&= \lim_{n \rightarrow \infty} \epsilon_n^d \sum_{\xi \in \epsilon_n \mathcal{L}} \sum_{(\rho\alpha\beta)} \sum_{(\tau\gamma\delta)} V_{(\rho\alpha\beta)(\tau\gamma\delta)} : \{(T_{\rho,n}(\theta_n t_n^\beta) - \theta_n t_n^\alpha) : (T_{\tau,n}(\theta_n)D_{\tau,n}(Z_n) + D_{\tau,n}(\theta_n)(Z_n))\} \\
&= \lim_{n \rightarrow \infty} \epsilon_n^d \sum_{\xi \in \epsilon_n \mathcal{L}} \sum_{(\rho\alpha\beta)} \sum_{(\tau\gamma\delta)} V_{(\rho\alpha\beta)(\tau\gamma\delta)} : \{(T_{\rho,n}(\theta_n t_n^\beta) - \theta_n t_n^\alpha) : D_{\tau,n}(\theta_n Z_n)\}
\end{aligned} \tag{A.11}$$

After again using the convergence properties of θ_n , it is then straightforward to show

$$\begin{aligned}
& \lim_{n \rightarrow \infty} A_4^n \\
&= \lim_{n \rightarrow \infty} \epsilon_n^d \sum_{\xi \in \epsilon_n \mathcal{L}} \sum_{(\rho\alpha\beta)} \sum_{(\tau\gamma\delta)} V_{(\rho\alpha\beta)(\tau\gamma\delta)} : (T_{\rho,n}(\theta_n t_n^\beta) - \theta_n t_n^\alpha) : (T_{\tau,n}(\theta_n t_n^\delta) - \theta_n t_n^\gamma).
\end{aligned} \tag{A.12}$$

The equations (A.9), (A.10), (A.11), and (A.12) applied to (A.7) give the conclusion of the Lemma. \square

Lemma 21. *Let W_n, r_n , and φ_n be defined as in the proof of Theorem 16 with $I_{h,n}$ the \mathcal{P}_1 interpolant onto $\mathcal{T}_{h,n}$. Then*

$$\begin{aligned}
& \|\nabla I_{h,n}(\varphi_n W_n) - \nabla(\varphi_n W_n)\|_{L^2(\mathbb{R}^d)} \rightarrow 0, \\
& \|I_{h,n}(\varphi_n r_n^\alpha) - (\varphi_n r_n^\alpha)\|_{L^2(\mathbb{R}^d)} \rightarrow 0.
\end{aligned} \tag{A.13}$$

Proof. Let T be any element of \mathcal{T}_n and I_T the linear interpolant onto this triangle. Then

$$\begin{aligned}
\|\nabla I_T(\varphi_n W_n) - \nabla(\varphi_n W_n)\|_{L^2(T)} &\lesssim h_T \|\nabla^2(\varphi_n W_n)\|_{L^2(T)} \\
&\lesssim h_T \|\nabla^2 \varphi_n \otimes W_n\|_{L^2(T)} + h_T \|\nabla \varphi_n \otimes \nabla W_n\|_{L^2(T)} \\
&\lesssim h_T \|W_n\|_{L^2(T)} + h_T \|\nabla W_n\|_{L^2(T)}.
\end{aligned} \tag{A.14}$$

We recall that $\nabla \varphi_n$ has support on $B_1(0)$ due to our choice of scaling and that $\int_{B_1(0)} W_n dx = 0$ due to our choice of equivalence class representative. Because of this and the estimate (A.14), it then follows that

$$\begin{aligned}
\|\nabla I_T(\varphi_n W_n) - \nabla(\varphi_n W_n)\|_{L^2(\mathbb{R}^d)} &\lesssim h_T \|W_n\|_{L^2(B_1(0))} + h_T \|\nabla W_n\|_{L^2(B_1(0))} \\
&\lesssim h_T \|\nabla W_n\|_{L^2(B_1(0))},
\end{aligned}$$

by the Poincaré inequality. Since $h_T = \mathcal{O}(\epsilon_n)$ on $L^2(B_1(0))$ due to the full mesh refinement assumption, we obtain the first result.

For the second one, the argument is the similar except that we have h_T^2 , we need not use the Poincaré inequality, and we do not immediately have that ∇r is bounded. However, we note that

$$\begin{aligned} h_T^2 \|\nabla r_n^\alpha\|_{L^2(T)} &\lesssim h_T^2 |T|^{1/2} \|\nabla r_n^\alpha\|_{L^\infty(T)} \\ &\lesssim h_T |T|^{1/2} \|r_n^\alpha\|_{L^\infty(T)} \lesssim h_T \|r_n^\alpha\|_{L^2(T)}, \end{aligned}$$

which could be used to obtain the result for r_n^α . \square

APPENDIX B. NOTATION

This section summarizes notation used in the manuscript.

- \mathcal{L} — a Bravais lattice
- \mathcal{M} — a multilattice
- $\mathcal{S} = \{0, \dots, S-1\}$ — the index set of atomic species
- ξ — an element of \mathcal{L} or $\epsilon\mathcal{L}$ for $\epsilon > 0$.
- $\alpha, \beta, \gamma, \delta, \iota, \chi$ — indexes denoting atomic species
- $\rho, \tau, \sigma \in \mathcal{L}$ — vectors between lattice sites
- \mathcal{R} — an interaction range whose elements are triples of the form $(\rho\alpha\beta) \in \mathcal{L} \times \mathcal{S} \times \mathcal{S}$
- $\mathcal{R}_1 := \{\rho \in \mathcal{L} : \exists(\rho\alpha\beta) \in \mathcal{R}\}$ — projection of \mathcal{R} onto lattice direction
- $r_{\text{cut}} := \max\{|\rho| : (\rho\alpha\beta) \in \mathcal{R}\}$ — a finite cut-off distance
- r_{cell} — the radius of the smallest ball inscribing the unit cell of \mathcal{L}
- $r_{\text{buff}} := \max\{r_{\text{cut}}, r_{\text{cell}}\}$
- $\mathbf{u} = (u_\alpha)_{\alpha=0}^{S-1}$ — vector of displacements of all species of atoms
- (U, \mathbf{p}) — displacement/shift description defined by $U = u_0$ and $p_\alpha = u_\alpha - u_0$
- \mathbf{y}^{ref} and \mathbf{p}^{ref} — the reference deformation and shifts
- $D_{(\rho\alpha\beta)}\mathbf{u}(\xi) = u_\beta(\xi + \rho) - u_\alpha(\xi)$, $D_{(\rho\alpha\beta)}(U, \mathbf{p}) = U(\xi + \rho) - U(\xi) + p_\beta(\xi + \rho) - p_\alpha(\xi)$
- $D\mathbf{u}(\xi) = (D_{(\rho\alpha\beta)}\mathbf{u}(\xi))_{(\rho\alpha\beta) \in \mathcal{R}}$, $D(U, \mathbf{p})(\xi) = (D_{(\rho\alpha\beta)}(U, \mathbf{p})(\xi))_{(\rho\alpha\beta) \in \mathcal{R}}$
- $\hat{V}_\xi(D\mathbf{y}(\xi))$ and $V_\xi(D\mathbf{u})$ — site potentials defined on deformations and displacements, respectively
- $\mathcal{E}^a(\mathbf{u})$ and $\mathcal{E}_{\text{hom}}^a(\mathbf{u})$ — energy difference functionals for defective and defect free lattice.
- \mathcal{T}_a — atomistic scale finite element mesh of triangles in $2D$ and tetrahedra in $3D$
- $\bar{\zeta}(x), \bar{\zeta}_\xi(x) = \bar{\zeta}(x - \xi)$ — nodal basis function of \mathcal{T}_a associated with the origin and ξ respectively
- $\omega_\rho(x) := \int_0^1 \bar{\zeta}(x + t\rho) dt$ — an auxiliary function
- Iu_α, IU, Ip_α or $\bar{u}_\alpha, \bar{U}, \bar{p}_\alpha$ — a piecewise linear interpolant with respect to \mathcal{T}_a
- $\tilde{I}u_\alpha, \tilde{I}U, \tilde{I}p_\alpha$ or $\tilde{u}_\alpha, \tilde{U}, \tilde{p}_\alpha$ — a $C^{2,1}$ interpolant with respect to \mathcal{T}_a
- $u^*(x) := (\bar{\zeta} * \bar{u})(x)$ — quasi-interpolant of u defined through convolution
- $|\cdot|$ — meaning depends on context: $|\cdot|$ is ℓ^2 norm of a vector, matrix, higher order tensor, or finite difference stencil. $|T|$ is area or volume of element T in a finite element partition, $|\gamma|$ is the order of a multiindex.
- $\|\cdot\|_{\ell^2(A)}$ — ℓ^2 norm over a set A . If $f : A \rightarrow \mathbb{R}^d$ is a vector-valued function, $\|f\|_{\ell^2(A)} = (\sum_{\alpha \in A} |f(\alpha)|^2)^{1/2}$.
- $\|\cdot\|_a$ — norm on admissible displacements defined by $\|\mathbf{u}\|_a^2 := \sum_{\alpha=0}^{S-1} \|\nabla Iu_\alpha\|_{L^2(\mathbb{R}^d)}^2 + \sum_{\alpha \neq \beta} \|Iu_\alpha - Iu_\beta\|_{L^2(\mathbb{R}^d)}^2$.
- \mathcal{U} — space of admissible displacements defined by

$$\mathcal{U} := \{\mathbf{u} = (u_\alpha)_{\alpha=0}^{S-1} : u_\alpha : \mathcal{L} \rightarrow \mathbb{R}^n, \|\mathbf{u}\|_a < \infty\} / \mathbb{R}^n$$

- \mathcal{U}_0 — space of test displacements defined by

$$\{(U, \mathbf{p}) : \text{supp}(\nabla IU), p_0 \equiv 0, \text{ and } \text{supp}(Ip_\alpha) \text{ are compact}\} / \mathbb{R}^n$$

- Ω — a finite polygonal domain
- φ — the blending function
- $\Omega_a := \text{supp}(1 - \varphi) + B_{2r_{\text{buff}}}$ — the atomistic domain
- $\Omega_b := \text{supp}(\nabla \varphi) + B_{2r_{\text{buff}}}$ — the blending region
- $\Omega_c := \text{supp}(\varphi) \cap \Omega + B_{2r_{\text{buff}}}$ — the continuum region
- $\Omega_{\text{core}} := \Omega \setminus \Omega_c$ — the defect core region
- \mathcal{T}_h — the (coarse) finite element mesh on Ω
- $h(x) := \max_{T: x \in T} \text{Diam}(T)$ — the mesh size function
- $R_t := \inf_R \{R > 0 : \Omega_t \subset B_R(0)\}$ — an exterior measure of a domain Ω_t
- $r_t := \sup_r \{r > 0 : B_r(0) \subset \Omega_t\}$ — an interior measure of a domain Ω_t
- $R_o := \inf_R \{R > 0 : \Omega \subset B_R(0)\}$ — an exterior measurement of Ω
- $r_i := \sup_r \{r > 0 : B_r(0) \subset \Omega\}$ — an interior measurement of Ω
- $\Omega_{\text{ext}} := \mathbb{R}^d \setminus B_{r_i/2}(0)$ — exterior of Ω
- I_h — the standard piecewise linear nodal interpolant on \mathcal{T}_h
- S_h — the Scott-Zhang quasi-interpolant on \mathcal{T}_h .
- $W_{\text{CB}}(U, \mathbf{p})$ — Cauchy–Born strain energy density function
- $\mathcal{E}^c(U, \mathbf{p})$ — Cauchy–Born energy functional
- $\mathcal{U}_h := \{u \in C^0(\Omega) : u|_T \in \mathcal{P}_1(T), \quad \forall T \in \mathcal{T}_h\}$ — a finite element space
- $\mathcal{U}_h := \mathcal{U}_h / \mathbb{R}^n$ space of admissible finite element displacements
- $\mathcal{U}_{h,0} := \{u \in C^0(\mathbb{R}^d) : u|_T \in \mathcal{P}_1(T), \quad \forall T \in \mathcal{T}_h, u = 0 \text{ on } \mathbb{R}^d \setminus \Omega\}$ — finite element space satisfying homogeneous boundary conditions
- $\mathcal{U}_{h,0} := \mathcal{U}_{h,0} / \mathbb{R}^n$ — finite element quotient space
- $\mathcal{P}_{h,0} := \{0\} \times (\mathcal{U}_{h,0})^{S-1}$ — finite element space for shifts
- $\|(U, \mathbf{p})\|_{\text{ml}}^2 := \|\nabla U\|_{L^2(\mathbb{R}^d)}^2 + \sum_{\alpha=0}^{S-1} \|p_\alpha\|_{L^2(\mathbb{R}^d)}^2 = \|\nabla U\|_{L^2(\mathbb{R}^d)}^2 + \|\mathbf{p}\|_{L^2(\mathbb{R}^d)}^2$ — norm on finite element spaces
- $\|\mathbf{p}\|_{L^p} := \sum_{\alpha=0}^{S-1} \|p_\alpha\|_{L^p}, \|\nabla \mathbf{p}\|_{L^p} := \sum_{\alpha=0}^{S-1} \|\nabla p_\alpha\|_{L^p}$
- $\eta(x)$ — a smooth bump function or standard mollifying function depending on the context
- $T_R u_\alpha(x) = \eta(x/R) \left(I u_\alpha - \frac{1}{|A_R|} \int_{A_R} I u_0 dx \right)$ — a truncation operator
- $\Pi_h u_\alpha := S_h(T_{r_i} u_\alpha)$ — an projection operator from discrete displacements to finite element displacements
- $\Pi_h p_\alpha := \Pi_h(u_\alpha - u_0)$ — a projection operator on shifts
- $[S_d^c(U, \mathbf{q})(x)]_\beta$ and $[S_s^c(U, \mathbf{q})(x)]_{\alpha\beta}$ — continuum stress function associated with displacements and shifts
- $[S_d^a(U, \mathbf{q})(x)]_\beta$ and $[S_s^a(U, \mathbf{q})(x)]_{\alpha\beta}$ — atomistic stress function associated with displacements and shifts
- $V_{(\rho\alpha\beta)(\tau\gamma\delta)}(\cdot) : v : w := w^\top [V_{(\rho\alpha\beta)(\tau\gamma\delta)}(\cdot)] v \quad \forall v, w \in \mathbb{R}^n$
- $\mathbb{C} : D(W, \mathbf{q}) : D(Z, \mathbf{r}) := \sum_{(\rho\alpha\beta) \in \mathcal{R}} \sum_{(\tau\gamma\delta) \in \mathcal{R}} V_{(\rho\alpha\beta)(\tau\gamma\delta)} : D_{(\rho\alpha\beta)}(W, \mathbf{q}) : D_{(\tau\gamma\delta)}(Z, \mathbf{r})$
- $\mathbb{C} : \nabla(W, \mathbf{q}) : \nabla(Z, \mathbf{r}) := \sum_{(\rho\alpha\beta) \in \mathcal{R}} \sum_{(\tau\gamma\delta) \in \mathcal{R}} V_{(\rho\alpha\beta)(\tau\gamma\delta)} : (\nabla_\rho W + q_\beta - q_\alpha) : (\nabla_\tau Z + r_\beta - r_\alpha)$
- φ_n — a sequence of blending functions
- $\psi_n := 1 - \varphi_n$
- $\theta_n := \sqrt{\psi_n}$
- $B_r, B_r(x)$ — Ball of radius r about the origin or ball of radius r about x .

- $\text{supp}(f)$ — support of a function f .
- $\text{Diam}(U)$ — diameter of the set U measured with the Euclidean norm.
- $(\mathbb{R}^n)^{\mathcal{R}}$ — direct product of vectors with $|\mathcal{R}|$ terms.
- $^\top$ — transpose of a matrix.
- \otimes — tensor product.
- ∇^j — j th derivative of a function defined on \mathbb{R}^d .
- ∂_γ — multiindex notation for derivatives.
- $L^p(U)$ — Standard Lebesgue spaces.
- $W^{k,p}(U)$ — Standard Sobolev spaces.
- $W_{\text{loc}}^{k,p}(U) = \{f : U \rightarrow \mathbb{R}^d : f \in W^{k,p}(V) \forall V \subset\subset U\}$.
- $H^k(U) = W^{k,2}(U)$, $H_0^1(U) = \{f \in H^k(U) : \text{Trace}(f) = 0 \text{ on } \partial U\}$.
- C^k — space of k times continuously differentiable functions
- $f_U f dx$ — average value of f over U .

REFERENCES

- [1] A. Abdulle, P. Lin, and A. Shapeev. Numerical methods for multilattices. *Multiscale Model. Simul.*, 10(3):696–726, 2012.
- [2] A. Abdulle, P. Lin, and A. Shapeev. A priori and a posteriori $W^{1,\infty}$ error analysis of a qc method for complex lattices. *SIAM J. Numer. Anal.*, 51(4):2357–2379, 2013.
- [3] F. Abraham, J. Broughton, N. Bernstein, and E. Kaxiras. Spanning the continuum to quantum length scales in a dynamic simulation of brittle fracture. *Europhysics Letters*, 44(6):783, 1998.
- [4] M. Arroyo and T. Belytschko. Finite crystal elasticity of carbon nanotubes based on the exponential cauchy-born rule. *Phys. Rev. B*, 69:115415, Mar 2004.
- [5] S. Badia, P. Bochev, M. Gunzburger, R. Lehoucq, and M. Parks. Blending methods for coupling atomistic and continuum models. In J. Fish, editor, *Bridging the scales in science and engineering*, pages 165–186. Oxford University Press, 2009.
- [6] S. Badia, P. Bochev, R. Lehoucq, M. Parks, J. Fish, M. Nuggehally, and M. Gunzburger. A force-based blending model for atomistic-to-continuum coupling. *International Journal for Multiscale Computational Engineering*, 5(5), 2007.
- [7] S. Badia, M. Parks, P. Bochev, M. Gunzburger, and R. Lehoucq. On atomistic-to-continuum coupling by blending. *Multiscale Modeling & Simulation*, 7(1):381–406, 2008.
- [8] P. Bauman, H. Ben Dhia, N. Elkhodja, J. Oden, and S. Prudhomme. On the application of the Arlequin method to the coupling of particle and continuum models. *Computational Mechanics*, 42:511–530, 2008.
- [9] M. Born and K. Huang. *Dynamical Theory of Crystal Lattices*. Clarendon Press, first edition, 1954.
- [10] S. Brenner and R. Scott. *The mathematical theory of finite element methods*, volume 15. Springer, 2008.
- [11] A.L. Cauchy. De la pression ou la tension dans un systeme de points materiels. In *Exercices de Mathematiques*. 1828.
- [12] D. Datta, C. Picu, and M. Shephard. Composite grid atomistic continuum method: an adaptive approach to bridge continuum with atomistic analysis. *International Journal for Multiscale Computational Engineering*, 2(3), 2004.
- [13] M. Dobson, R. Elliott, M. Luskin, and E. Tadmor. A multilattice quasicontinuum for phase transforming materials: Cascading cauchy born kinematics. *Journal of Computer-Aided Materials Design*, 14(1):219–237, 2007.
- [14] M. Dobson and M. Luskin. Analysis of a force-based quasicontinuum approximation. *ESAIM: Mathematical Modelling and Numerical Analysis*, 42:113–139, 0 2008.
- [15] M. Dobson, M. Luskin, and C. Ortner. Sharp stability estimates for the force-based quasicontinuum approximation of homogeneous tensile deformation. *Multiscale Modeling & Simulation*, 8(3):782–802, 2010.
- [16] W. E, J. Lu, and J.Z. Yang. Uniform accuracy of the quasicontinuum method. *Phys. Rev. B*, 74:214115, 2006.
- [17] V. Ehrlicher, C. Ortner, and A. V. Shapeev. Analysis of boundary conditions for crystal defect atomistic simulations. *Archive for Rational Mechanics and Analysis*, 222(3):1217–1268, 2016.
- [18] B. Eidel and A. Stukowski. A variational formulation of the quasicontinuum method based on energy sampling in clusters. *Journal of the Mechanics and Physics of Solids*, 57(1):87–108, 2009.
- [19] J. Ericksen. On the cauchy-born rule. *Mathematics and Mechanics of solids*, 13(3-4):199–220, 2008.
- [20] J. Hubbard and B. Hubbard. *Vector calculus, linear algebra, and differential forms : a unified approach*. Matrix Editions, fourth edition, 2009.
- [21] T. Hudson and C. Ortner. Analysis of stable screw dislocation configurations in an anti-plane lattice model. *SIAM J. Math. Anal.*, 41:291–320, 2015.
- [22] B. Van Koten and C. Ortner. Symmetries of 2-lattices and second order accuracy of the cauchy-born model. *SIAM Multiscale Modelling and Simulation*, 11:615–634, 2013.
- [23] X. Li, M. Luskin, and C. Ortner. Positive definiteness of the blended force-based quasicontinuum method. *Multiscale Modeling & Simulation*, 10(3):1023–1045, 2012.
- [24] X. Li, M. Luskin, C. Ortner, and A.V. Shapeev. Theory-based benchmarking of the blended force-based quasicontinuum method. *Computer Methods in Applied Mechanics and Engineering*, 268:763–781, 2014.
- [25] X. Li, C. Ortner, A.V. Shapeev, and B. Van Koten. Analysis of blended atomistic/continuum hybrid methods. *Numerische Mathematik*, 134(2):275–326, 2016.
- [26] J. Lu and P. Ming. Convergence of a force-based hybrid method in three dimensions. *Communications on Pure and Applied Mathematics*, 66(1):83–108, 2013.

- [27] J. Lu and P. Ming. Stability of a force-based hybrid method with planar sharp interface. *SIAM Journal on Numerical Analysis*, 52:2005–2026, 2014.
- [28] M. Luskin and C. Ortner. Atomistic-to-continuum coupling. *Acta Numerica*, 22:397–508, 4 2013.
- [29] M. Luskin, C. Ortner, and B. Van Koten. Formulation and optimization of the energy-based blended quasi-continuum method. *Computer Methods in Applied Mechanics and Engineering*, 253:160–168, 2013.
- [30] C. Makridakis, D. Mitsoudis, and P. Rosakis. On atomistic-to-continuum couplings without ghost forces in three dimensions. *Applied Mathematics Research eXpress*, 2014(1):87–113, 2014.
- [31] R. Miller and E. Tadmor. A unified framework and performance benchmark of fourteen multiscale atomistic/continuum coupling methods. *Modeling and Simulation in Materials Science and Engineering*, 17(5):053001, 2009.
- [32] D. Olson. *Formulation and Analysis of an Optimization-Based Atomistic-to-Continuum Coupling Algorithm*. PhD thesis, University of Minnesota, 2015.
- [33] D. Olson, P. Bochev, M. Luskin, and A. Shapeev. Development of an optimization-based atomistic-to-continuum coupling method. In I. Lirkov, S. Margenov, and J. Wanievski, editors, *Large-Scale Scientific Computing*, volume 8353 of *Lecture Notes in Computer Science*, pages 33–44. Springer Berlin Heidelberg, 2014.
- [34] D. Olson and C. Ortner. Regularity and locality of point defects in multilattices. *Applied Mathematics Research eXpress*, To appear, 2017.
- [35] D. Olson, A. Shapeev, P. Bochev, and M. Luskin. Analysis of an optimization-based atomistic-to-continuum coupling method for point defects. *ESAIM: M2AN*, 50(1):1–41, 2016.
- [36] M. Ortiz, R. Phillips, and E. Tadmor. Quasicontinuum analysis of defects in solids. *Philosophical Magazine A*, 73(6):1529–1563, 1996.
- [37] C. Ortner. A posteriori existence in numerical computations. *SIAM J. Numer. Anal.*, 47(4):2550–2577, 2009.
- [38] C. Ortner and A. Shapeev. Interpolants of Lattice Functions for the Analysis of Atomistic/Continuum Multiscale Methods. *ArXiv e-prints*, April 2012. 1204.3705.
- [39] C. Ortner and E. Süli. A note on linear elliptic systems on \mathbb{R}^d . *ArXiv e-prints*, 2012. 1202.3970.
- [40] C. Ortner and F. Theil. Justification of the Cauchy–Born approximation of elastodynamics. *Arch. Ration. Mech. Anal.*, 207:1025–1073, 2013.
- [41] C. Ortner and L. Zhang. Atomistic/continuum blending with ghost force correction. *ArXiv e-prints*, 1407.0053, 2014.
- [42] R. Scott and S. Zhang. Finite element interpolation of nonsmooth functions satisfying boundary conditions. *Mathematics of Computation*, 54(190):483–493, 1990.
- [43] P. Seleson, S. Beneddine, and S. Prudhomme. A force-based coupling scheme for peridynamics and classical elasticity. *Computational Materials Science*, 66:34–49, 2013.
- [44] A. Shapeev, D. Olson, and M. Luskin. *Unpublished Manuscript*, 2015.
- [45] A. V. Shapeev. Consistent energy-based atomistic/continuum coupling for two-body potentials in three dimensions. *SIAM J. Sci. Comput.*, 34(3):B335–B360, 2012.
- [46] A.V. Shapeev. Consistent energy-based atomistic/continuum coupling for two-body potentials in one and two dimensions. *SIAM J. Multiscale Model. Simul.*, 9:905–932, 2011.
- [47] V. B. Shenoy, R. Miller, E. B. Tadmor, D. Rodney, R. Phillips, and M. Ortiz. An adaptive finite element approach to atomic-scale mechanics—the quasicontinuum method. *J. Mech. Phys. Solids*, 47(3):611–642, 1999.
- [48] L. Shilkrot, R. Miller, and W. Curtin. Coupled atomistic and discrete dislocation plasticity. *Physical Review Letters*, 89(2):025501, 2002.
- [49] T. Shimokawa, J.J. Mortensen, J. Schjøtz, and K.W. Jacobsen. Matching conditions in the quasicontinuum method: Removal of the error introduced at the interface between the coarse-grained and fully atomistic region. *Phys. Rev. B*, 69:214104, Jun 2004.
- [50] F. Stillinger and T. Weber. Computer simulation of local order in condensed phases of silicon. *Physical review B*, 31(8):5262, 1985.
- [51] E. Tadmor and R. Miller. *Modeling Materials Continuum, Atomistic and Multiscale Techniques*. Cambridge University Press, first edition, 2011.
- [52] S.P. Xiao and T. Belytschko. A bridging domain method for coupling continua with molecular dynamics. *Computer methods in applied mechanics and engineering*, 193(17):1645–1669, 2004.
- [53] Jerry Z Yang and E. Weinan. Generalized cauchy-born rules for elastic deformation of sheets, plates, and rods: Derivation of continuum models from atomistic models. *Physical Review B*, 74(18):184110, 2006.